NAA-SR-8617
VOLUME I
REACTOR TECHNOLOGY
TID-4500 (29th Ed.)
SNAP REACTORS,
SNAP PROGRAM,
M-3679 (34th Ed.)

SNAP TECHNOLOGY HANDBOOK

VOLUME I

LIQUID METALS

By

G. F. BURDI

ATOMICS INTERNATIONAL

A DIVISION OF NORTH AMERICAN AVIATION, INC.
P.O. BOX 309 CANOGA PARK, CALIFORNIA

CONTRACT: AT(11-1)-GEN-8
ISSUED: AUG -1 1964

DISCLAIMER

DISTRIBUTION

This report has been distributed according to the category "Reactor Technology" as given in "Standard Distribution Lists for Unclassified Scientific and Technical Reports" TID-4500 (29th Ed.), April 1, 1964. A total of 850 copies was printed.

Price $2.75
Available from the Office of Technical Services
Department of Commerce
Washington 25, D. C.

INSERT LATEST PAGES. DESTROY SUPERSEDED PAGES.

LIST OF EFFECTIVE PAGES

NOTE: The portion of the text affected by the changes is indicated by a vertical line in the outer margin of the page.

TOTAL NUMBER OF PAGES IN THIS PUBLICATION IS 151 CONSISTING OF THE FOLLOWING:

*The asterisk indicates pages changed, added, or deleted by the current change

ADDITIONAL COPIES OF THIS PUBLICATION MAY BE OBTAINED FROM ATOMICS INTERNATIONAL

CONTENTS

CONTENTS

TABLES

FIGURES

FIGURES

FIGURES

INTRODUCTION

Extensive use of liquid metals as working fluids in various reactor programs, i.e., SNAP 10A/2/8, necessitates a handbook to correlate and present the current information which is available to the engineer. The present work is not intended to be all inclusive but contains important excerpts from commonly used references along with recent developments, arranged for the convenience of the design engineer. Data selected for presentation has passed the test of being in reasonable agreement with the majority of published work; some older data not well substantiated by recent experiments has not been included. The liquid metals considered to be the most useful for present and future applications are mercury, sodium, sodium-potassium, potassium, rubidium, and lithium. As additional information becomes available, periodic revisions will be incorporated in this SNAP TECHNOLOGY HANDBOOK.

ACKNOWLEDGMENT

The author expresses his appreciation to P. D. Cohn, C. J. Baroczy, and L. Bernath for their valuable criticisms and suggestions.

1.0 PROPERTIES

1.1 GENERAL PROPERTIES

1.1.1 Mercury (Hg; at. no. 80; at. wt 200.61)[1,2,3,4,5]

Mercury is a mobile, silvery-white liquid slightly heavier than lead. It dissolves in nitric or concentrated sulfuric acids but is not soluble in non-oxidizing strong acids or in strong bases. Mercury is the most dense liquid metal and exhibits the highest gaseous ionization potential of all elements, excluding the inert gases. It is also the most fusible and volatile liquid metal, does not react with oxygen at room temperature, and is inert toward water. Upon prolonged exposure to moist air, an oxide film (usually representing oxidized trace impurities) may form on mercury surfaces.

Mercury readily forms alloys with the alkali metals, aluminum, bismuth, cadmium, gold, lead, magnesium, silver, tin, and zinc; when mercury comes into contact with sodium, NaK, or potassium, heat is given off. Some of the properties of these sodium and potassium amalgams are given below.[5]

TABLE 1.1

HEAT OF FORMATION OF SODIUM AND POTASSIUM AMALGAMS

Amalgam	Melting Point (°F)	Wt % of Na or K	Heat of Formation (from liquid mercury) (Btu/lb-mol)
$NaHg_2$	668	5.4	-29,200
$Na_{12}Hg_{13}$	441	9.6	?
NaHg	426	10.3	-20,550
$NaHg_4$	320	2.8	?
KHg_2	518	8.9	-35,620
KHg_3	392	6.1	-52,400
K_2Hg_9	343	4.1	?
KHg_9	158	2.1	?

Not all of the heats of formation are given due to lack of information and experiments. Properties on the ternary compounds were unavailable. It is important to note that the amount of liberated heat increases with increasing mercury-to-NaK weight ratio.

Mercury is presently available commercially in 76-lb flasks @$208 to $210 per flask with a purity of 99.7%. The principal producers (1949) are Bonanza Mines, Inc., Cardero Mining Company, and Sonoma Quicksilver Mines, Inc.

1.1.2 Sodium (Na; at. no. 11; at. wt 22.991;)[2,3,6]

Solid sodium is a relatively soft, silvery-white metal. Molten sodium is also a silvery-white metal which has a high reactivity with most gases or liquids other than the noble gases and nitrogen. Solid sodium does not burn in dry air at ordinary temperatures, but owing to the formation of an oxide film, it tarnishes rapidly in moist air. Molten sodium burns under atmospheric conditions to form a dense sodium monoxide fume, but under an oxygen atmosphere a yellow flame of burning sodium results giving off sodium monoxide and sodium peroxide. When sodium comes in contact with water, it reacts violently and ignites the liberated hydrogen. One of the most violent reactions occurs when alkali metals are brought into contact with carbon tetrachloride which results in erratic detonation. This reaction will also occur when an alkali metal is brought into contact with other polyhalogenated hydrocarbons. Vigorous reactions between sodium and halogens, acidic oxides, mercury, or alloys with lead, tin, zinc, or bismuth also occur. Reference 3 gives certain conditions under which the combination of the above metals with sodium results in no reaction.

Alloy compounds of sodium with mercury, potassium, bismuth, cadmium, antimony, arsenic, gold, lead, tin, and some other metals are possible.

Commercial sodium (~99.8% pure) – with common impurities such as calcium, potassium, hydrogen, chlorides, and oxygen present in amounts exceeding 10 ppm – is produced by E. I. DuPont de Nemours and Company, Ethyl Corporation, MSA Research Corporation (Commercial Division), and National Distillers Chemical Company. Price ranges from ~16¢/lb in tank car lots to 50¢/lb for 1 or 2 lb bricks.

1.1.3 Sodium-Potassium (NaK)[1,3,7,8]

Above its melting point, NaK appears as a mobile, silvery liquid. Although NaK reacts similarly to sodium and potassium, it is considered more active than either of the two metals alone; because NaK is in the liquid state at room temperature (composition of NaK ranges from 50 to 90 wt % potassium). Because potassium is the most reactive of the two elements, it determines the chemical properties of NaK to a great extent (see Section 1.1.4 for discussion of potassium). Exothermic reactions occur when NaK comes into contact with water forming oxides and hydroxides of sodium and potassium and also hydrogen gas. At room temperature NaK reacts with the oxygen in air to form a surface scum of sodium oxide and potassium superoxide. The oxide precipitating from the NaK at 392°F is entirely sodium monoxide.

Commercial NaK is manufactured by the same producers as those listed for sodium, in addition to the Mine Safety Appliance Co. The cost was 60¢/lb for NaK-56; 80¢/lb for NaK-78 [7] (The K wt % is given when referring to NaK.). Common impurities in ppm in the distilled NaK are 20 iron, 20 copper, 20 silicon, 40 aluminum, 10 magnesium, and 20 ppm of calcium. NaK used for reactor applications is usually further purified prior to introduction into a system. The above price varies greatly according to the purity desired.

1.1.4 Potassium (K; at. no. 19; at. wt 39.100)[2,3,7]

Potassium is a soft, silver-white alkali metal which differs from sodium in many ways. Unlike sodium, potassium combines with oxygen at room temperature to form a superoxide which may cause explosions. The cause of these explosions is not fully understood. Also, potassium forms an explosive carbonyl when brought into contact with carbon monoxide. Furthermore, potassium detonates with liquid bromine while sodium and lithium only react superficially. But similar to sodium, potassium reacts violently with water and ignites the liberated hydrogen. Reference 7 lists the many organic and inorganic reactions occurring with potassium.

Potassium is able to form alloy compounds with sodium, cesium, lithium, rubidium, magnesium, aluminum, gold, antimony, zinc, and cadmium.

Commercial potassium is available from producers of NaK and Na @~$1.00/lb in 150 ton quantities and @~$4.75/lb in 1 to 5 lb quantities (1961).

1.1.5 Rubidium (Rb; at. no. 37; at. wt 85.48)[2,3,9]

Rubidium is a soft, ductile, silvery-white metal. Neglecting cesium and francium, which is an unstable isotope, Rb is the most reactive alkali metal and reacts violently with water, igniting the liberated hydrogen. Rubidium ignites spontaneously in dry air characterized by a blue flame. The rest of the chemical properties closely resemble the other alkali metals.

Characteristic of the alkali metals, with Rb being no exception, is that the compounds formed are univalent. Rubidium can be alloyed with gold, cesium, potassium, and sodium and readily amalgamates with mercury.

The principal producers of commercial Rb (~99+% purity) are American Potash and Chemical Corporation, De Rerval Int. Rare Metals Corporation, and Fairmont Chemical Company, Inc., @~$440/lb in 1 lb quantities or $350/lb in 6 to 25 lb quantities.

1.1.6 Lithium (Li; at. no. 3; at. wt 6.940; Valence 1)[2,3]

Lithium is a silvery-white metal and is the least dense and least volatile of the alkali metals; however, Li is the hardest alkali metal. Below 212°F Li does not react with dry oxygen, but a freshly cut surface of Li turns yellow in moist air. When Li is exposed to cold water, a slow reaction results without igniting the liberated hydrogen. While other alkali metals are inert to nitrogen, Li in the presence of moisture reacts exothermically with nitrogen at ordinary temperatures, and at temperatures above its melting temperature, Li reacts rapidly with nitrogen to form Li_3N, a black hygroscopic nitride.

Lithium alloy compounds may be formed with magnesium, zinc, cadmium, bismuth, silicon, aluminum, tin, lead, mercury, silver, thallium, sodium, beryllium, barium, and calcium.

The principal producers of commercial Li (99.5% purity) are Foote Mineral Co., Lithium Corporation of America, Maywood Chemical Works, and Metalloy Corporation @~$9.00 to $11.00/lb. Lithium is available as granular particles, wire, or 8 by 1-1/2-in. diameter castings.

1.2 ENGINEERING PROPERTIES

The following sections contain engineering properties mostly from Reference 2 for Hg, Na, NaK, K, Rb, and Li and represent the most recent reliable data available. The reader is referred to the above reference for other properties and liquid metals not included in this report.

TABLE 1.2

ATMOSPHERIC BOILING AND MELTING POINTS OF Hg, Na, NaK, K, Rb, and Li[2, 10]

Metal	Melting Temperature (°F)	Boiling Temperature (°F)
Hg	-37.97	674
Na	208	1630
NaK	See Figures 1.1 and 1.2	
K	145.8	1395
Rb	102	1295
Li	357	2430

1.2.1 Density[2]

Figures 1.3 to 1.11 give the graphical representation of density vs temperature for Hg, Na, NaK, K, Rb, and Li in the liquid and saturated vapor states. The density of saturated NaK vapor was omitted because of the unavailability of data.

1.2.2 Thermal Conductivity[2,11,12]

Figures 1.12 to 1.21 graphically represent the thermal conductivity of Hg, Na, NaK, K, Rb, and Li. Again data were not available for saturated NaK vapor. For liquid Rb between 102 and 300°F, the thermal conductivity data were obtained from Reference 10.

1.2.3 Electrical Resistivity[2, 10, 13, 14]

All available data are shown in Figures 1.22 to 1.25 for the liquid metals in the liquid state. Electrical resistivity properties for liquid metals in the saturated vapor state were omitted due to lack of experimental results.

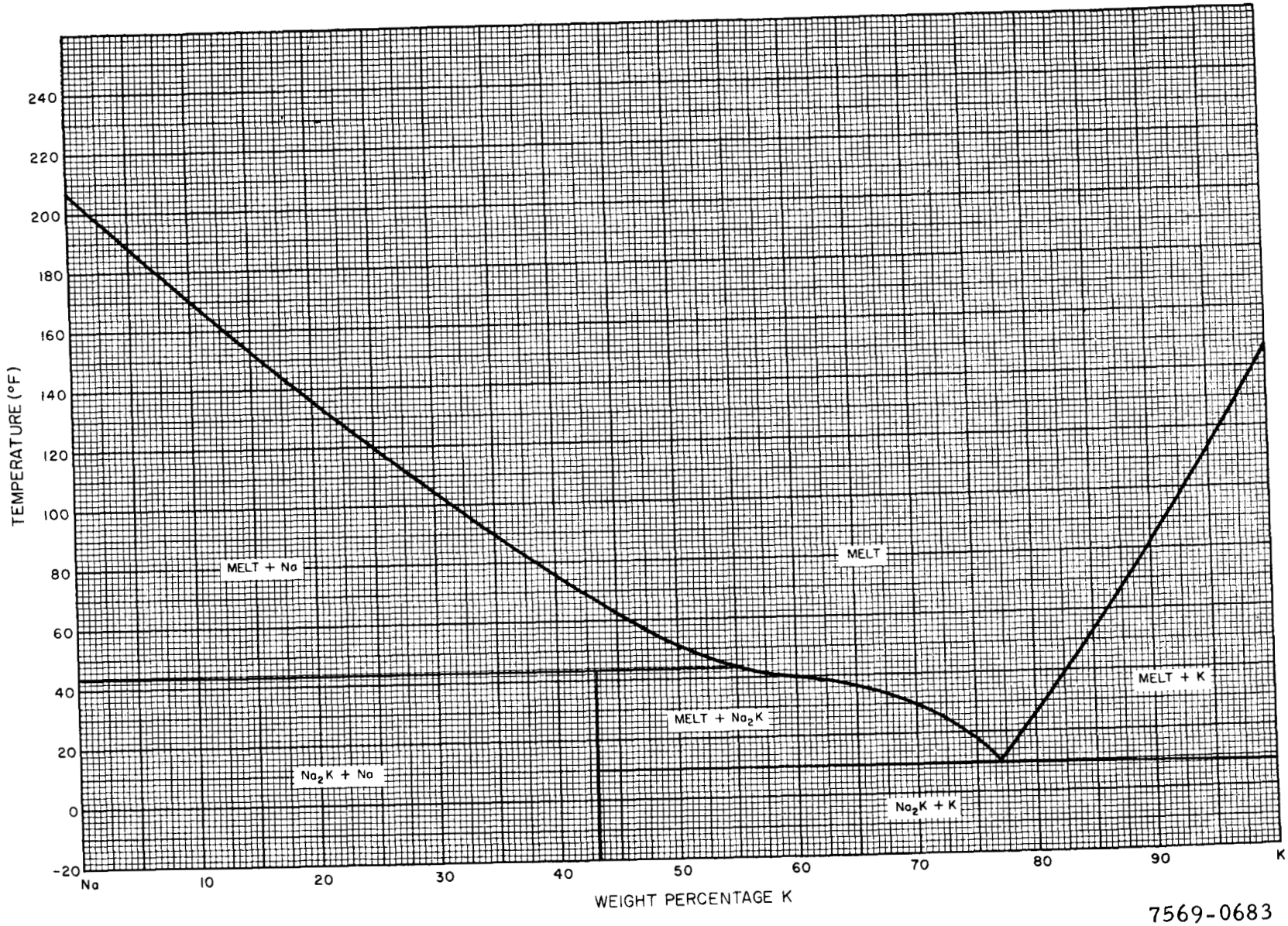

6-24-63

Figure 1.1 NaK Phase Diagram
(Reference 10)

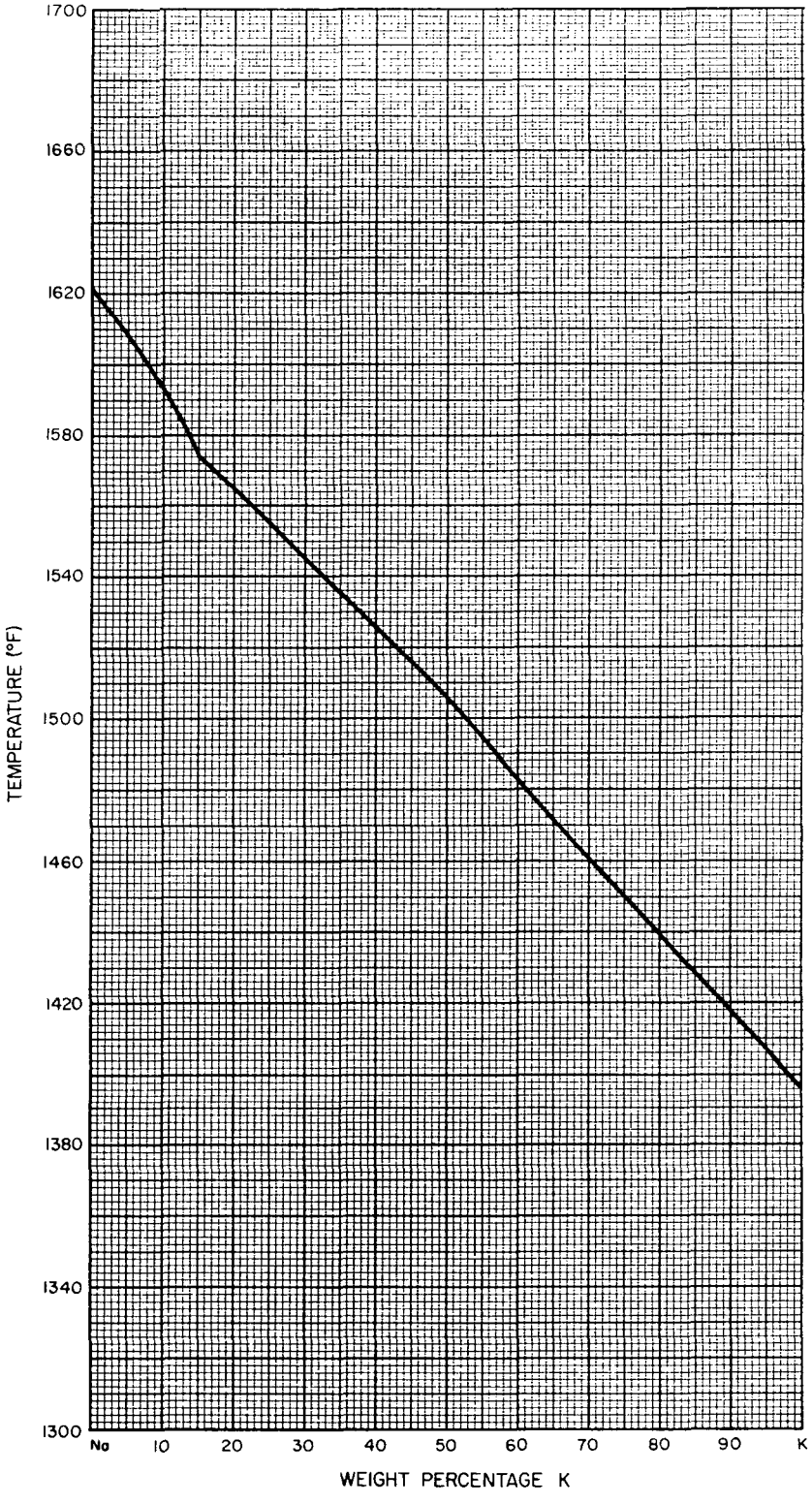

Figure 1.2 Boiling Point of NaK
(Reference 10)

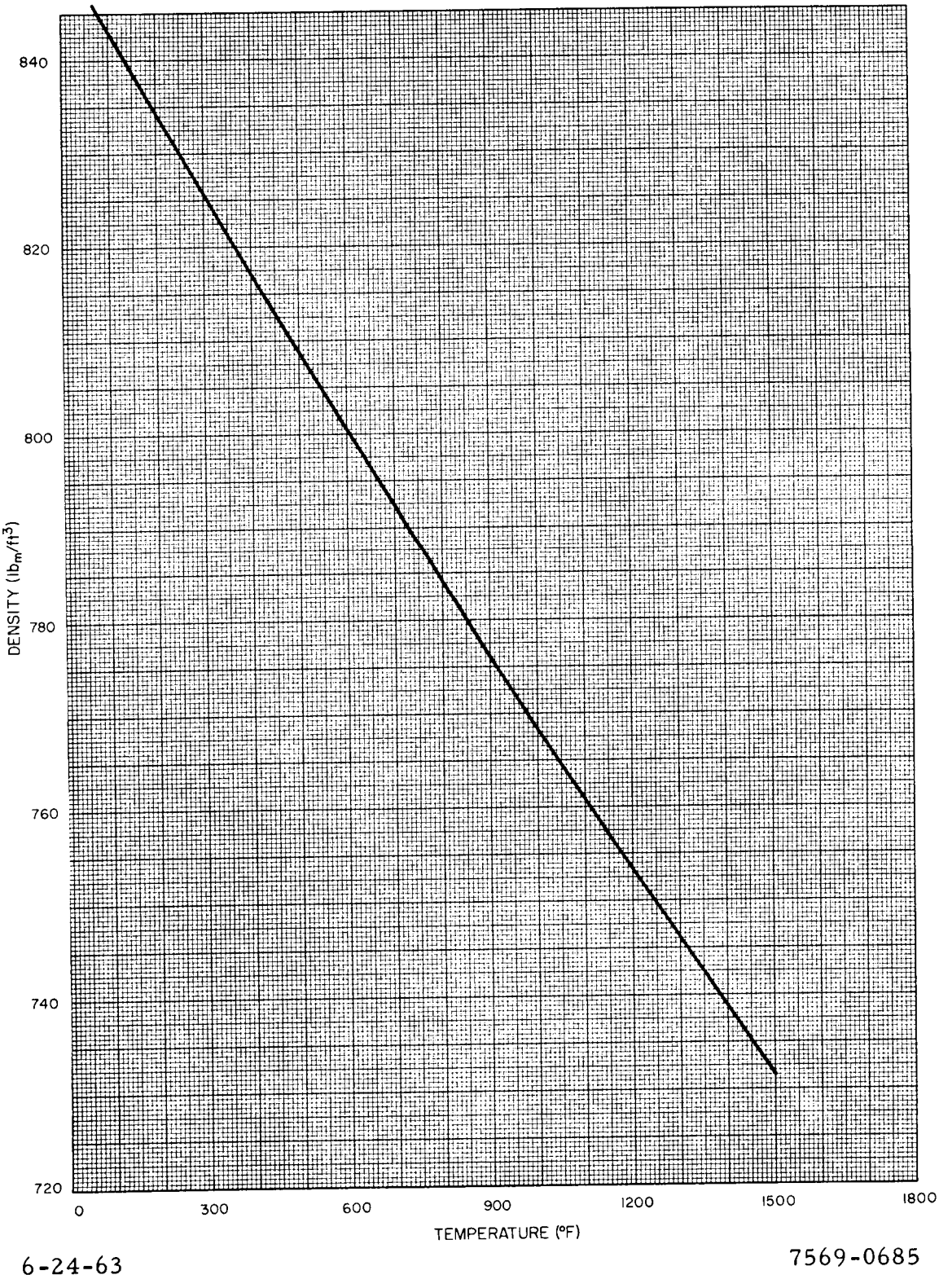

Figure 1.3 Density of Liquid Mercury
(Reference 2)

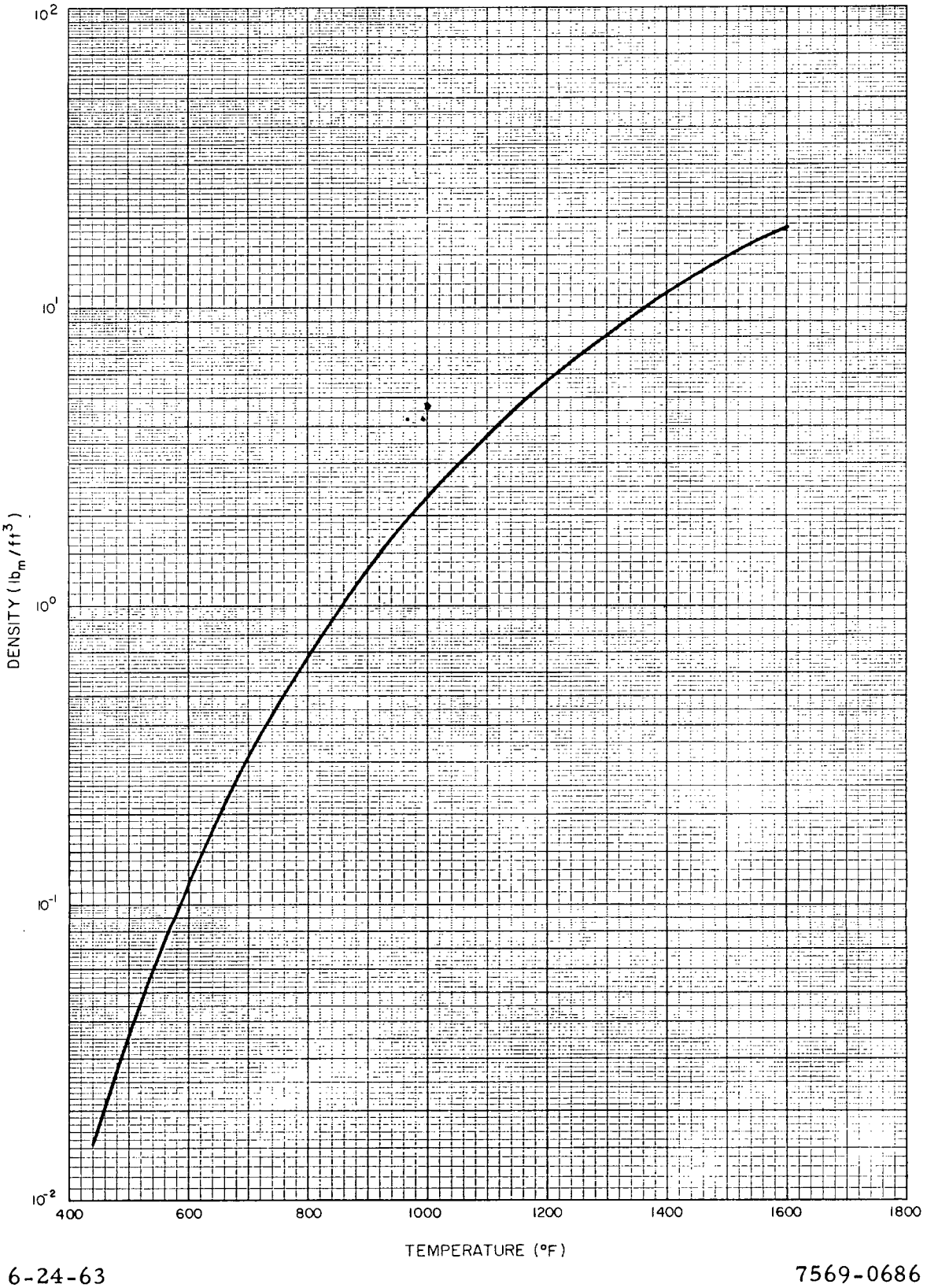

Figure 1.4 Density of Saturated Mercury Vapor (Reference 2)

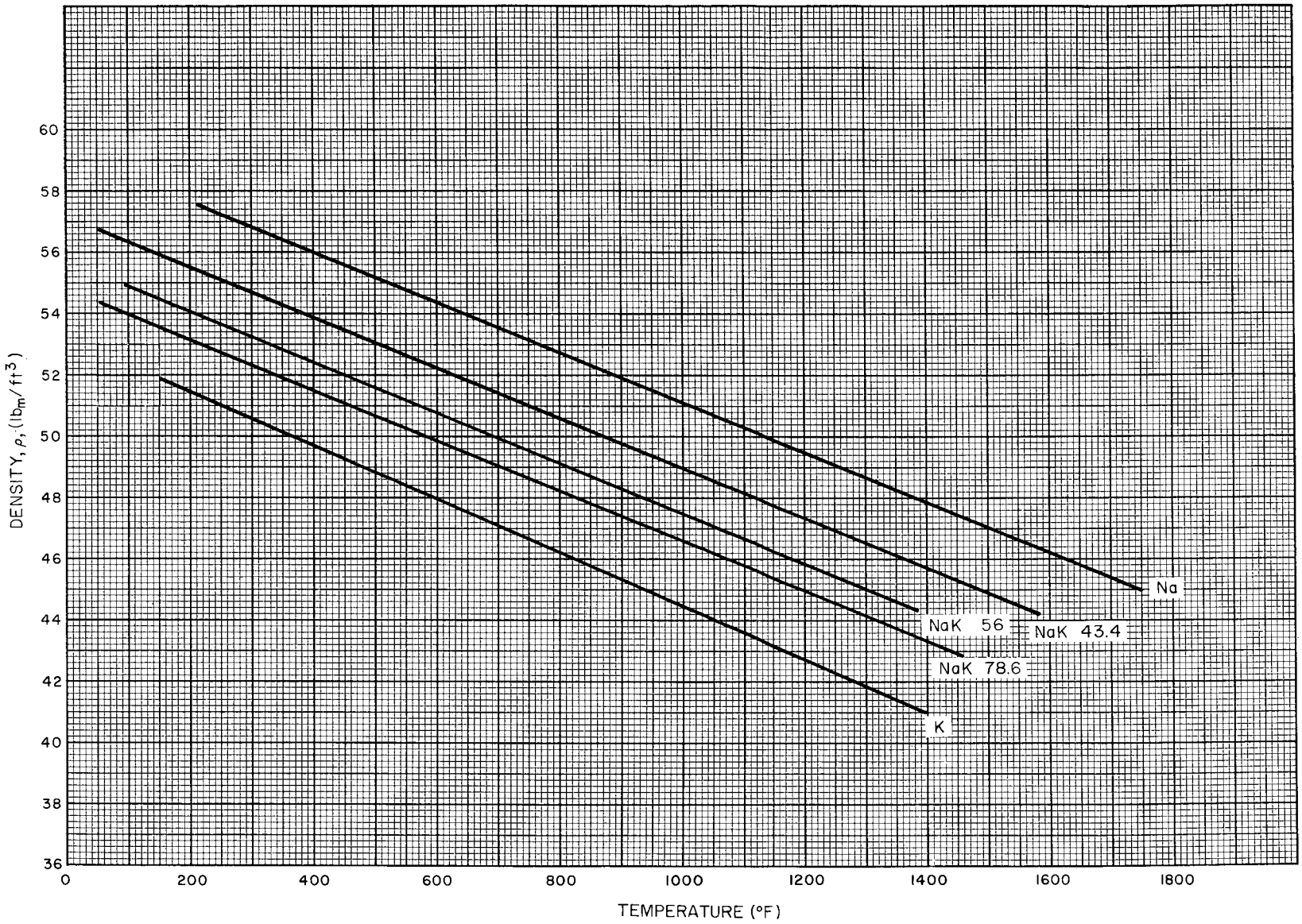

Figure 1.5 Density of Liquid Sodium, Potassium, and NaK
(Reference 2, 10)

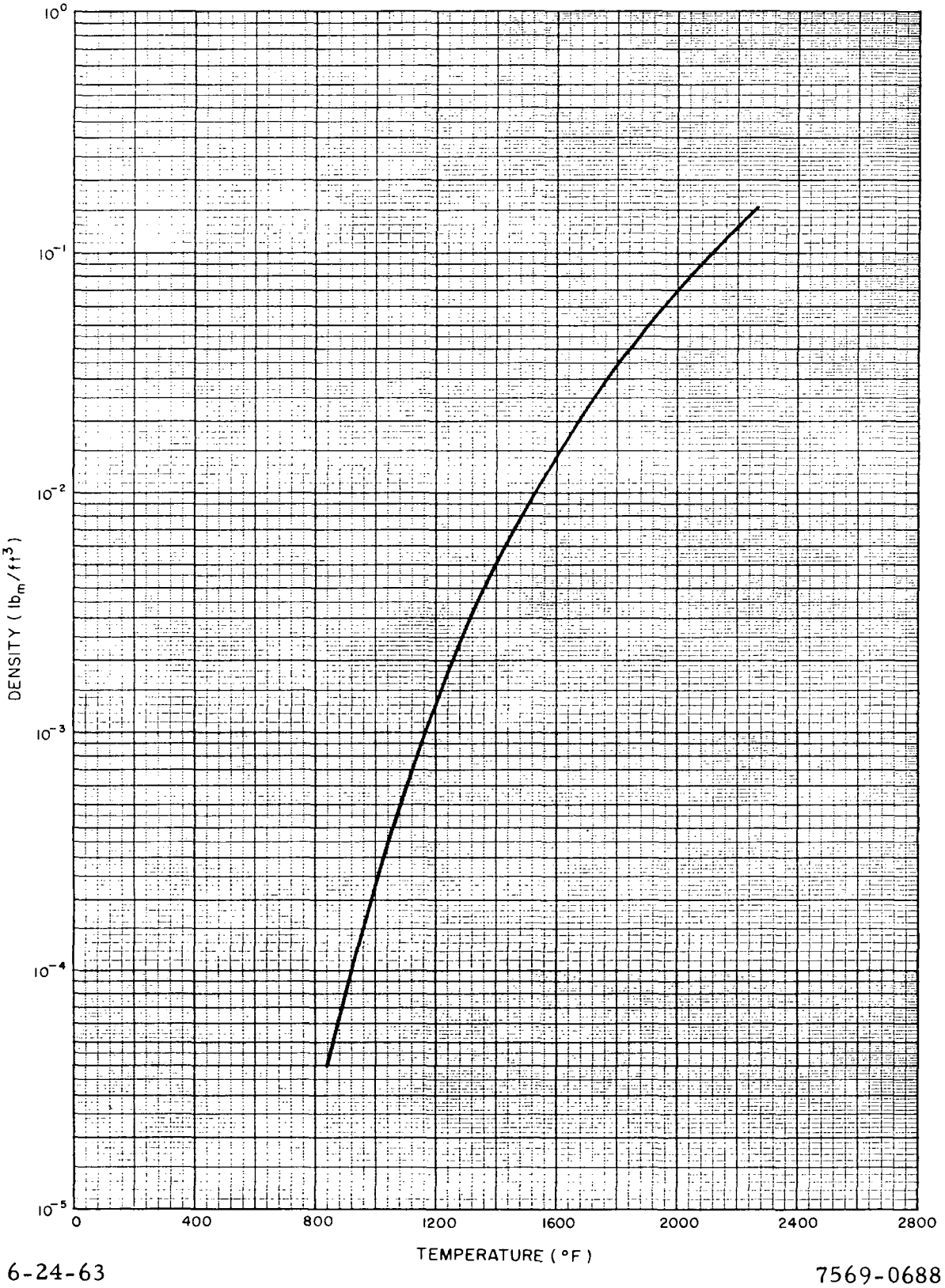

Figure 1.6 Density of Saturated Sodium Vapor
(Reference 2)

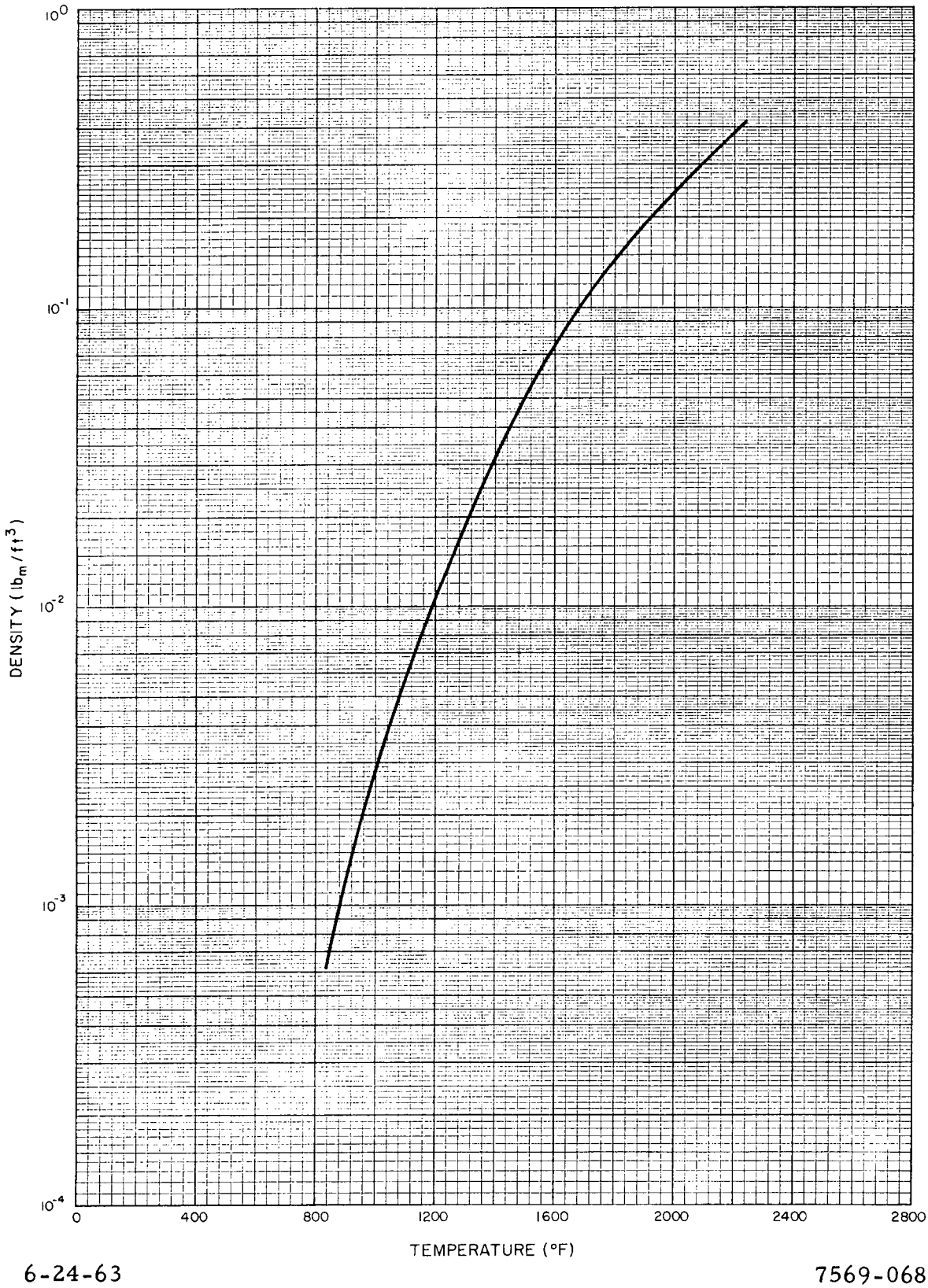

Figure 1.7 Density of Saturated Potassium Vapor (Reference 2)

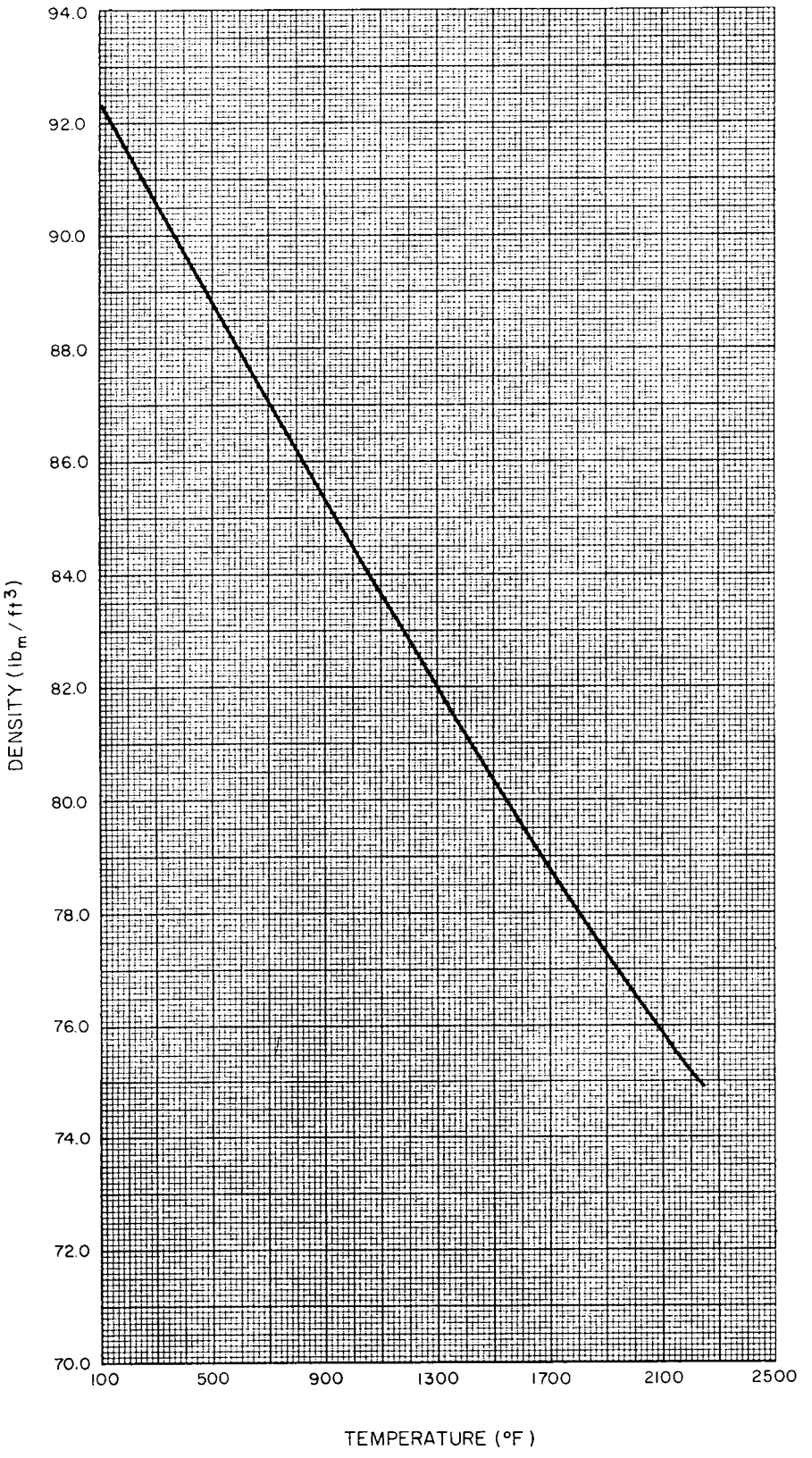

6-24-63 7569-0690

Figure 1.8 Density of Liquid Rubidium (Reference 2)

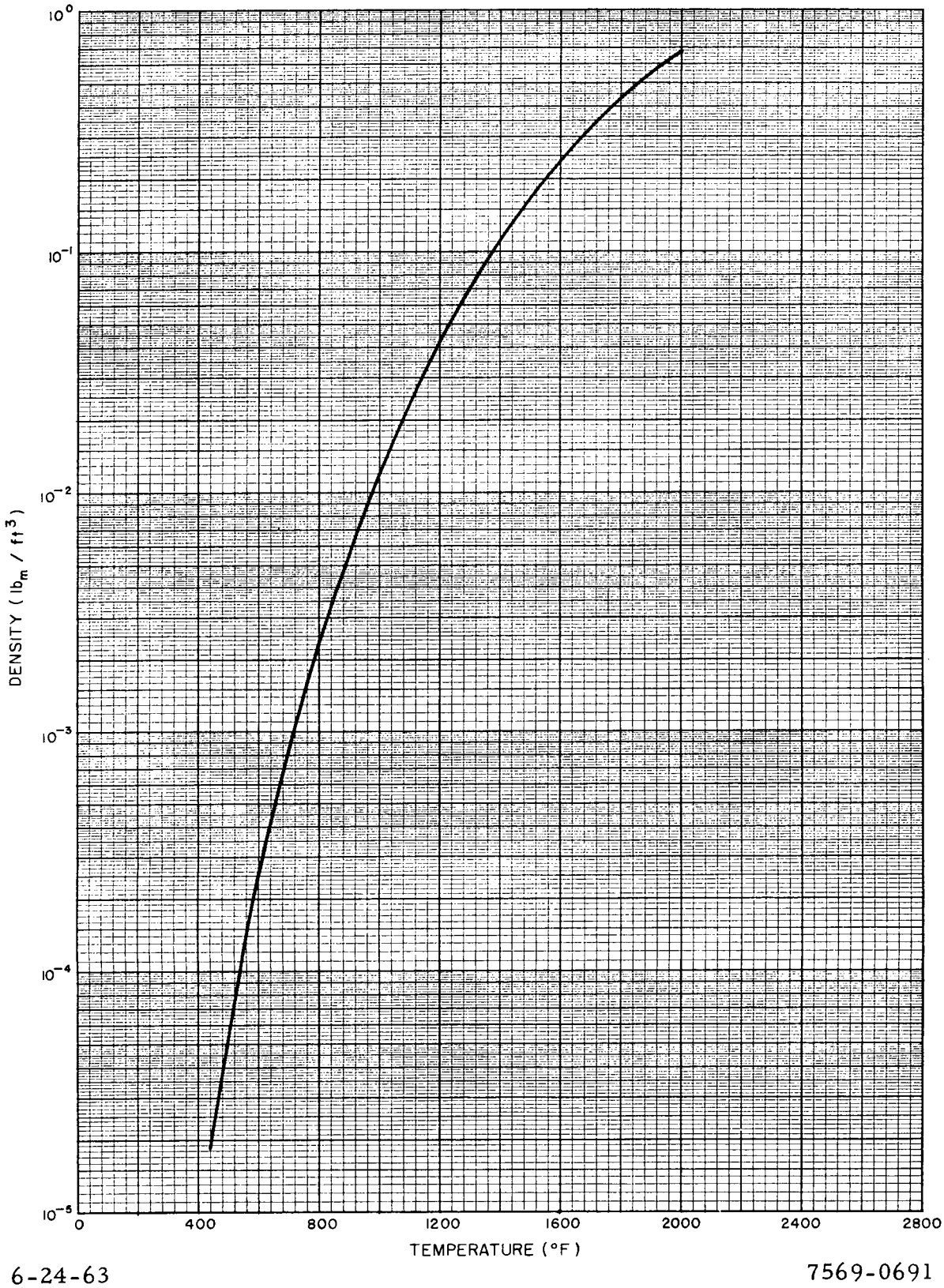

Figure 1.9 Density of Saturated Rubidium Vapor
(Reference 2)

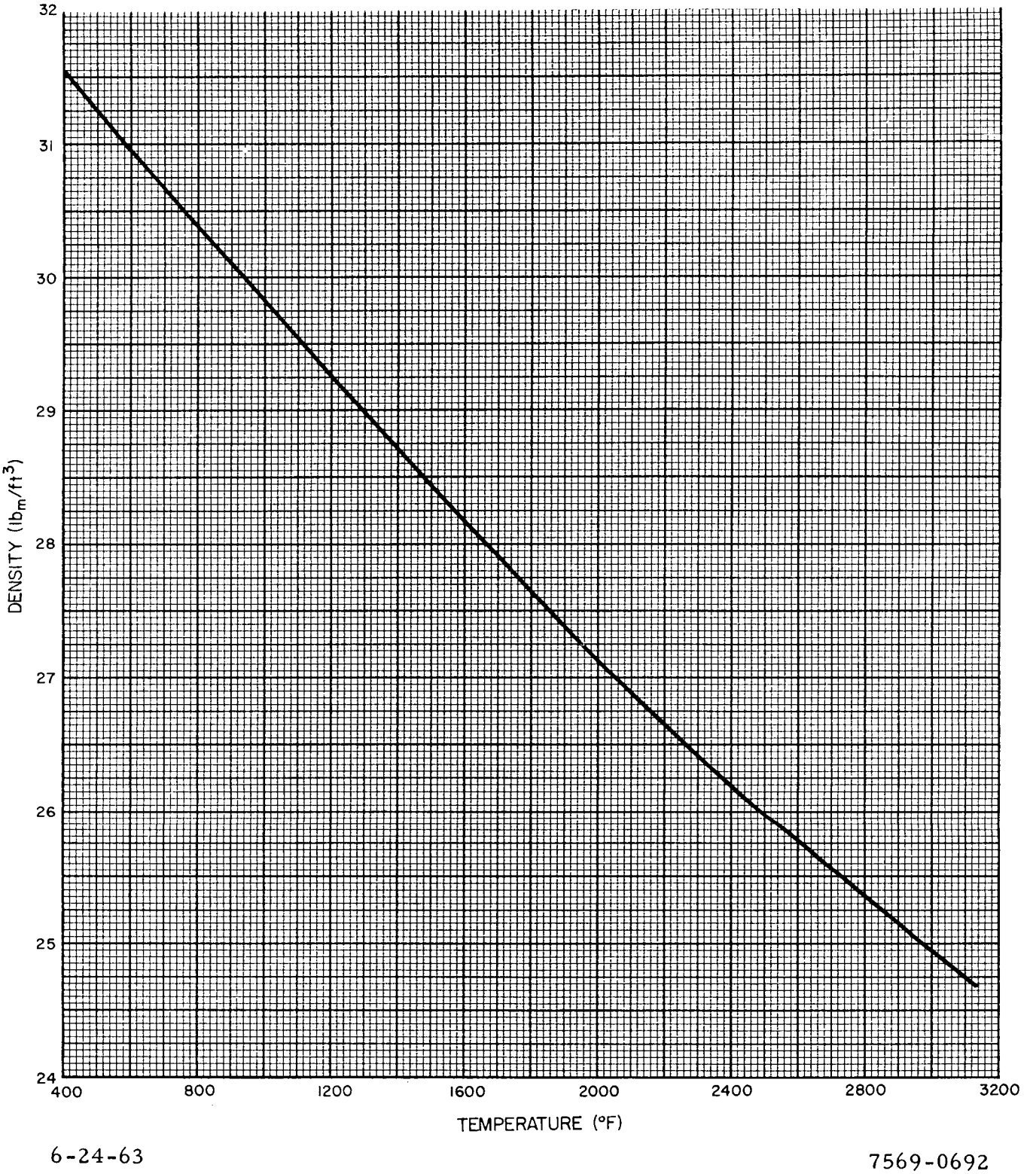

Figure 1.10 Density of Liquid Lithium
(Reference 2)

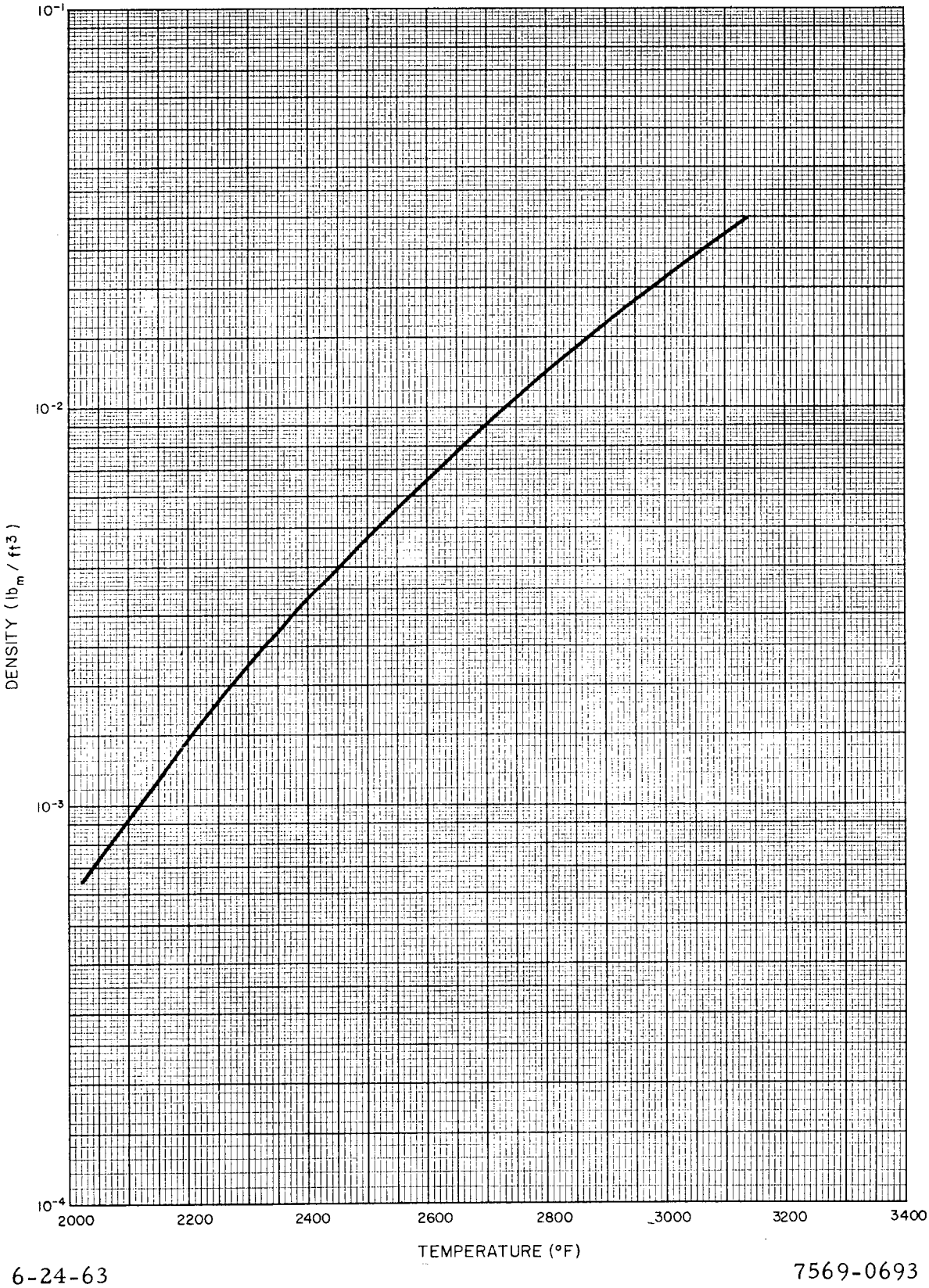

Figure 1.11 Density of Saturated Lithium Vapor
(Reference 2)

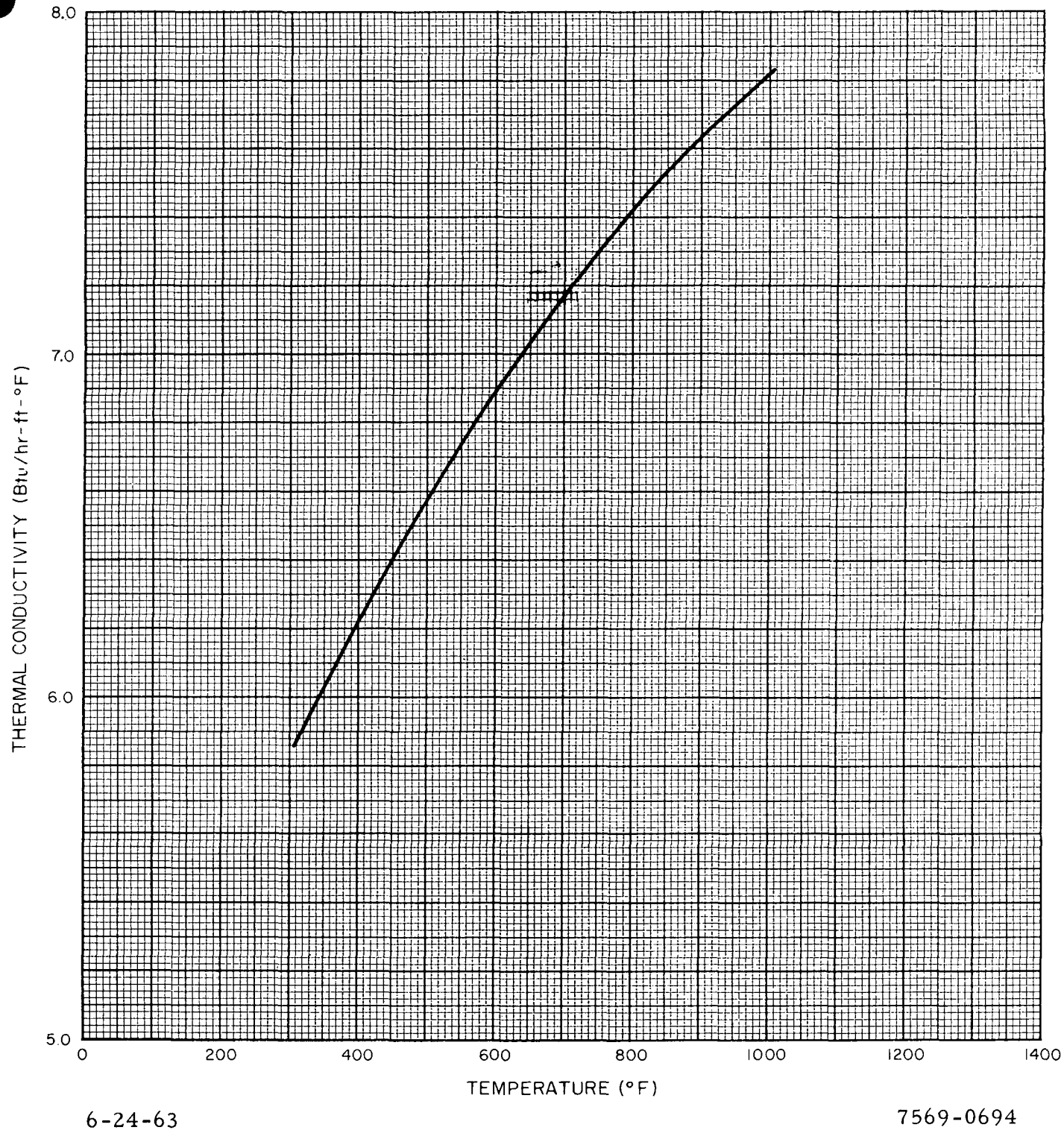

Figure 1.12 Thermal Conductivity of Liquid Mercury
(Reference 2)

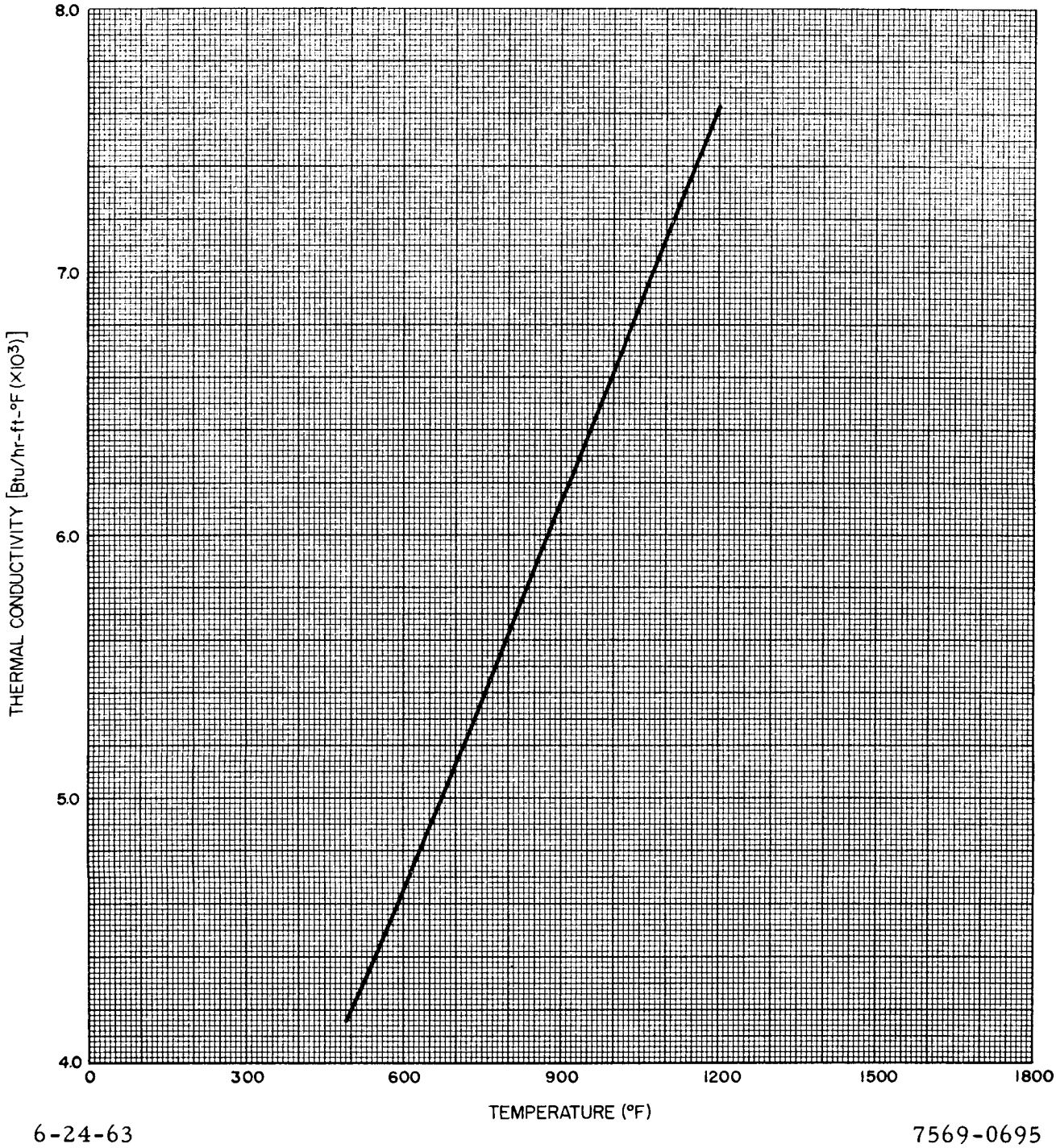

Figure 1.13 Thermal Conductivity at Saturated Mercury Vapor
(Reference 2)

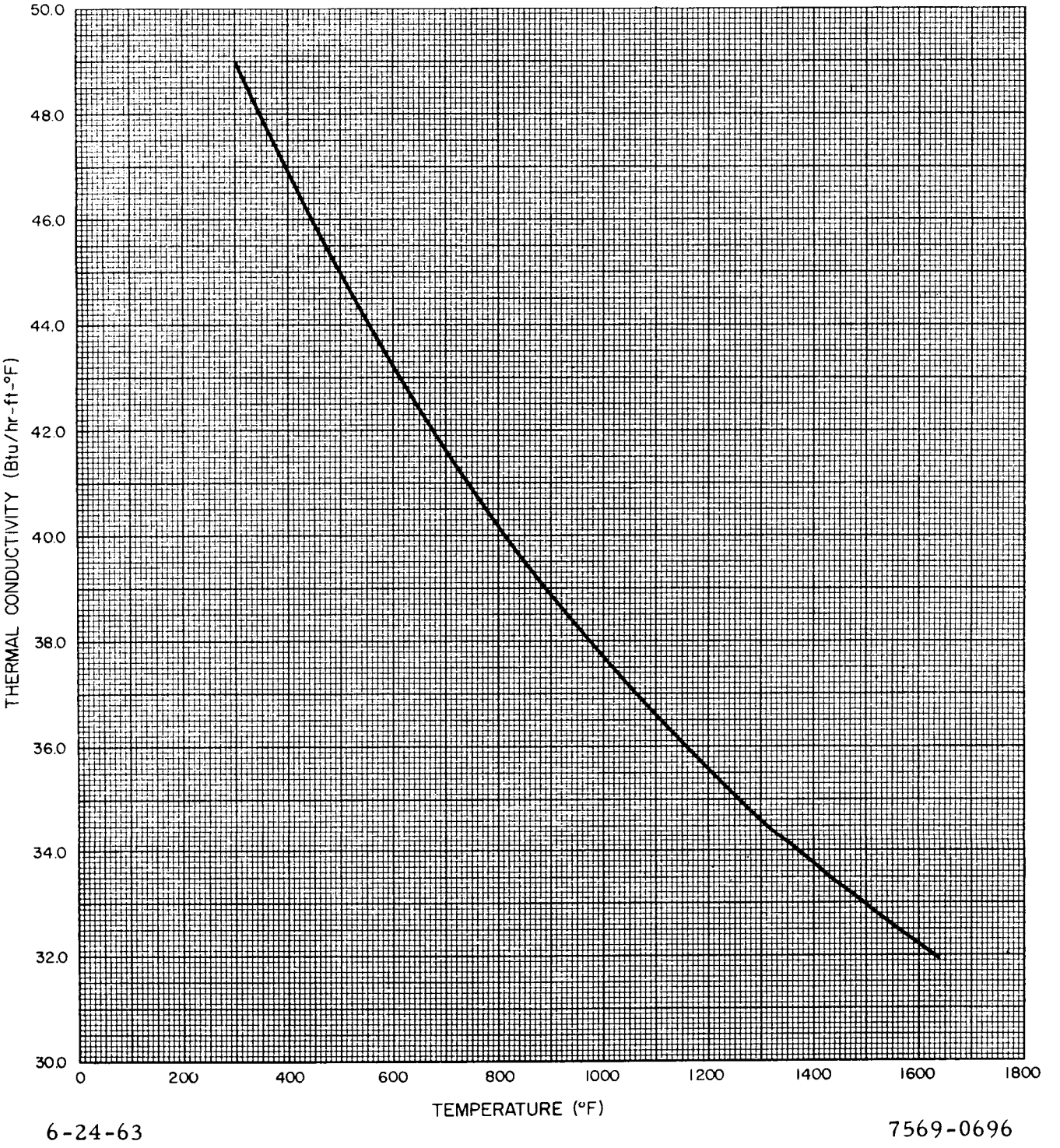

Figure 1.14 Thermal Conductivity of Liquid Sodium
(Reference 2)

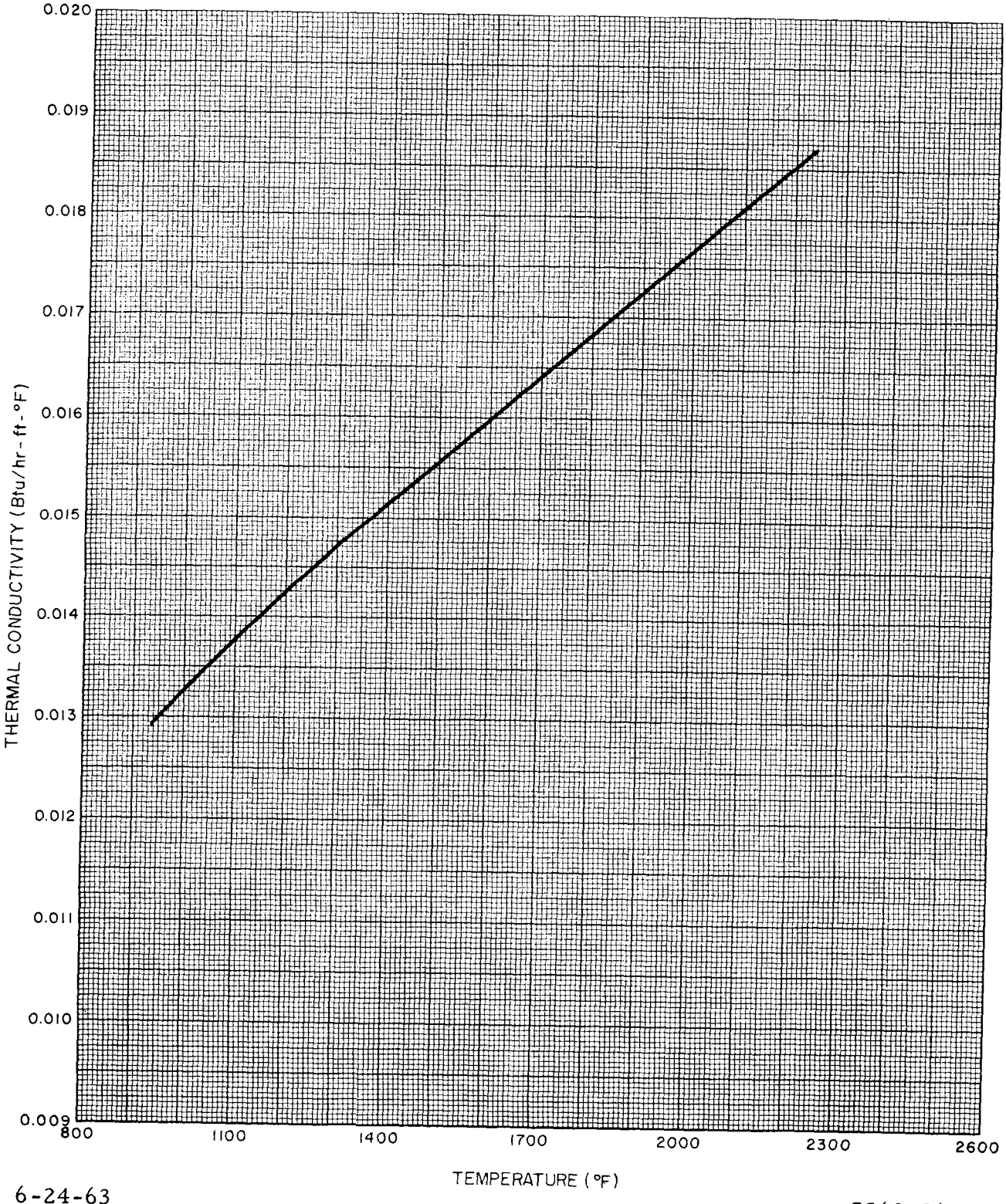

Figure 1.15 Thermal Conductivity of Saturated Sodium Vapor (Reference 2)

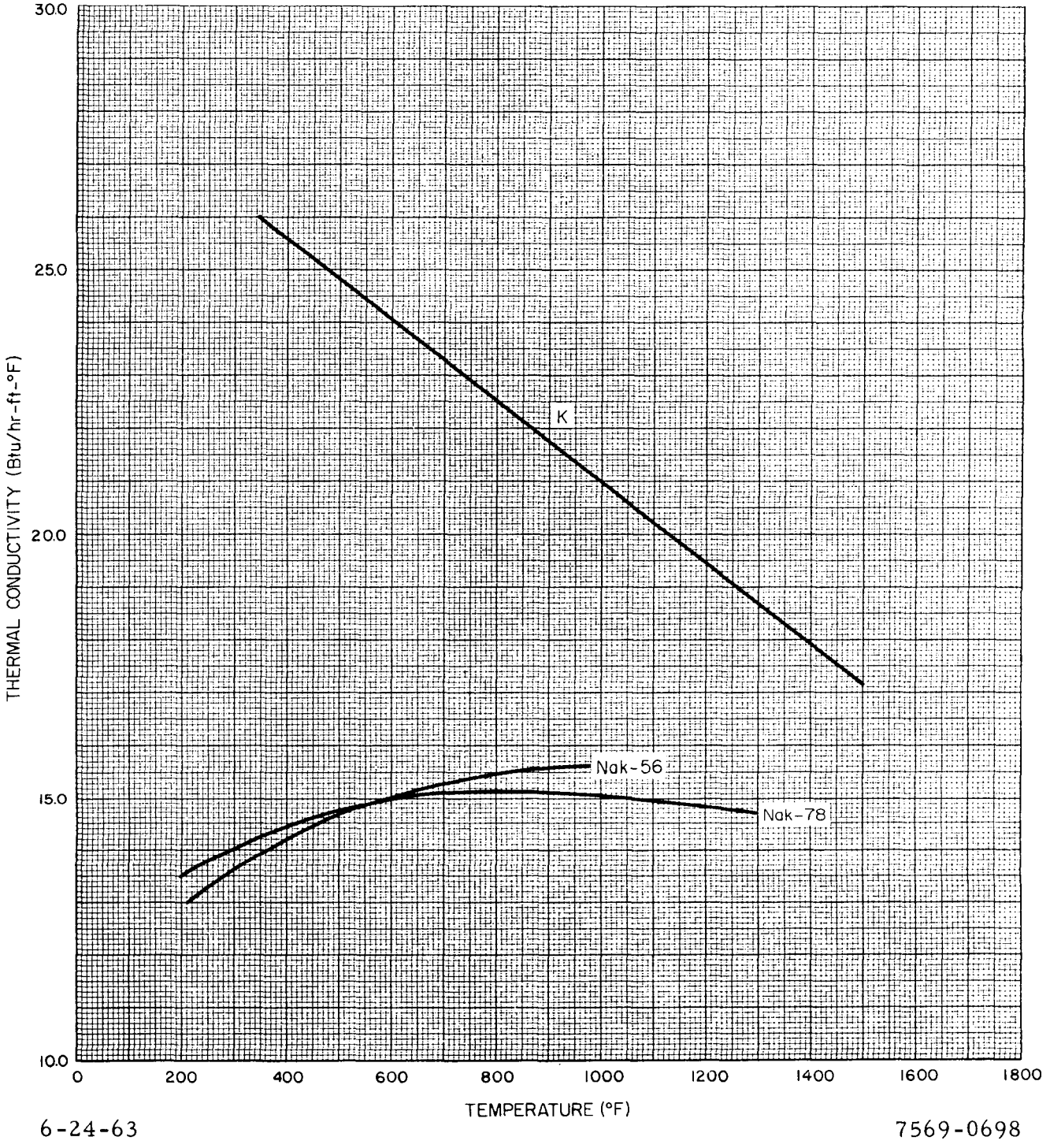

Figure 1.16 Thermal Conductivity of Potassium and NaK
(Reference 2 and 10)

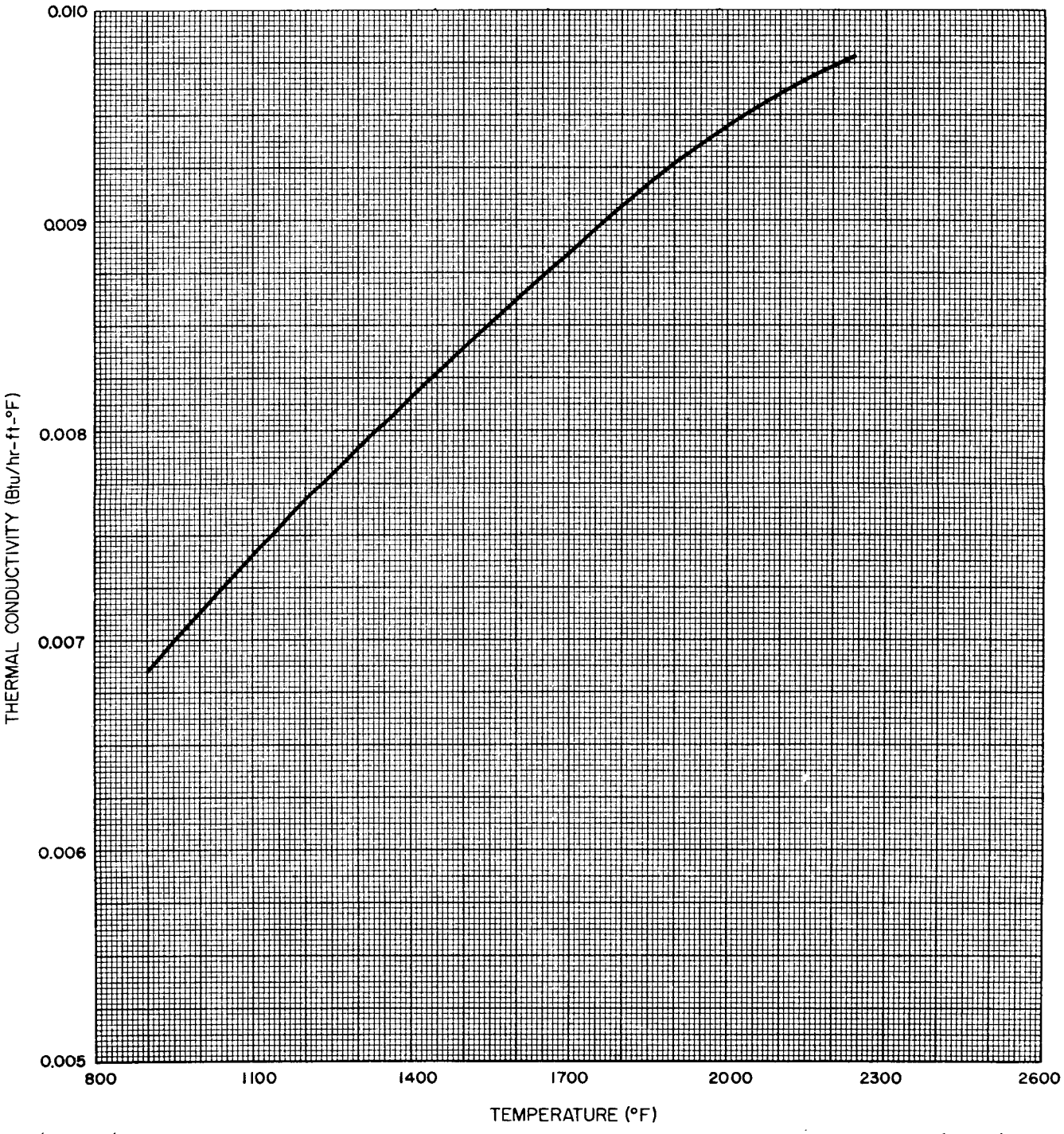

6-24-63 7569-0699

Figure 1.17 Thermal Conductivity of Saturated Potassium Vapor (Reference 2)

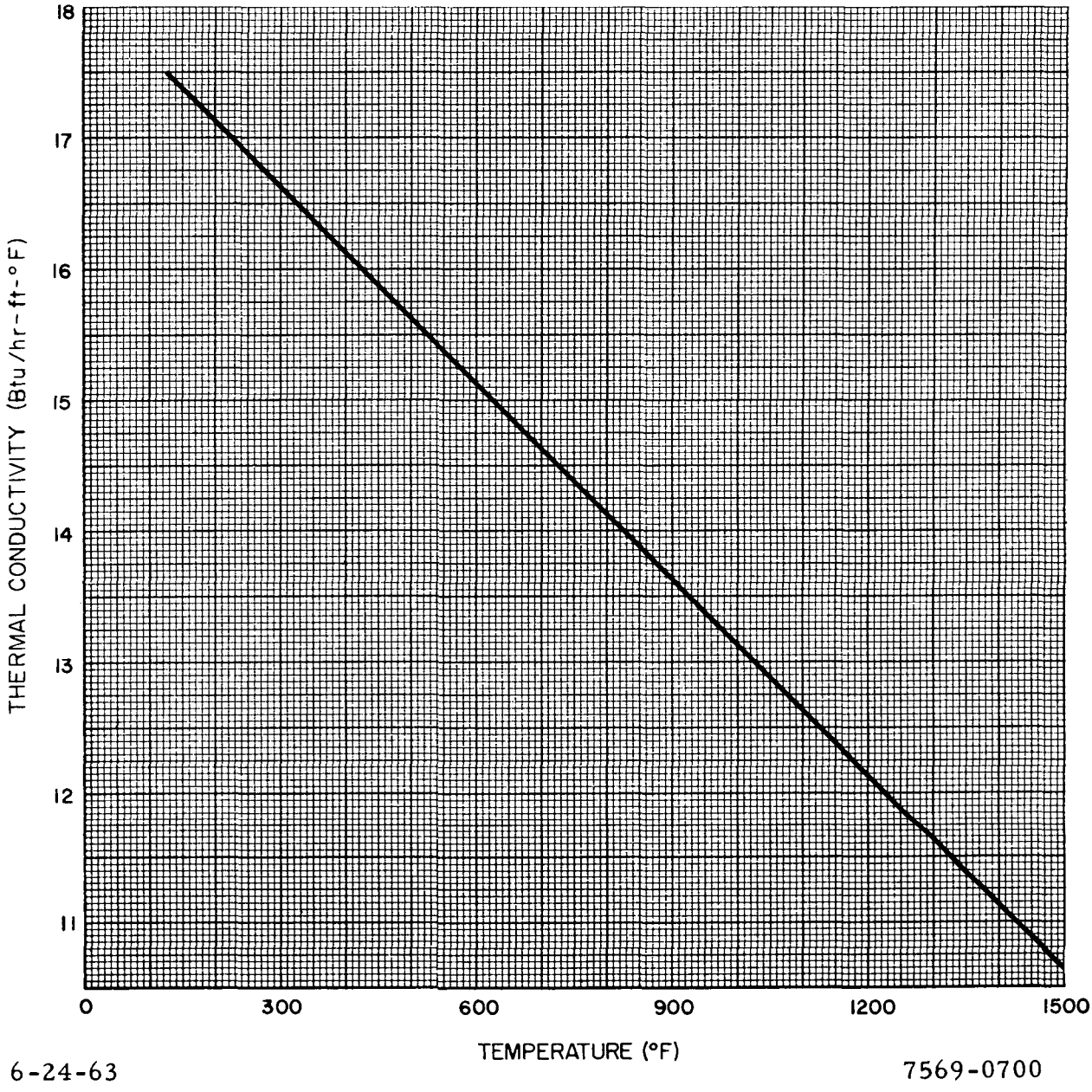

Figure 1.18 Thermal Conductivity of Liquid Rubidium
(Reference 2 and 11)

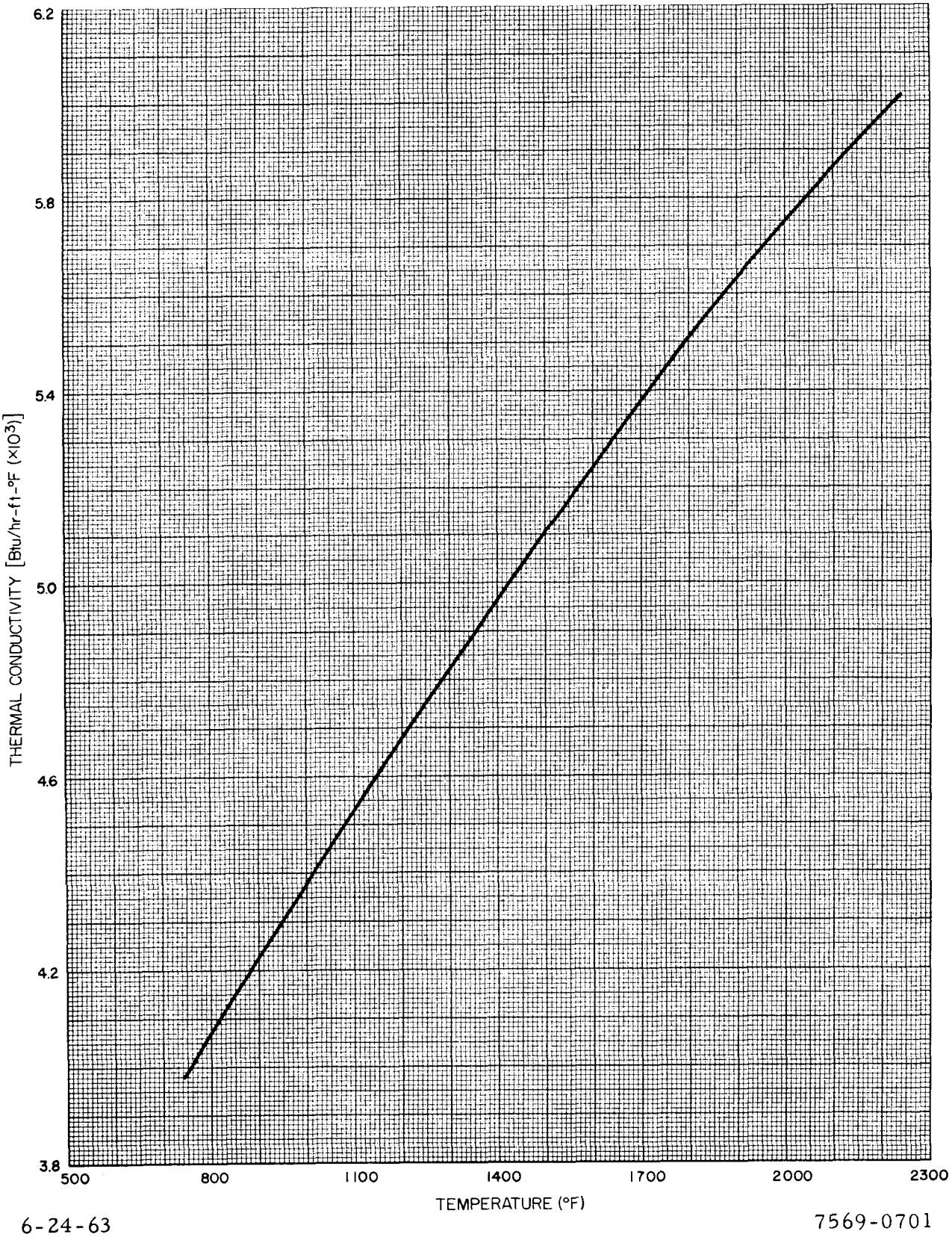

Figure 1.19 Thermal Conductivity of Saturated Rubidium Vapor (Reference 2)

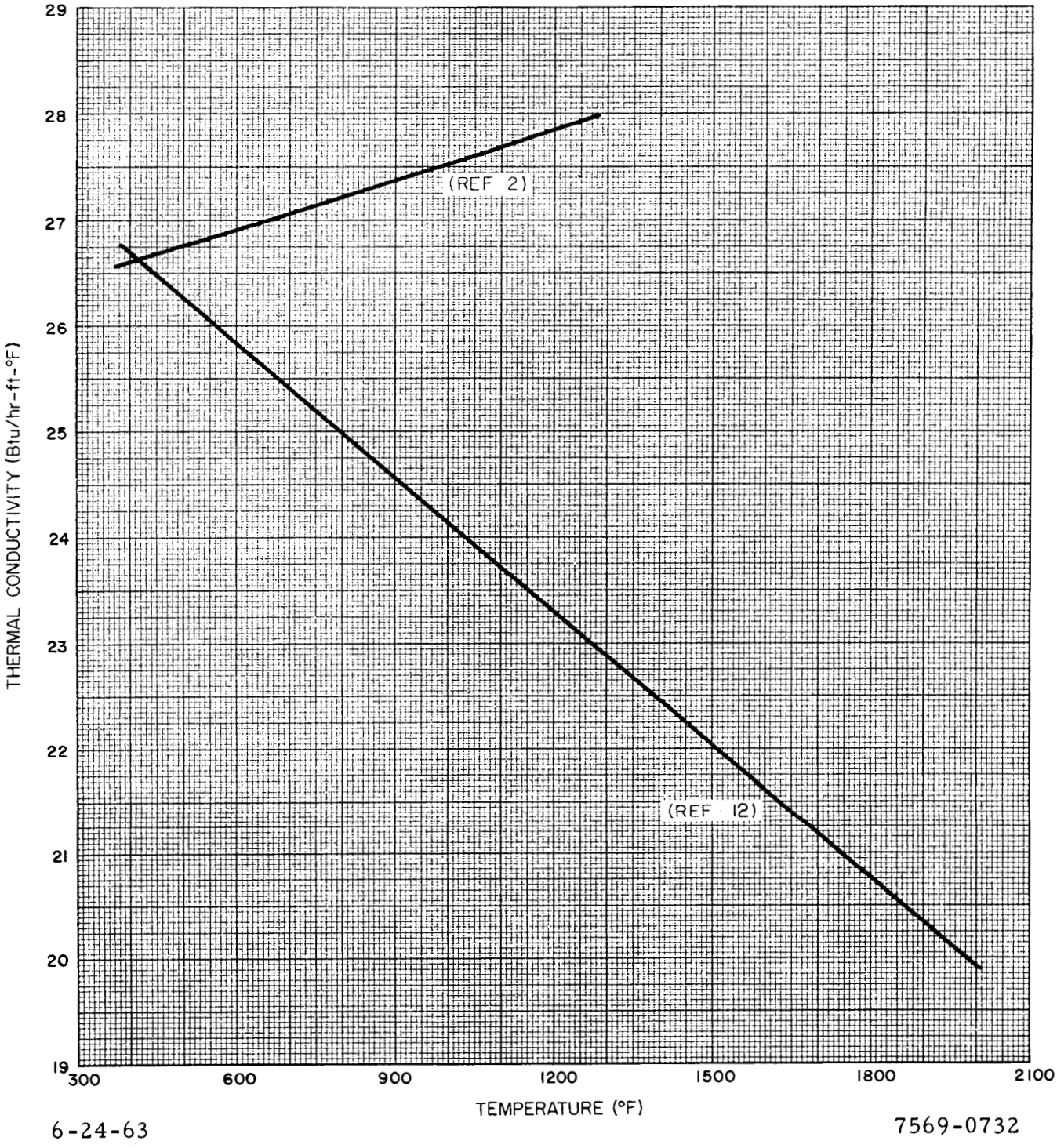

Figure 1.20 Thermal Conductivity of Liquid Lithium
(Reference 2 and 12)

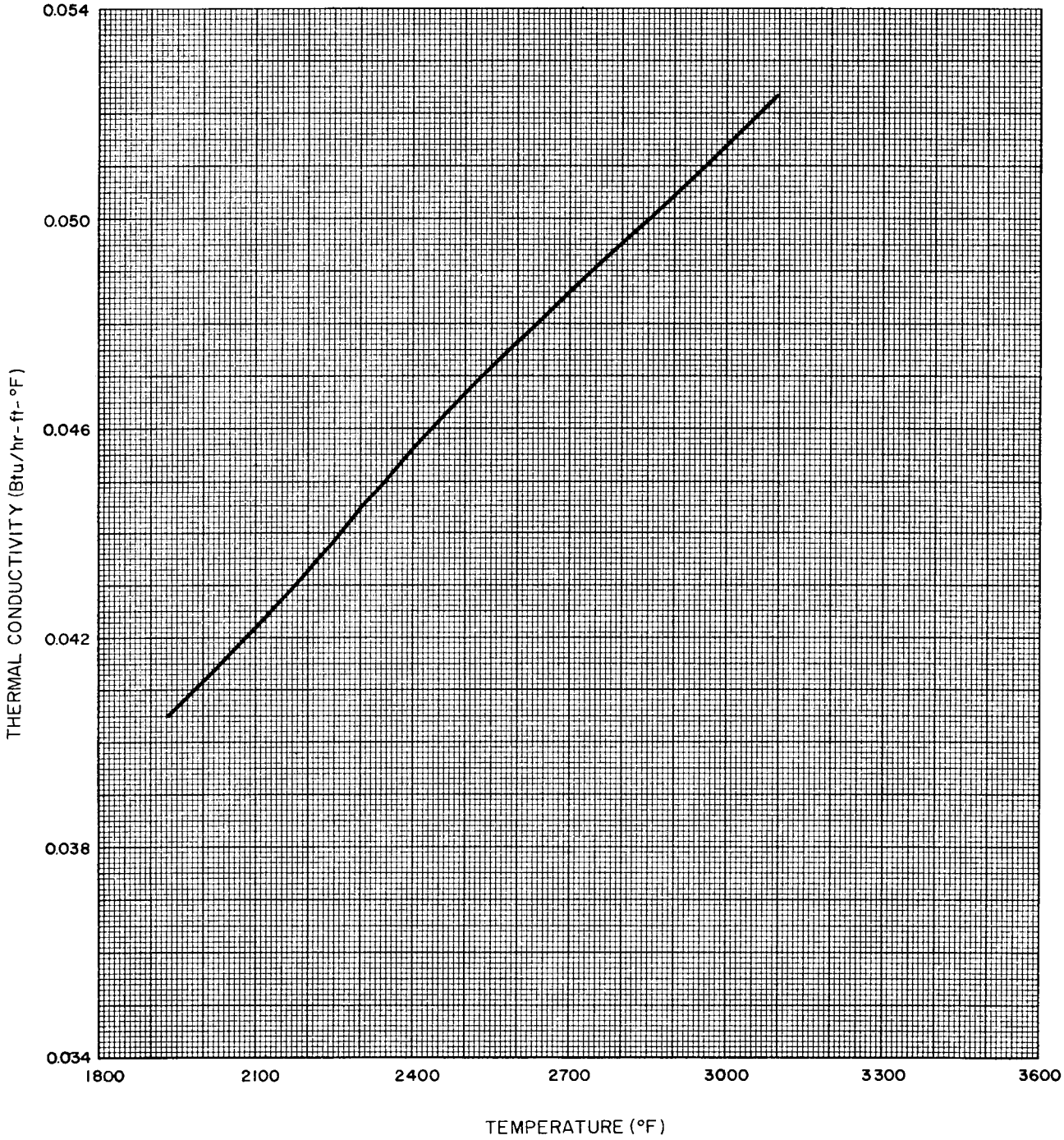

Figure 1.21 Thermal Conductivity of Saturated Lithium Vapor (Reference 2)

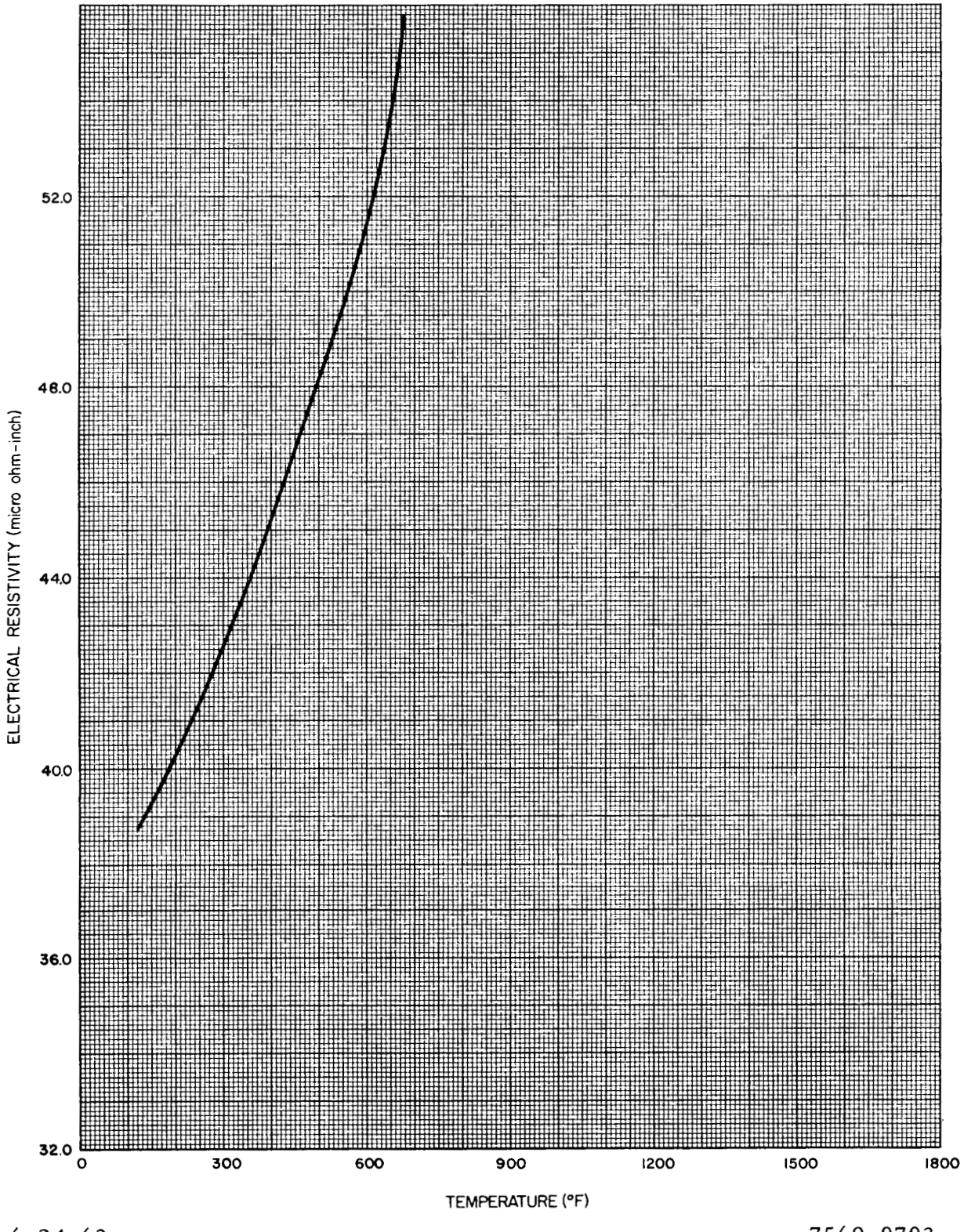

6-24-63 7569-0703

Figure 1.22 Electrical Resistivity of Liquid Mercury (Reference 2)

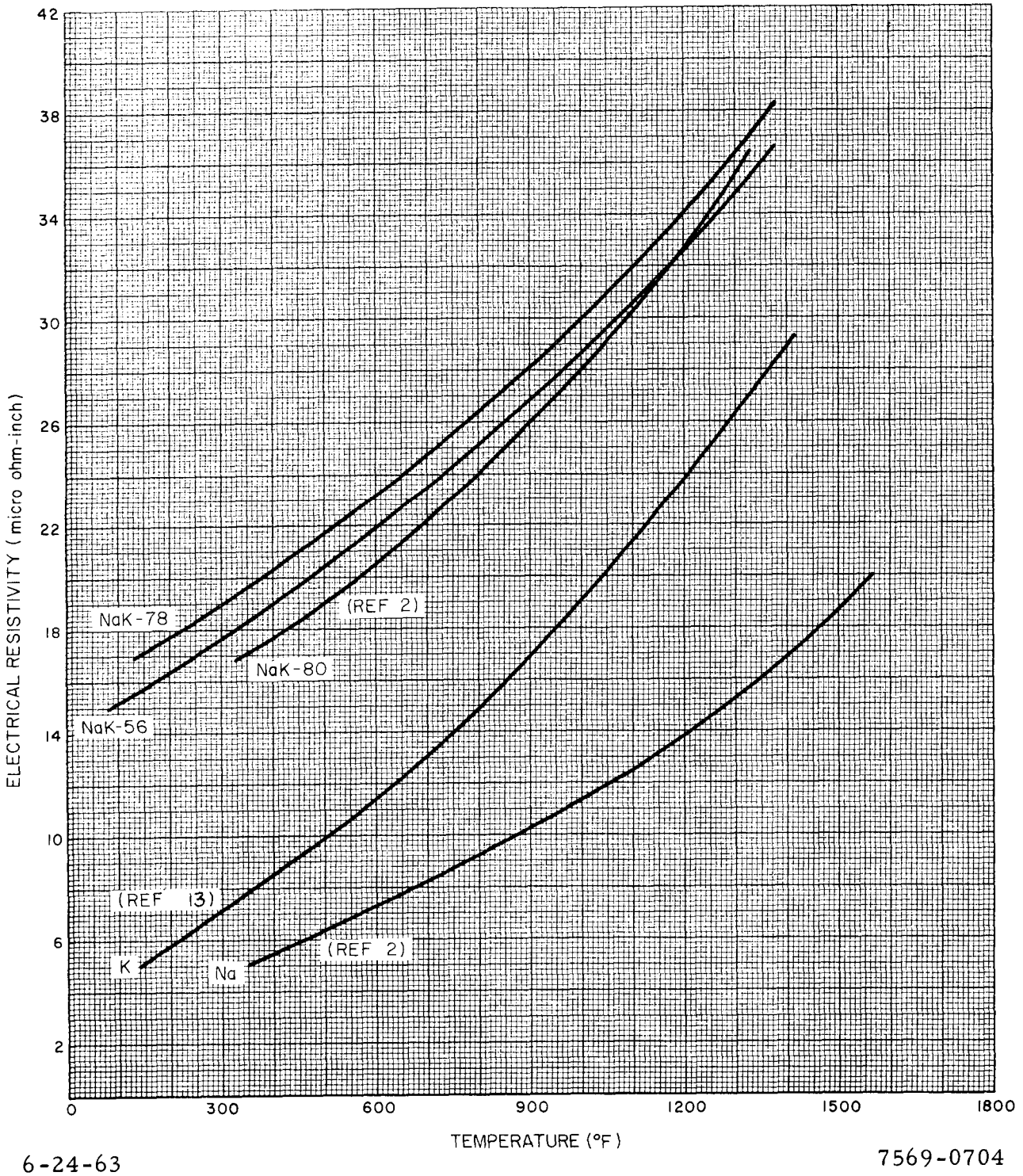

Figure 1.23 Electrical Resistivity of Sodium, Potassium, and NaK (Reference 2, 10, and 13)

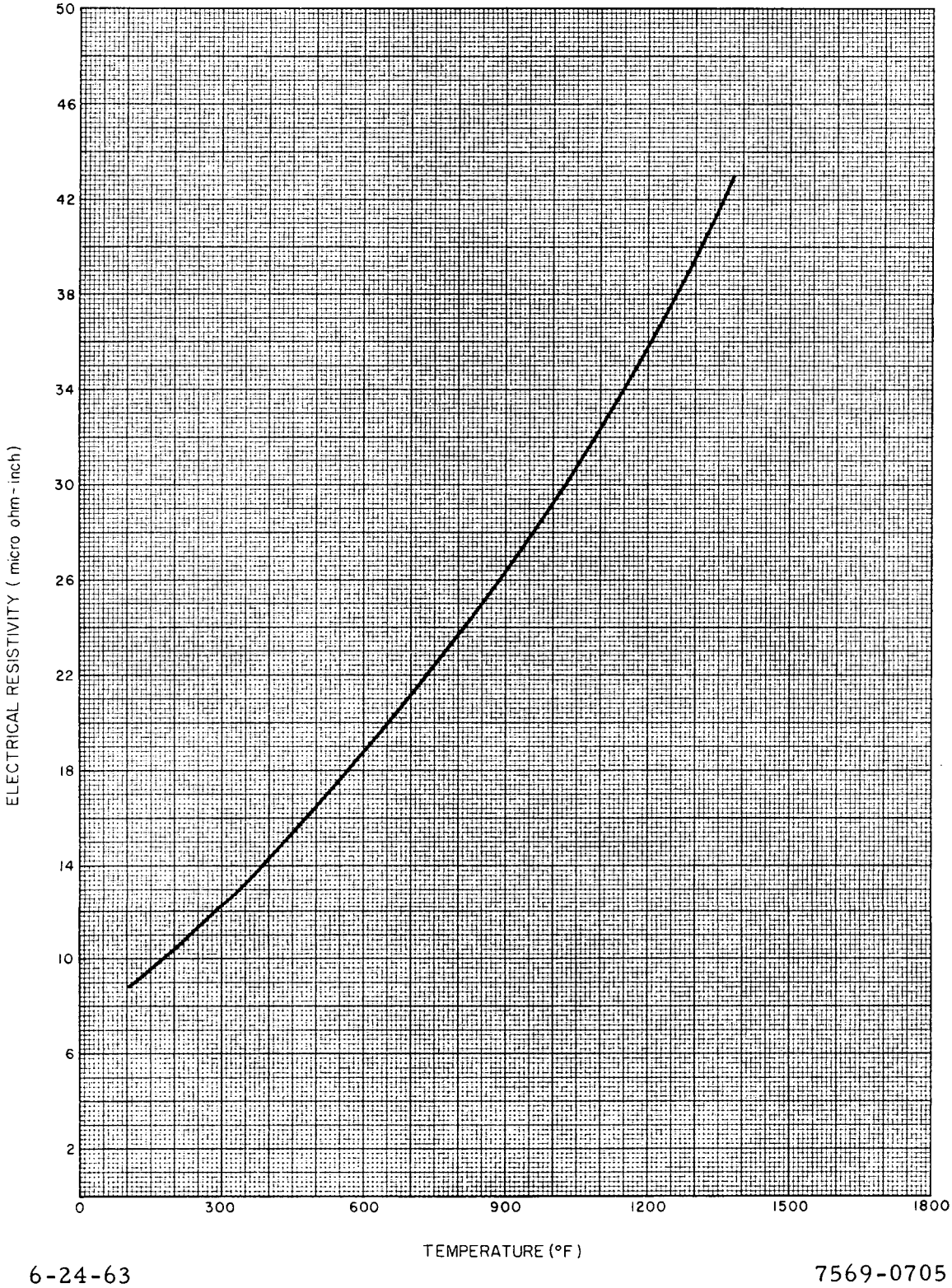

Figure 1.24 Electrical Resistivity of Liquid Rubidium
(Reference 13)

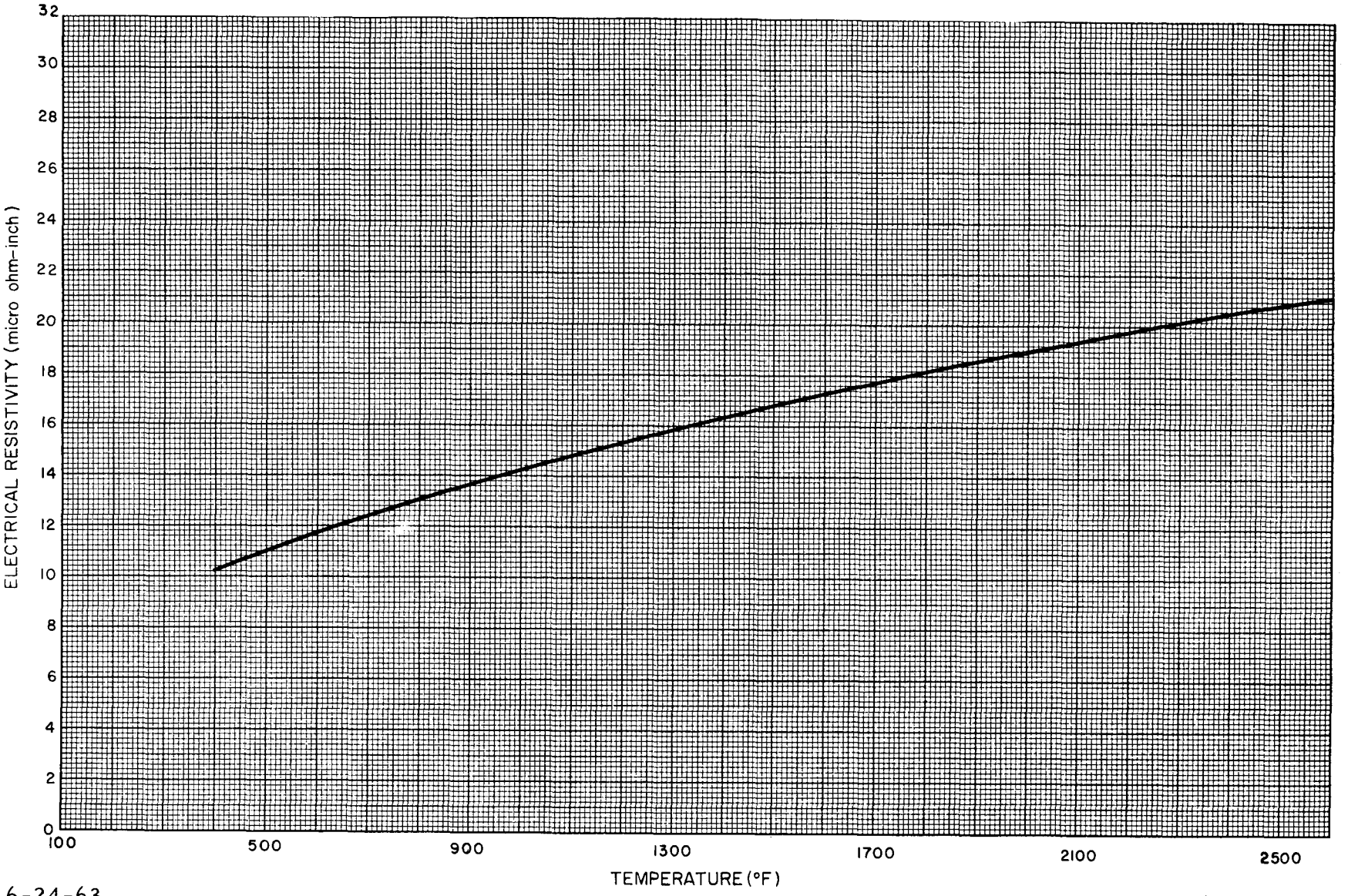

Figure 1.25 Electrical Resistivity of Lithium (Liquid)
(Reference 14)

1.2.4 Specific Heat[2, 15, 16, 17]

All of the available data on the specific heat of liquid metals are shown graphically in Figures 1.26 to 1.34. The specific heat of saturated NaK vapor was omitted due to the lack of data on this alloy.

1.2.5 Surface Tension[2, 18, 19]

Figures 1.35 to 1.40 graphically represent the surface tension properties of the selected liquid metals.

1.2.6 Vapor Pressure[2]

Figure 1.41 compares the vapor pressure properties of the selected liquid metals.

1.2.7 Absolute Viscosity[2, 10, 12]

Viscosity properties of the selected liquid metals are shown in Figures 1.42 to 1.50 with the exception of NaK in its saturated vapor state. Little interest has been shown by researchers in the saturated NaK vapor properties.

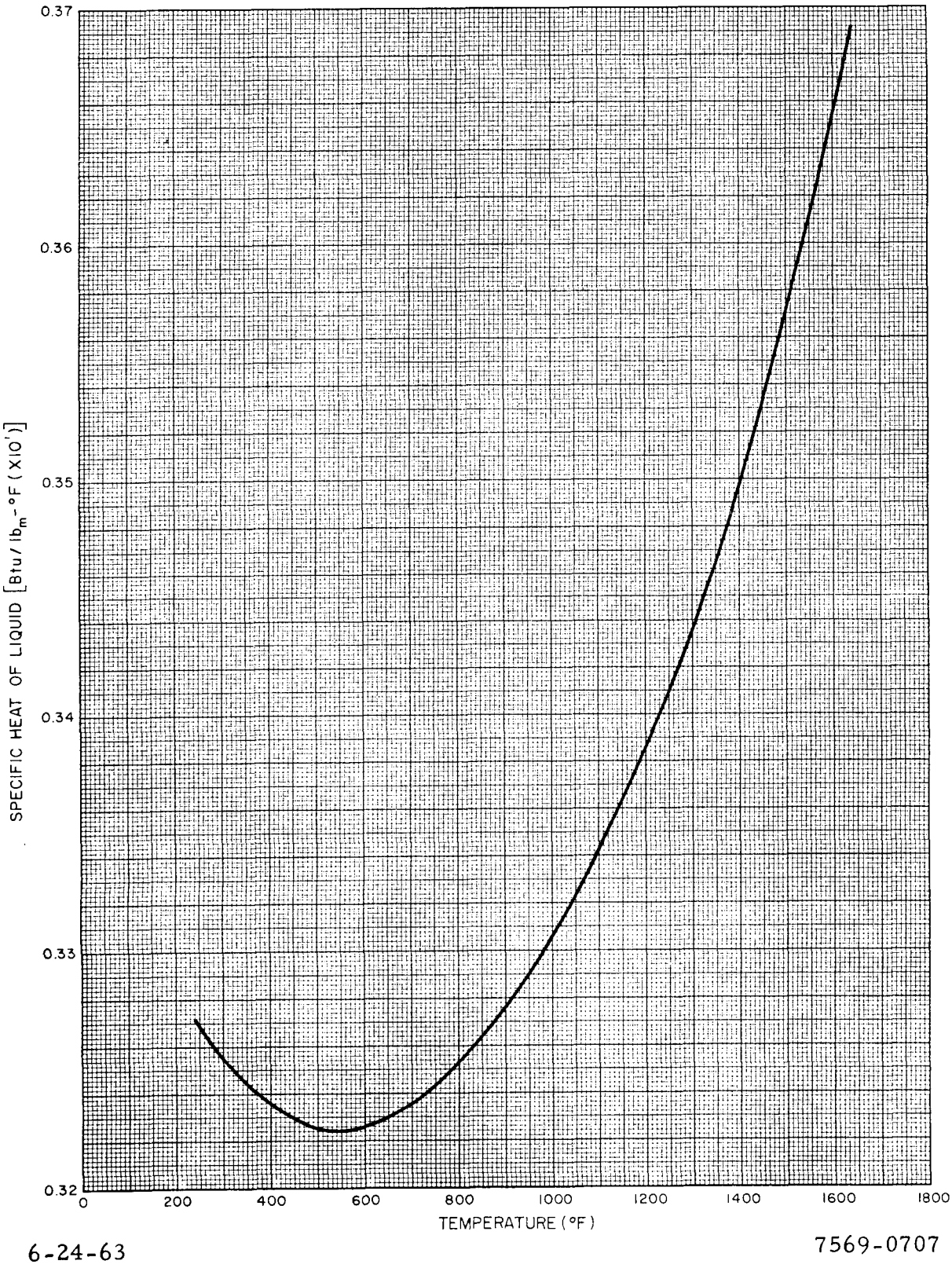

Figure 1.26 Specific Heat of Liquid Mercury
(Reference 2)

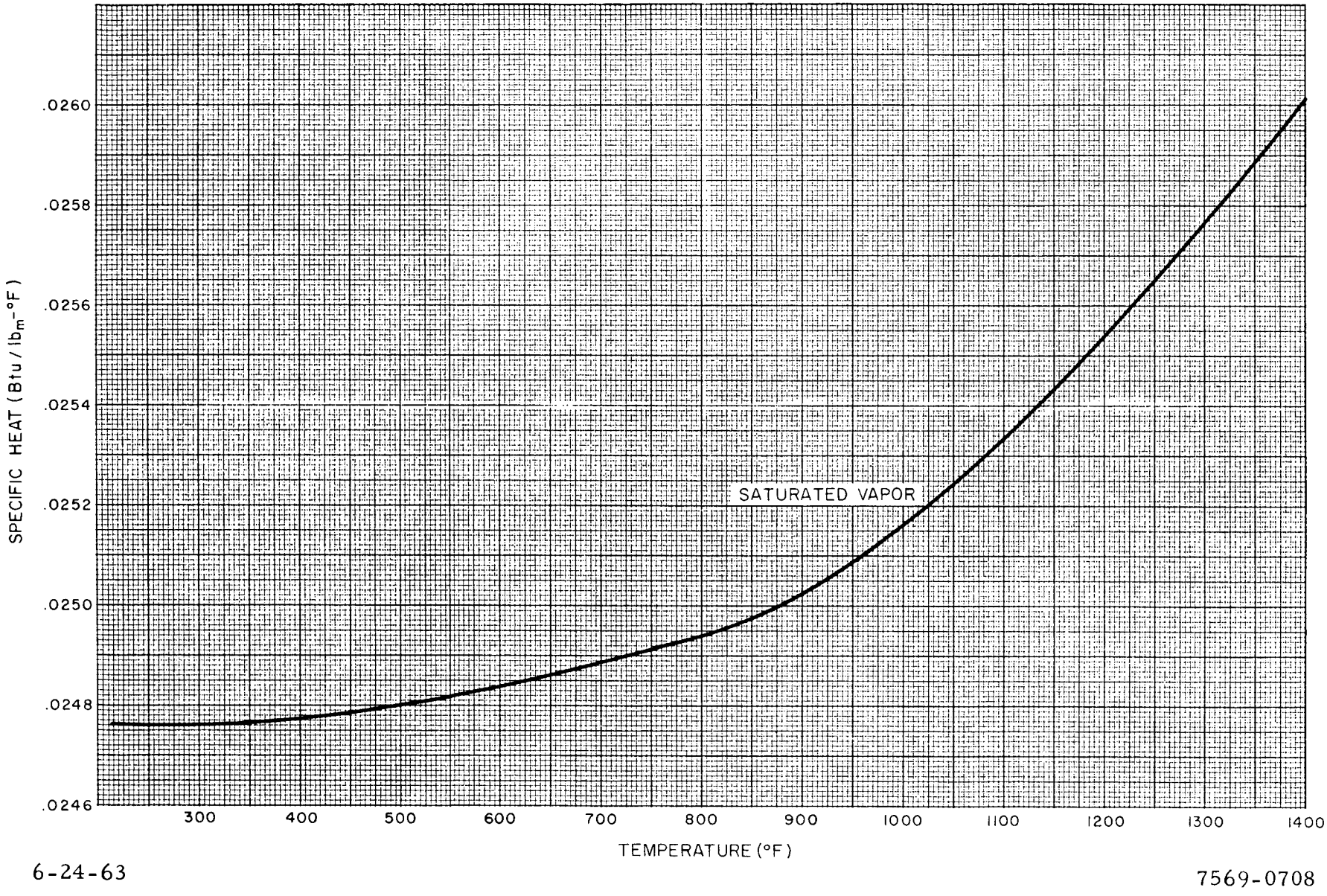

Figure 1.27 Specific Heat of Mercury Vapor
(Reference 15)

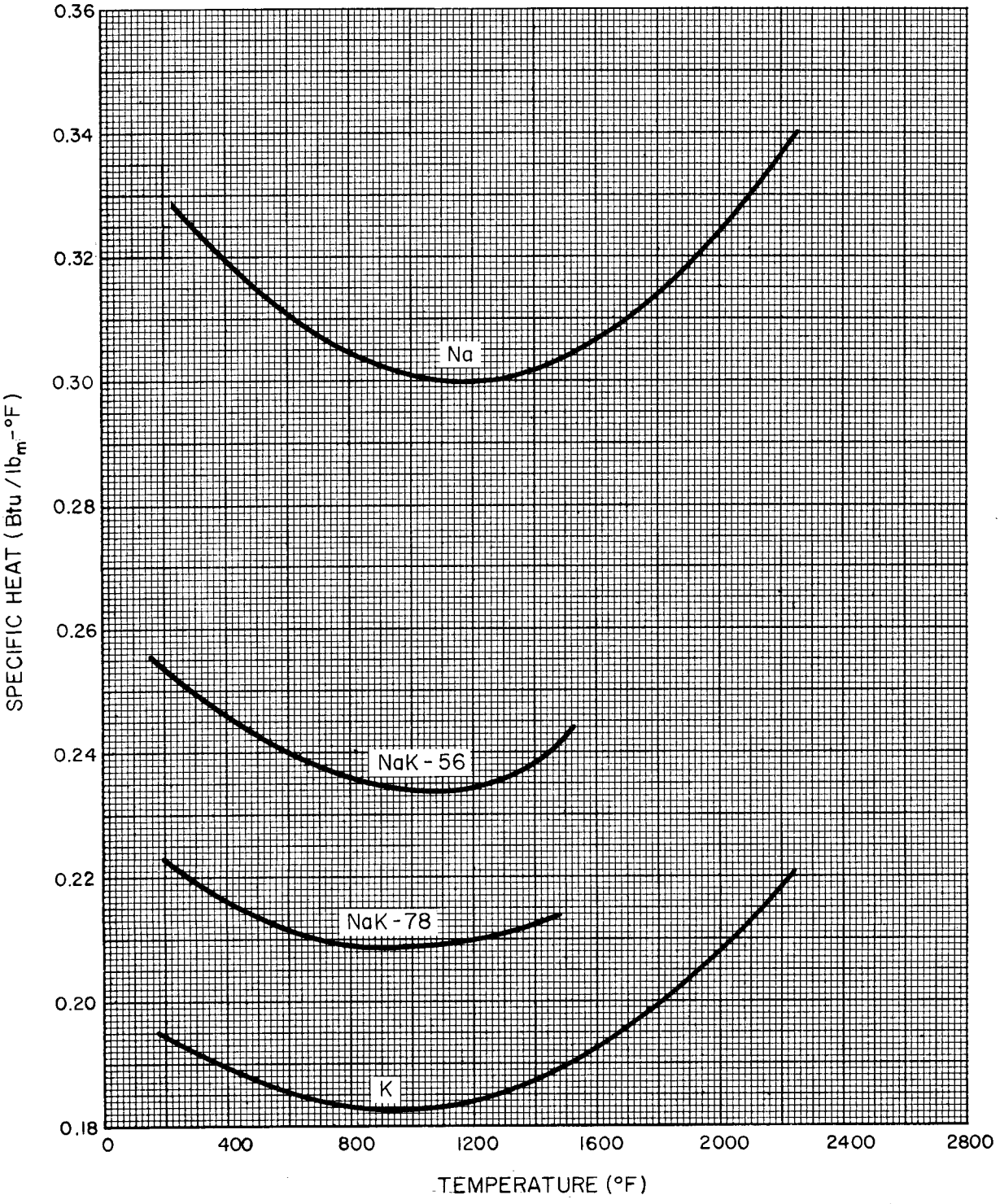

Figure 1.28 Specific Heat of Sodium, Potassium, and NaK (liquid) (Reference 2 and 10)

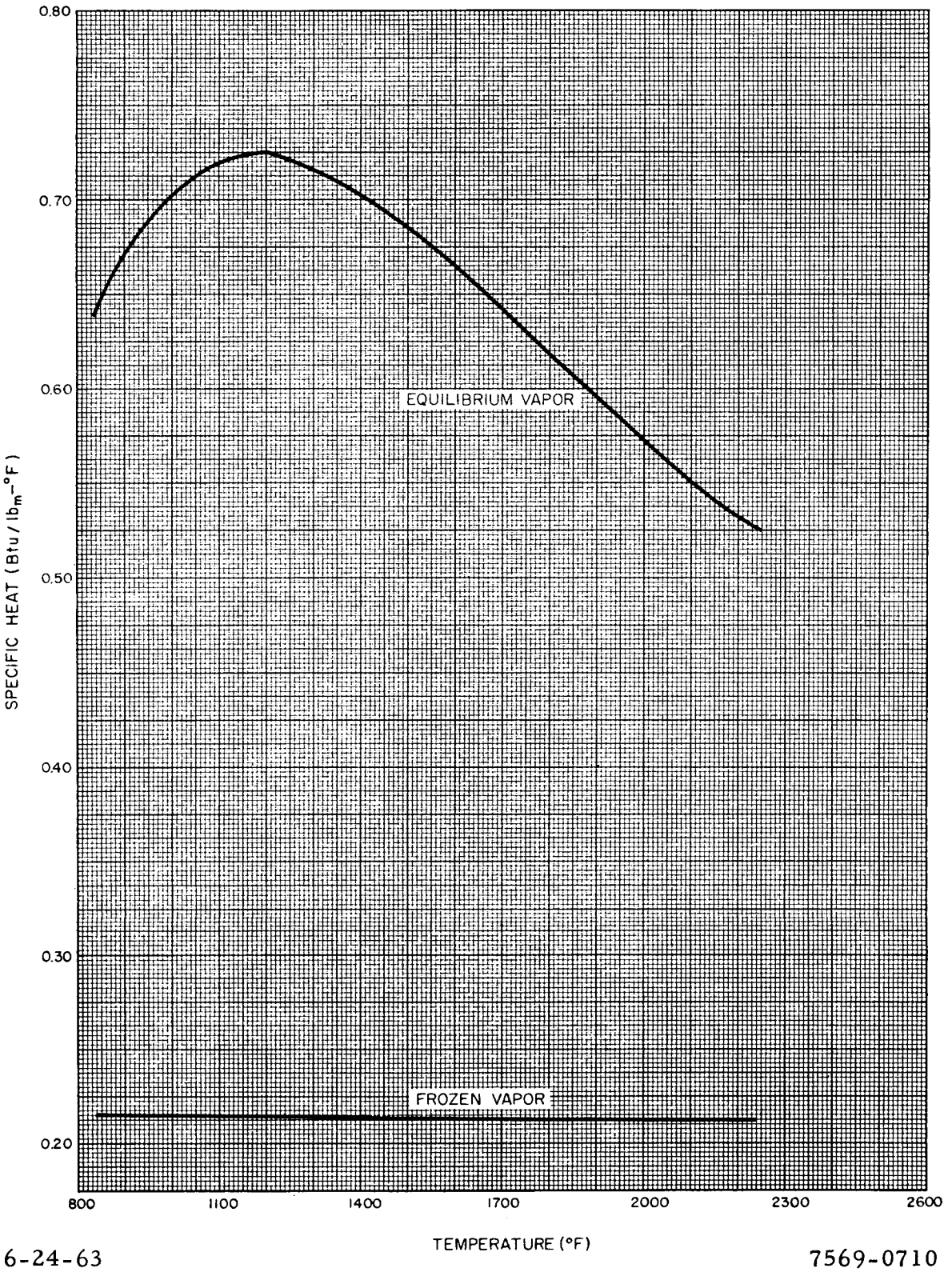

Figure 1.29 Specific Heat of Saturated Sodium Vapor (Reference 2)

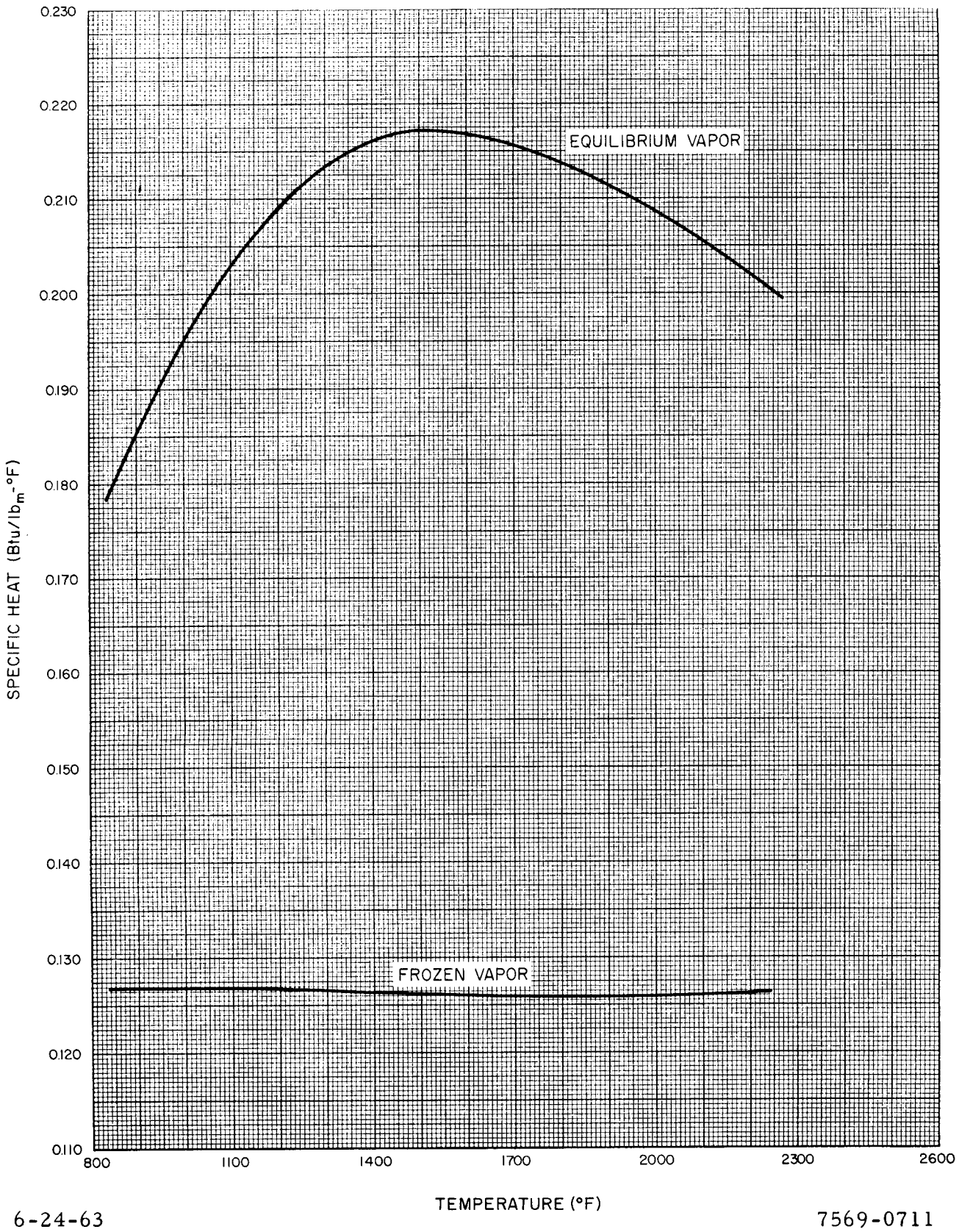

Figure 1.30 Specific Heat of Saturated Potassium Vapor (Reference 2)

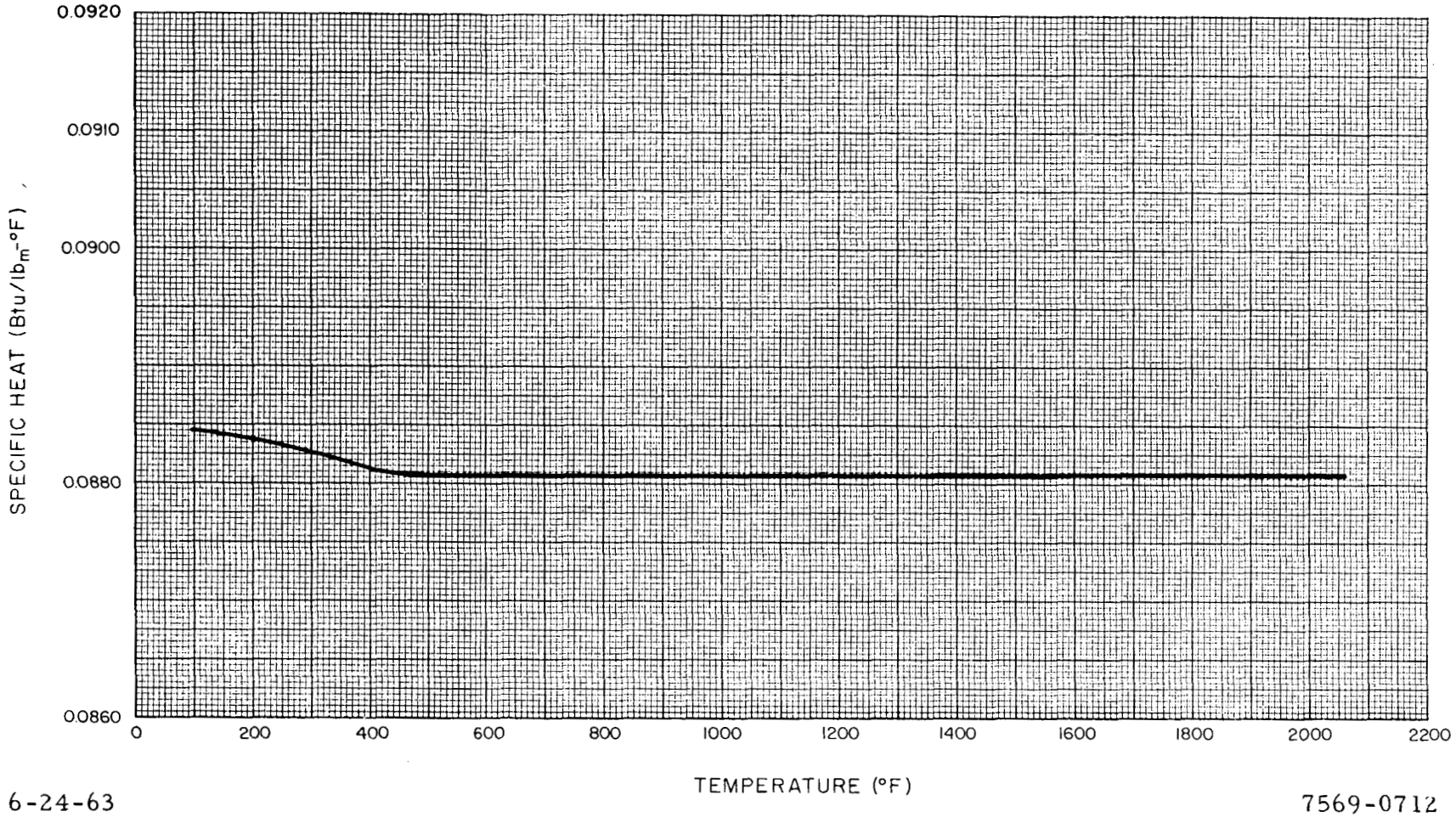

Figure 1.31 Specific Heat of Liquid Rubidium
(Reference 16)

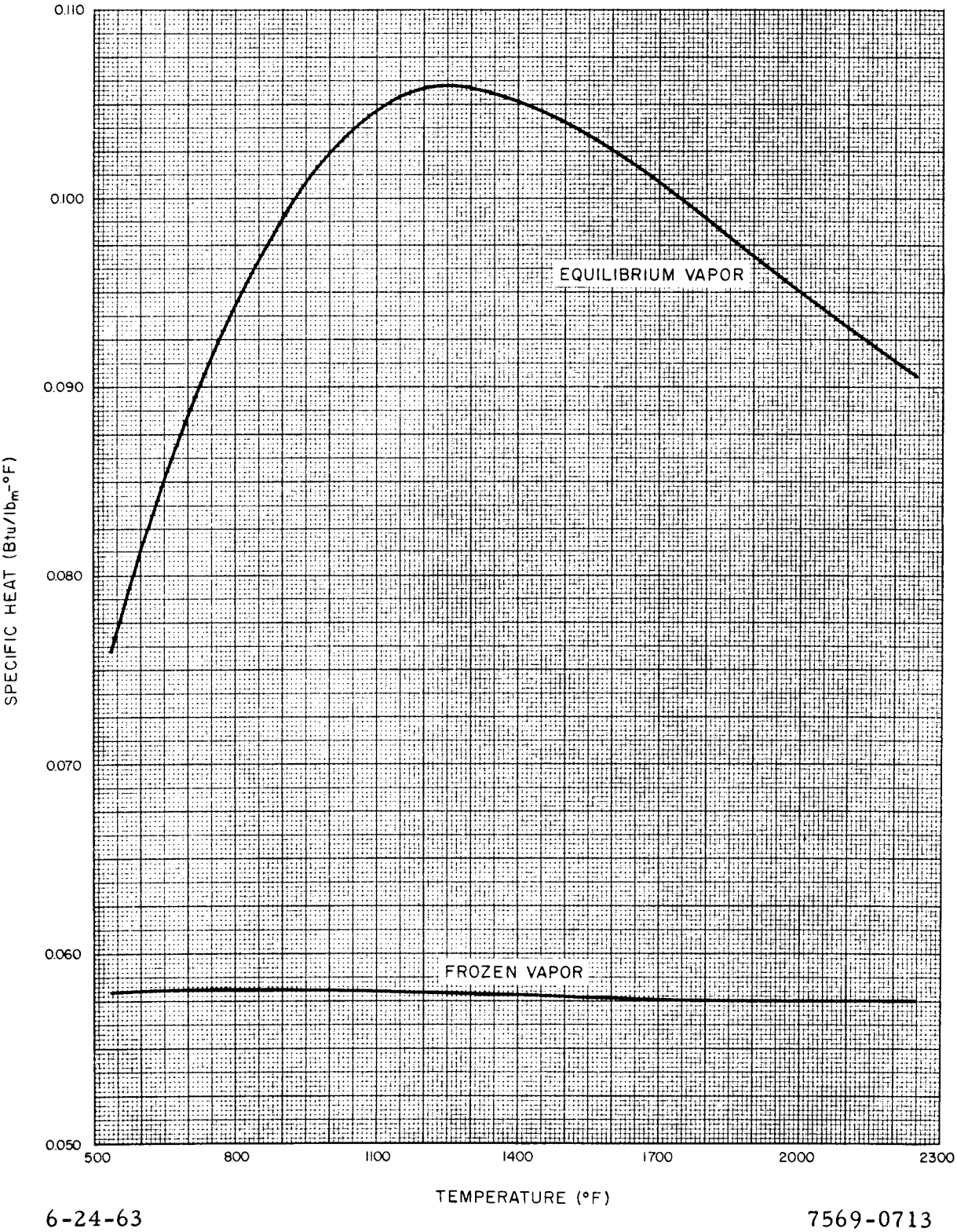

Figure 1.32 Specific Heat of Saturated Rubidium Vapor (Reference 2)

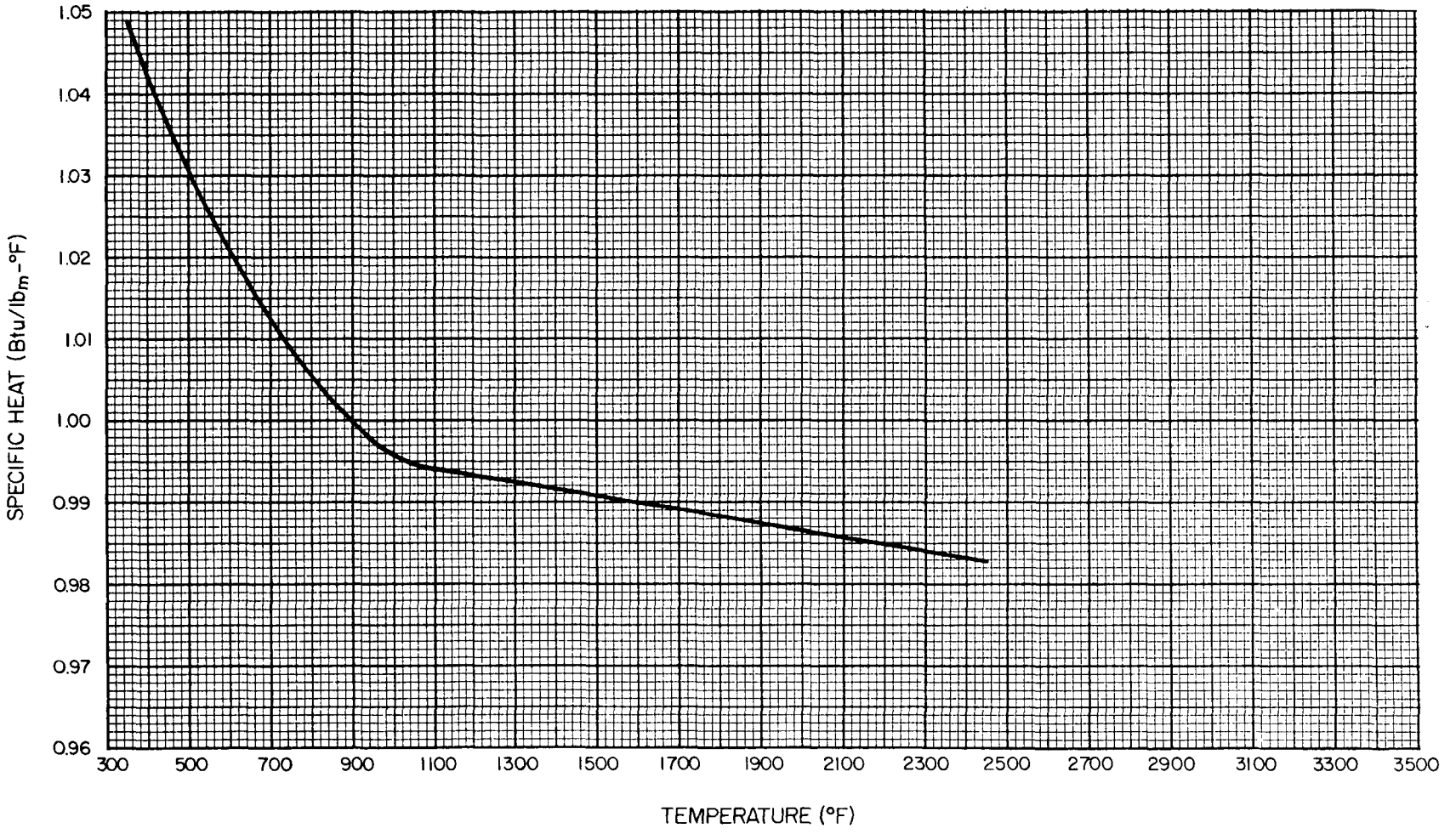

6-24-63

7569-0714

Figure 1.33 Specific Heat of Liquid Lithium
(Reference 17)

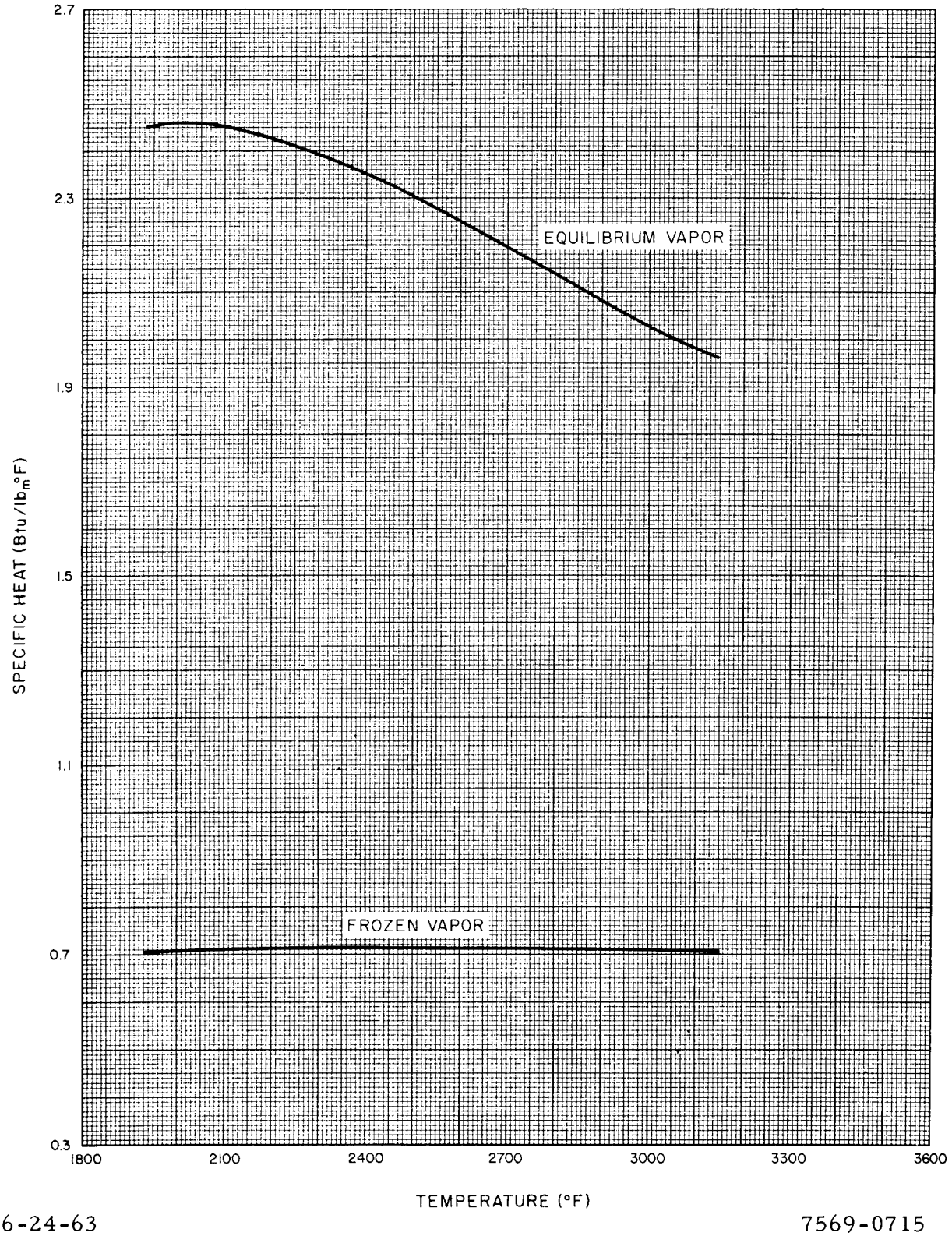

Figure 1.34 Specific Heat of Saturated Lithium Vapor (Reference 2)

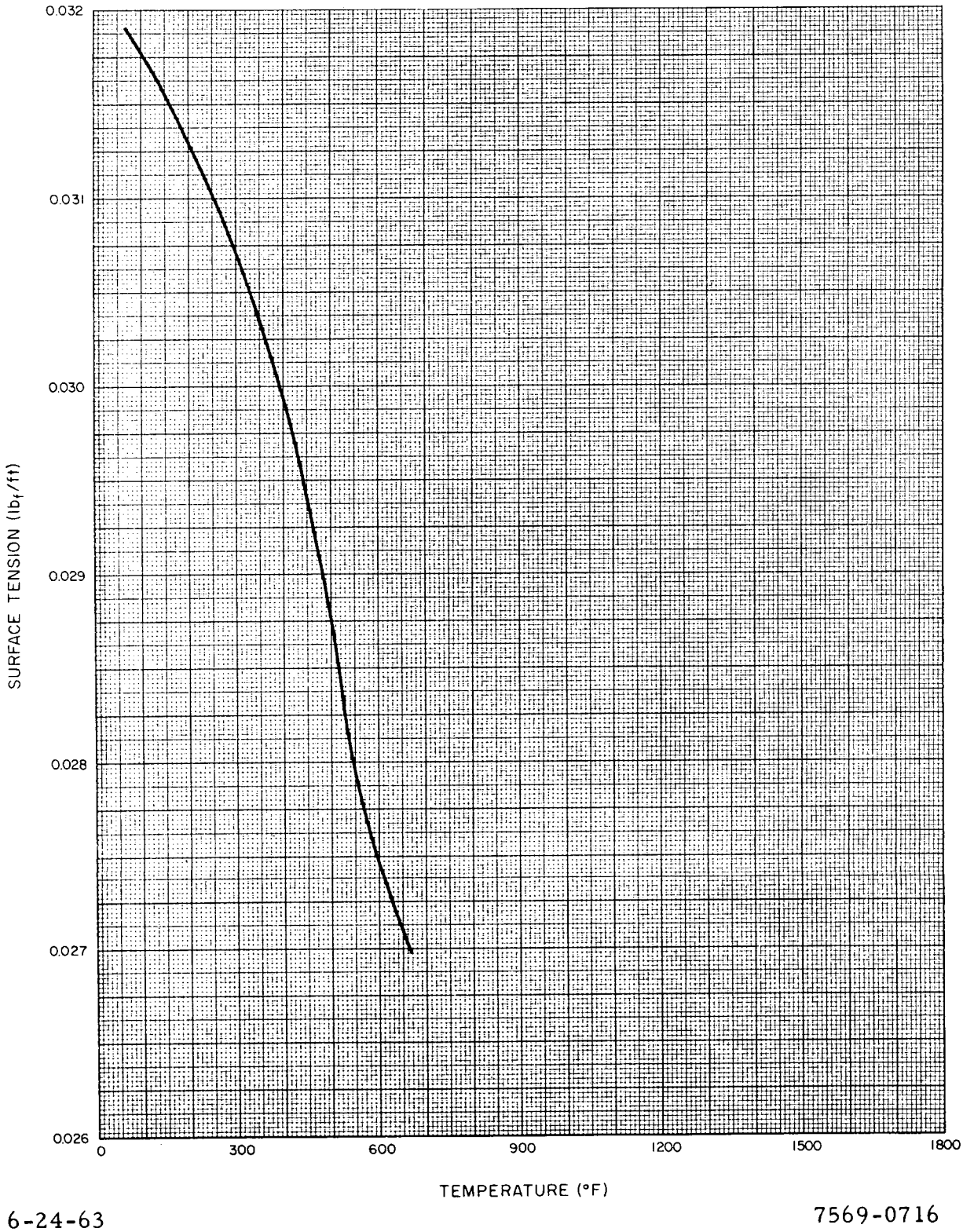

Figure 1.35 Surface Tension of Liquid Mercury
(Reference 2)

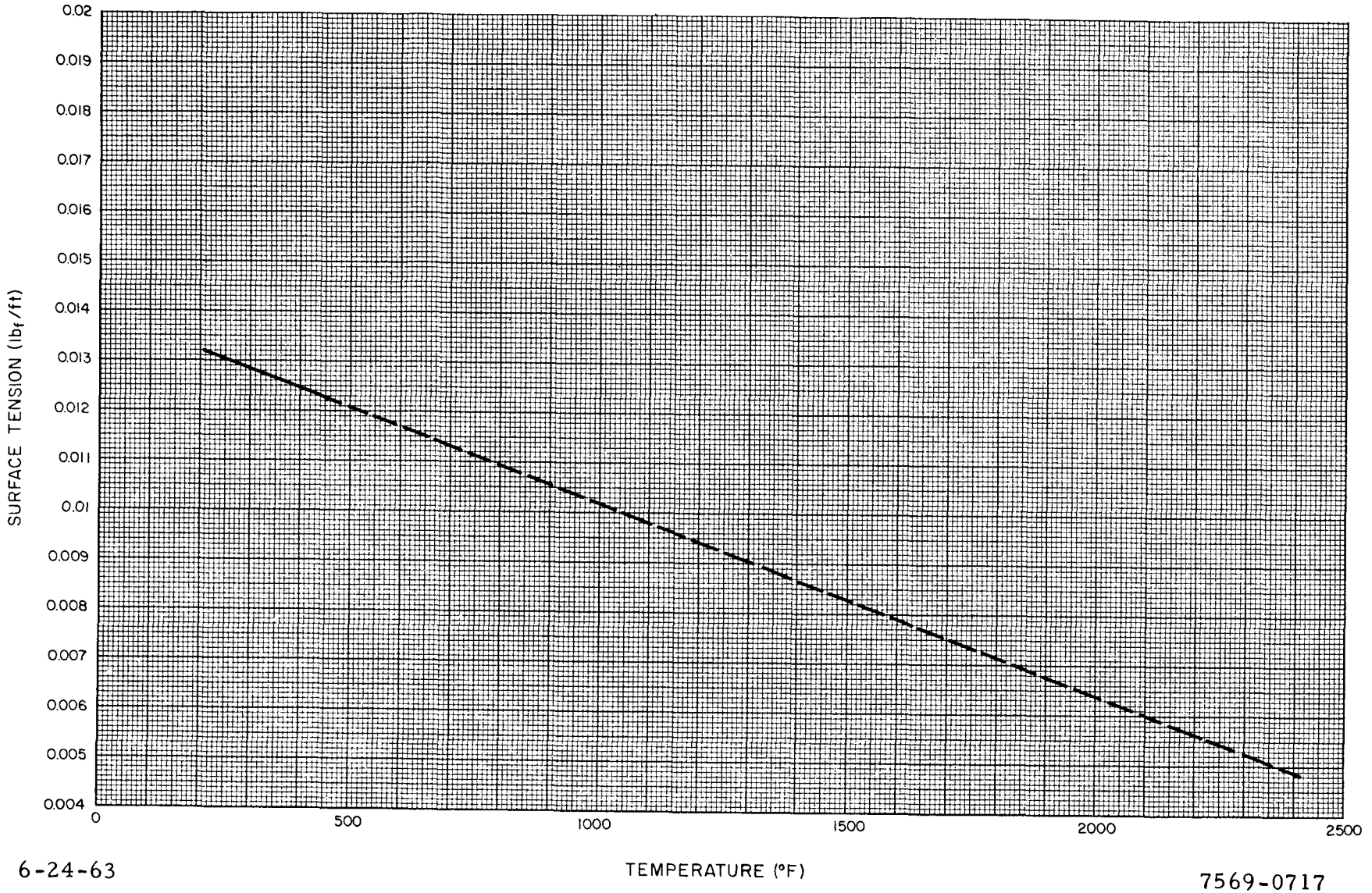

Figure 1.36 Surface Tension of Sodium (Liquid)
(Reference 19)

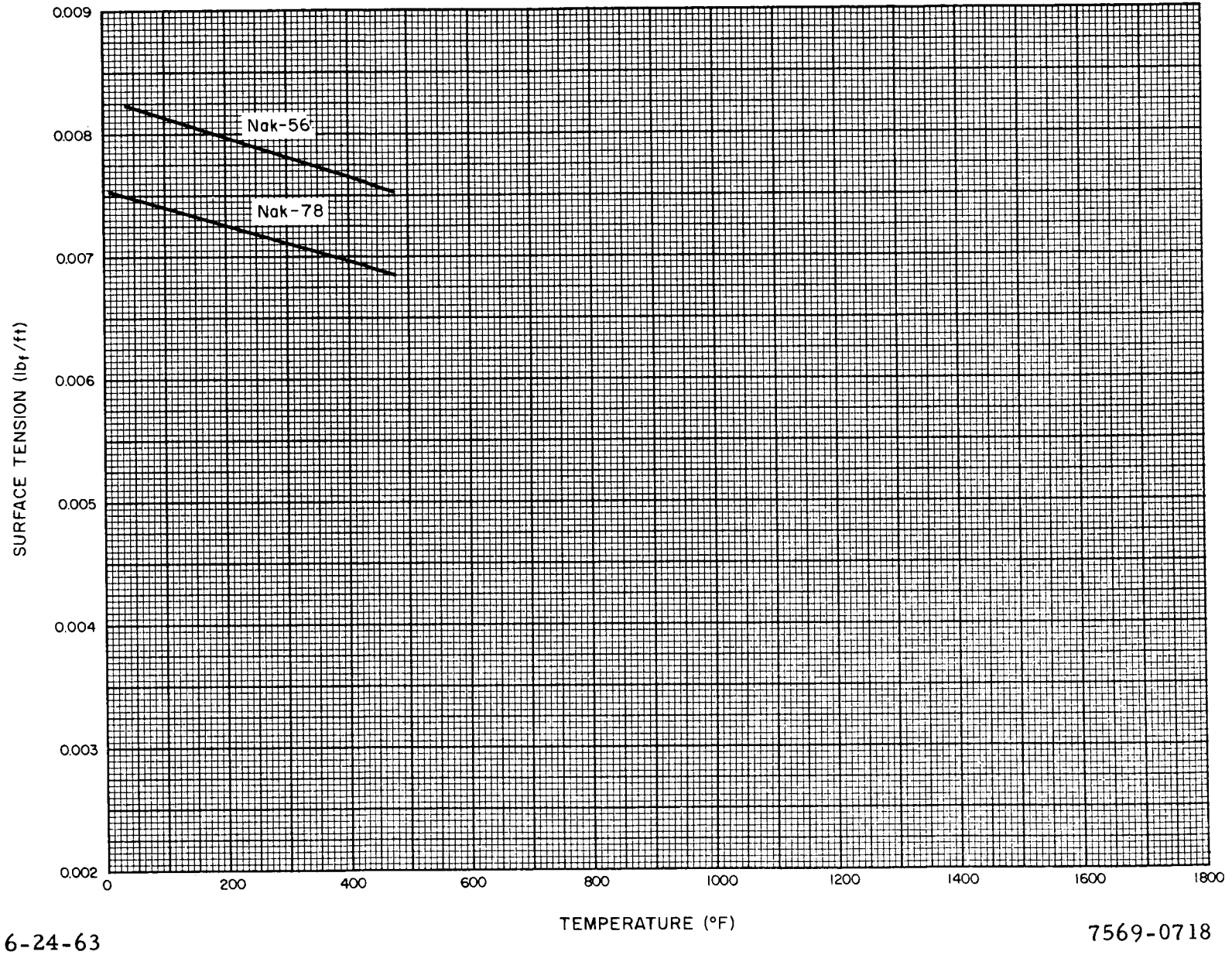

Figure 1.37 Surface Tension of Liquid NaK
(Reference 10)

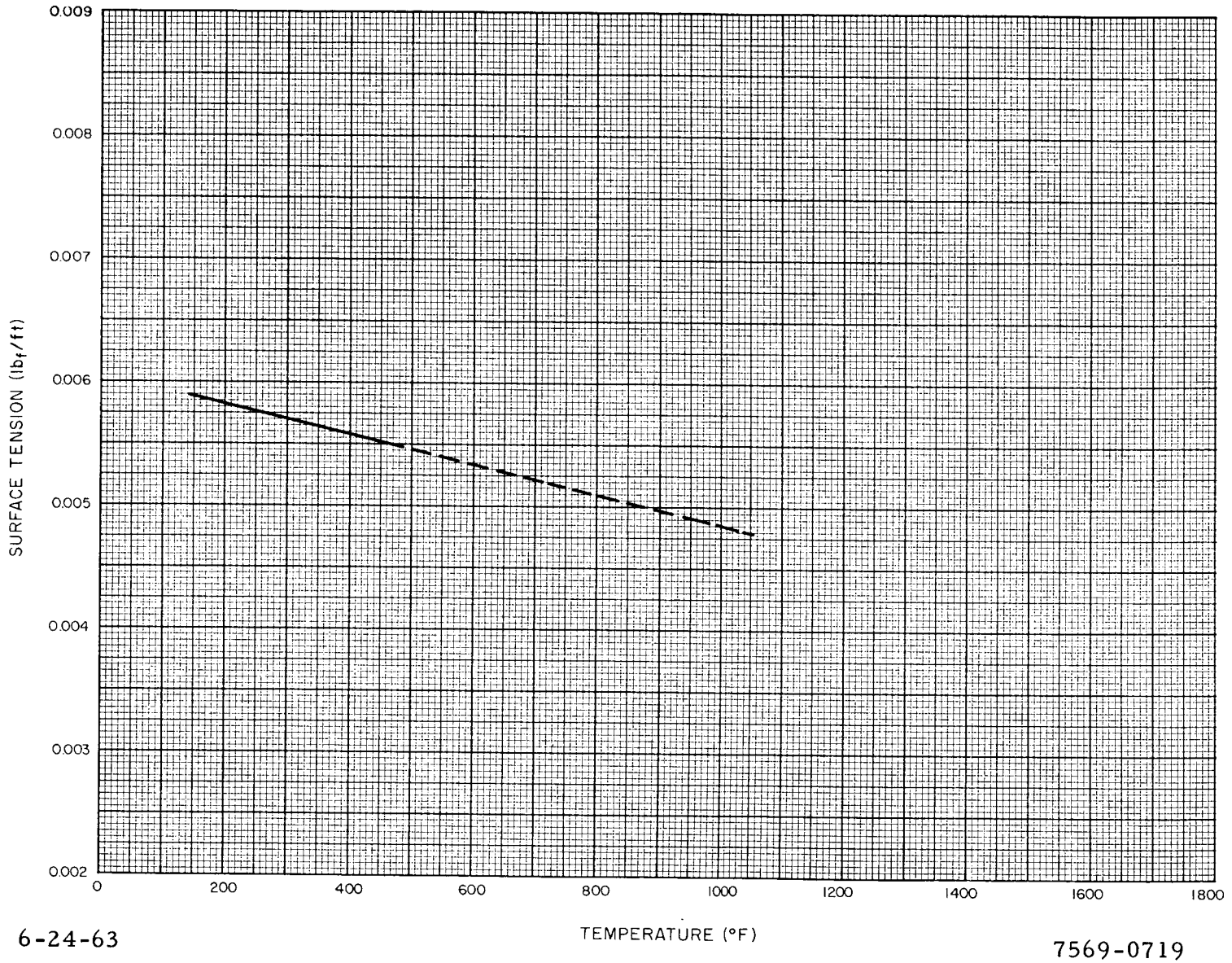

Figure 1.38. Surface Tension of Liquid Potassium
(Reference 3 and 7)

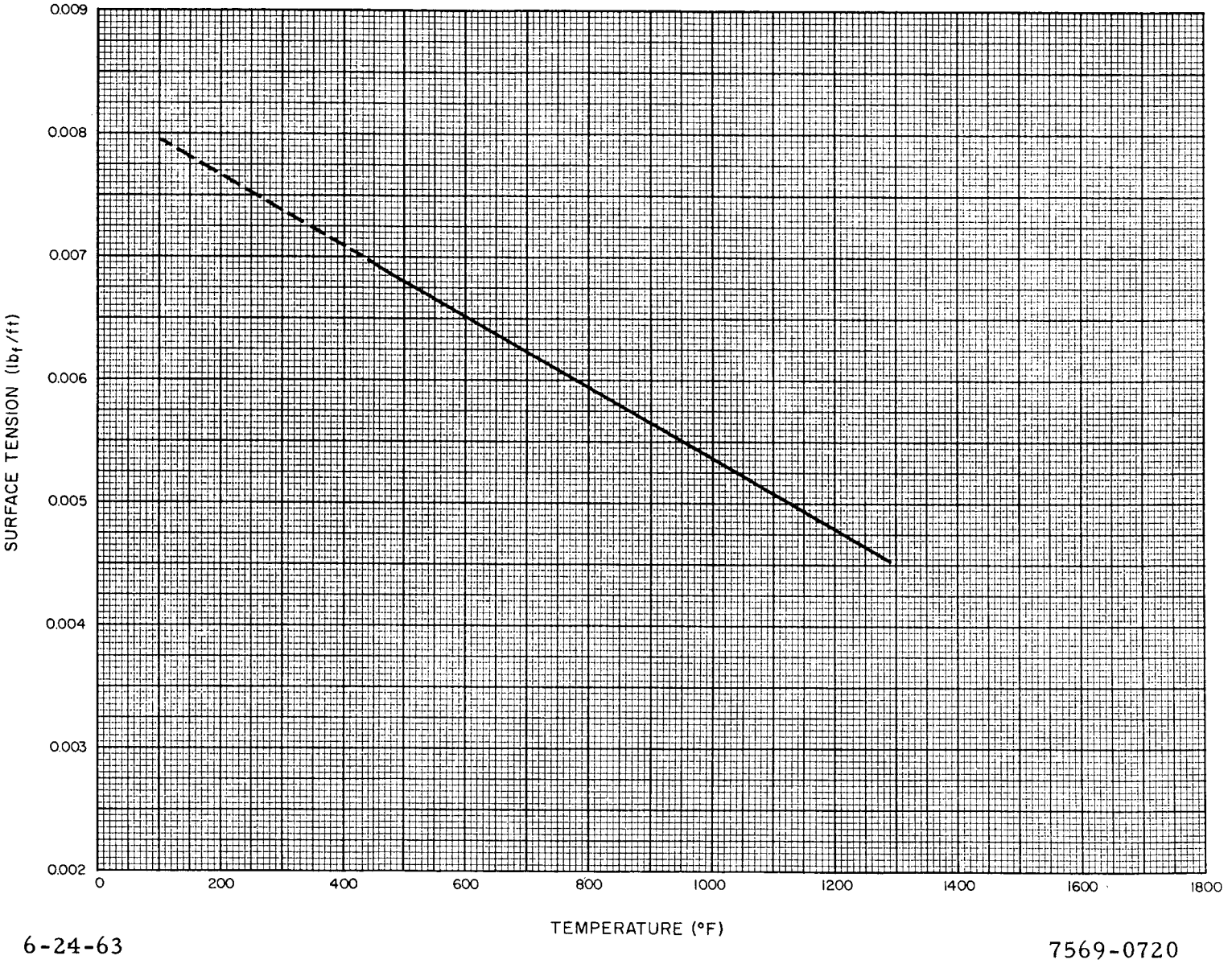

Figure 1.39 Surface Tension of Liquid Rubidium
(Reference 11)

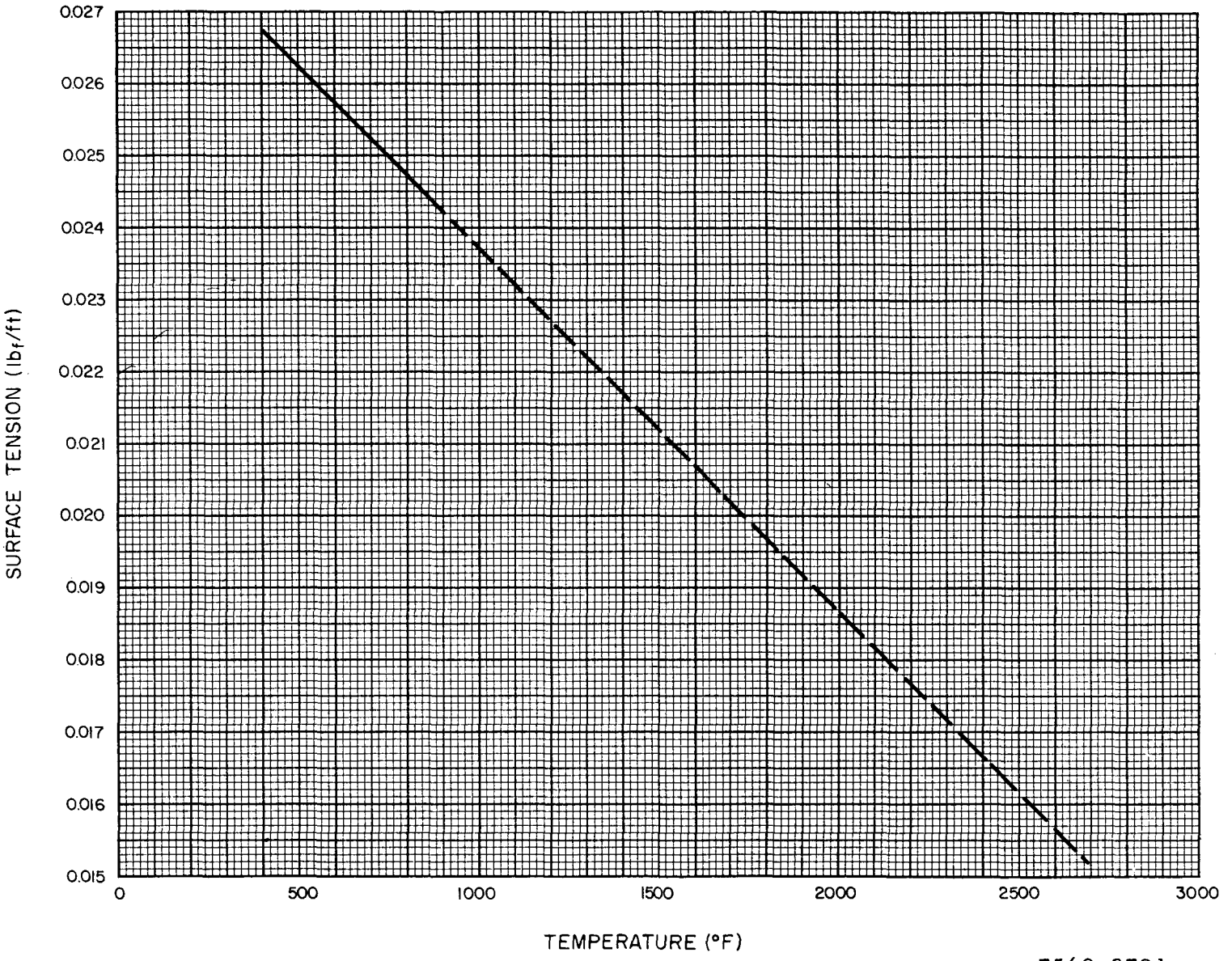

Figure 1.40 Surface Tension of Liquid Lithium
(Reference 14)

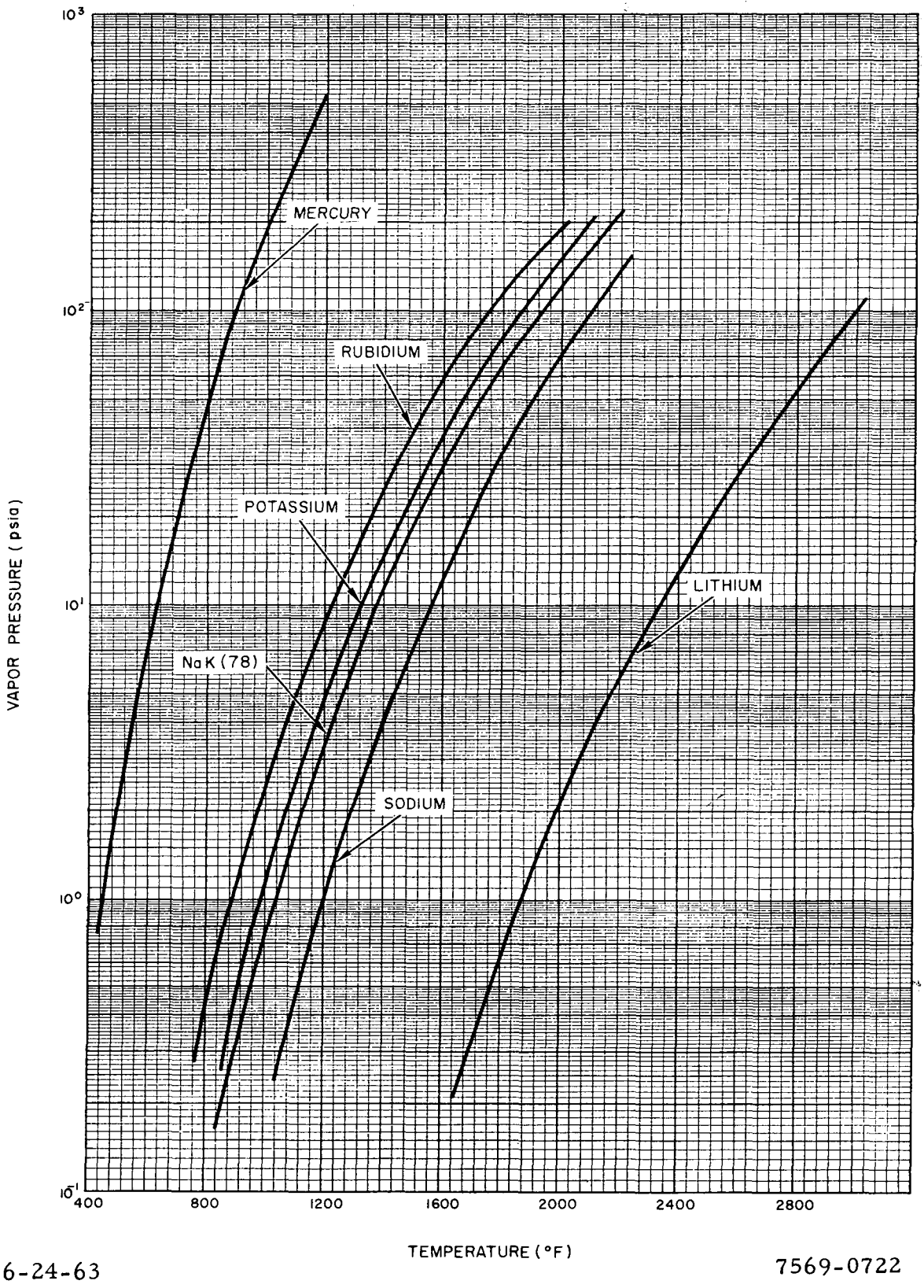

Figure 1.41 Comparison of Vapor Pressures of Alkali Metals and Mercury (Reference 2)

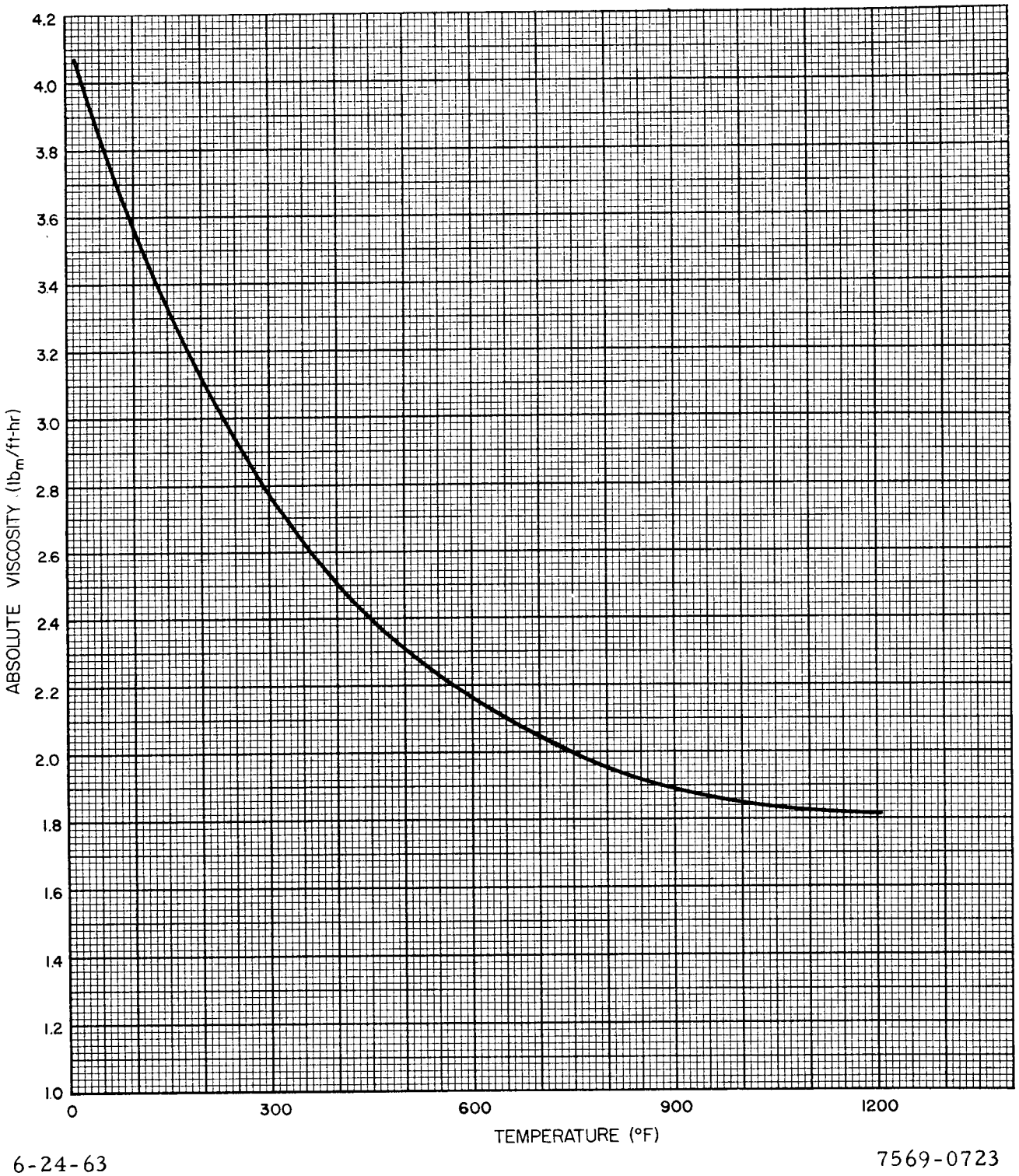

Figure 1.42 Absolute Viscosity of Liquid Mercury
(Reference 2)

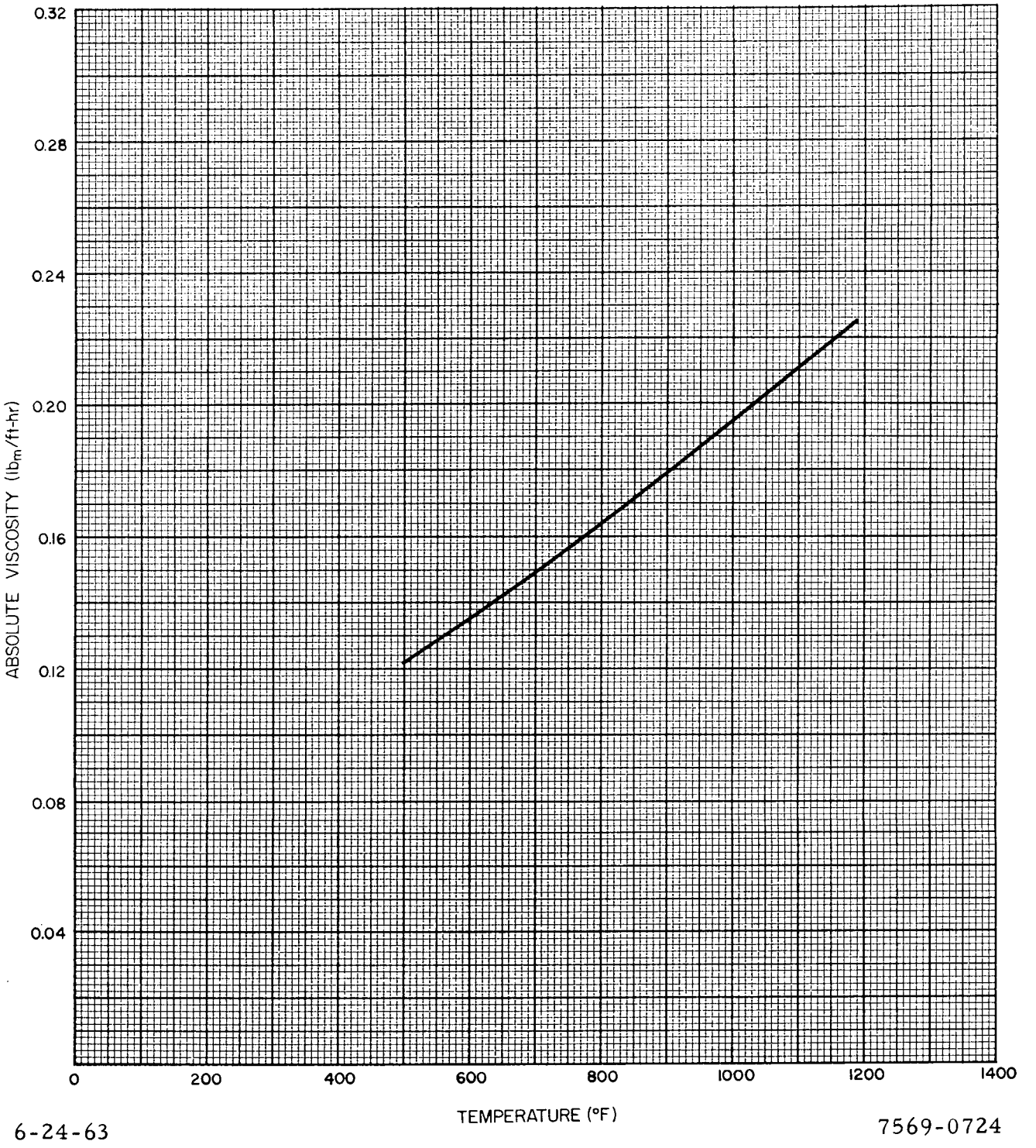

Figure 1.43 Absolute Viscosity of Saturated Mercury Vapor (Reference 2)

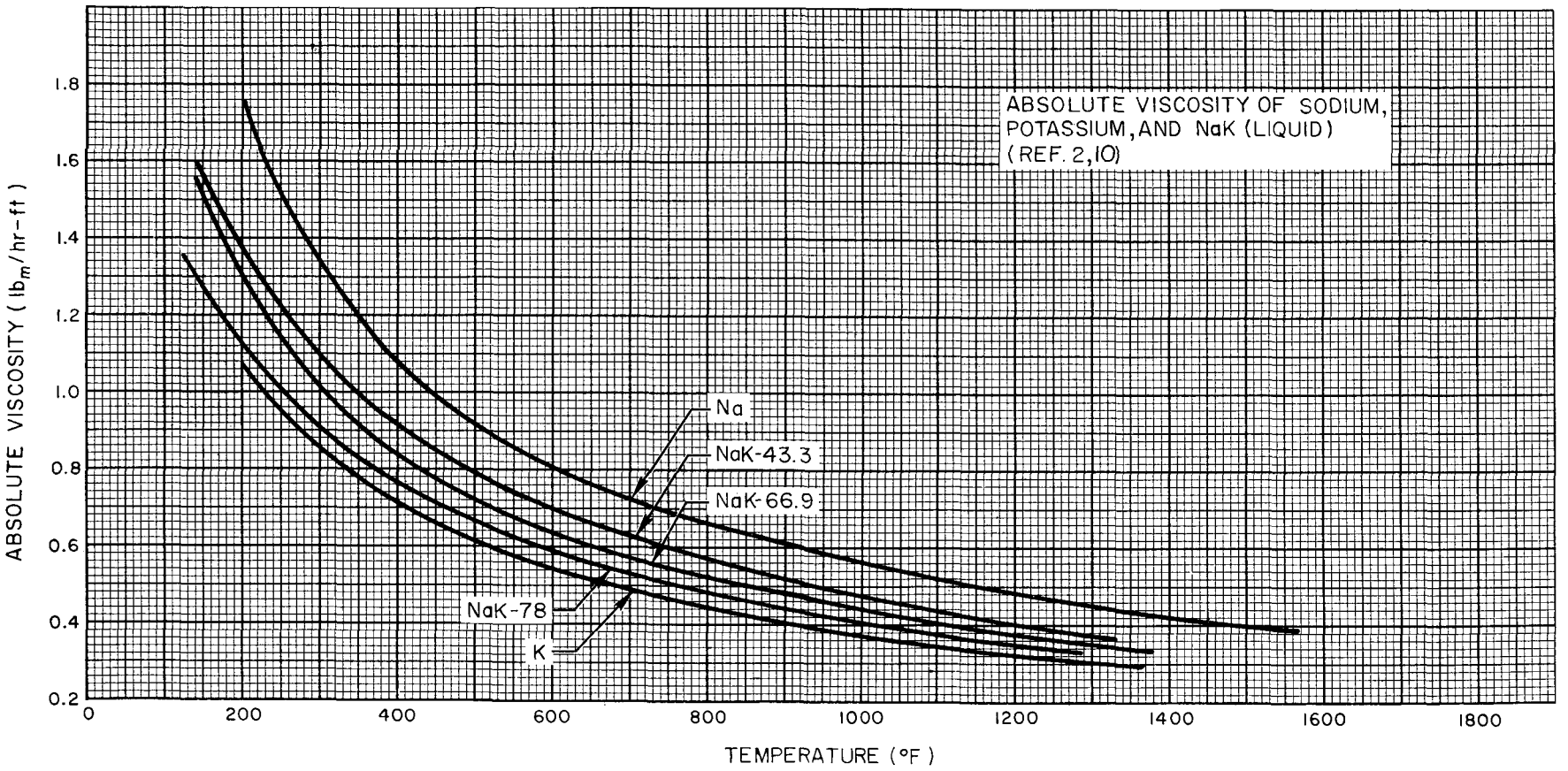

Figure 1.44 Absolute Viscosity of Sodium, Potassium, and NaK (liquid) (Reference 2, 10)

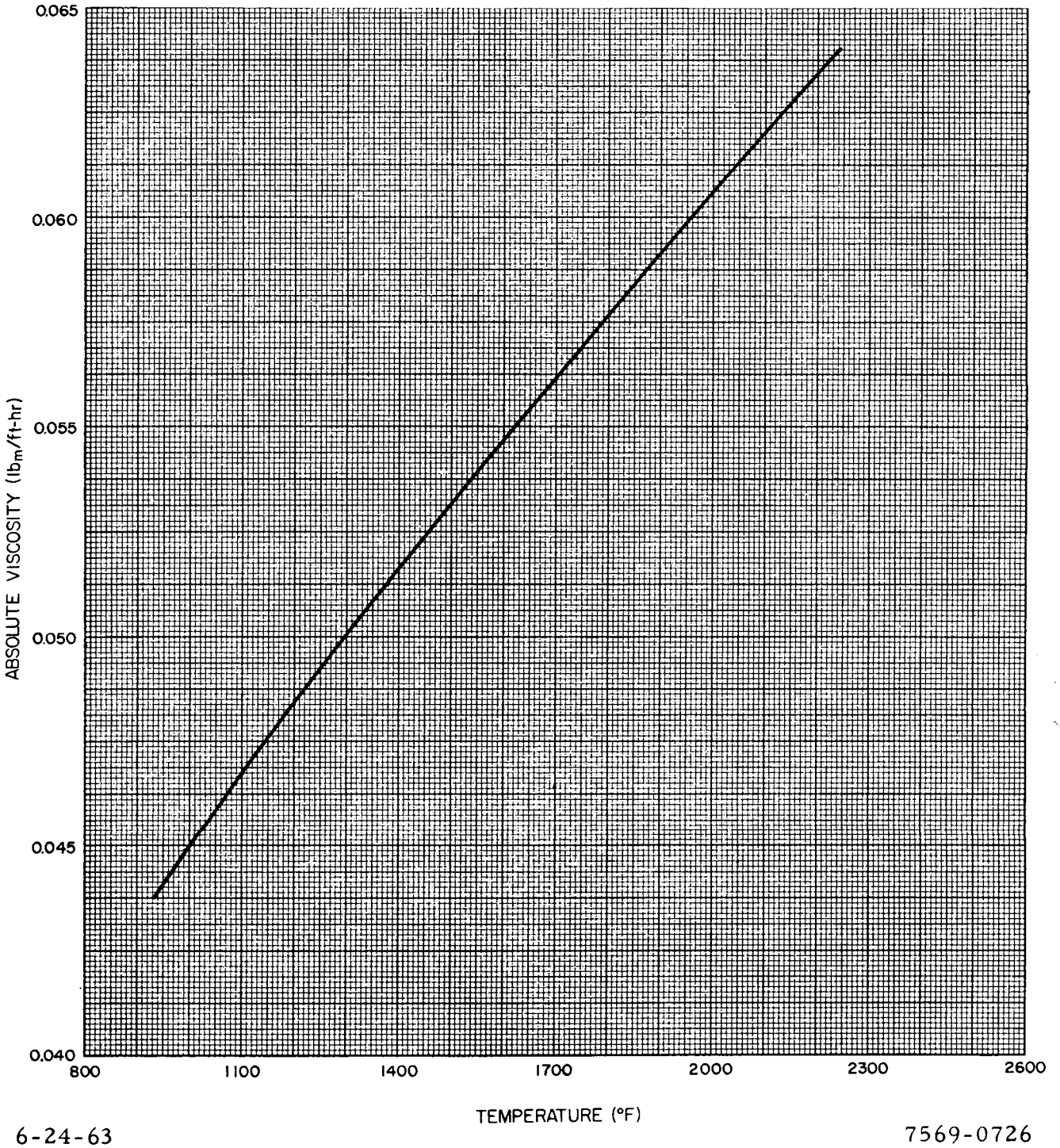

Figure 1.45 Absolute Viscosity of Saturated Sodium Vapor (Reference 2)

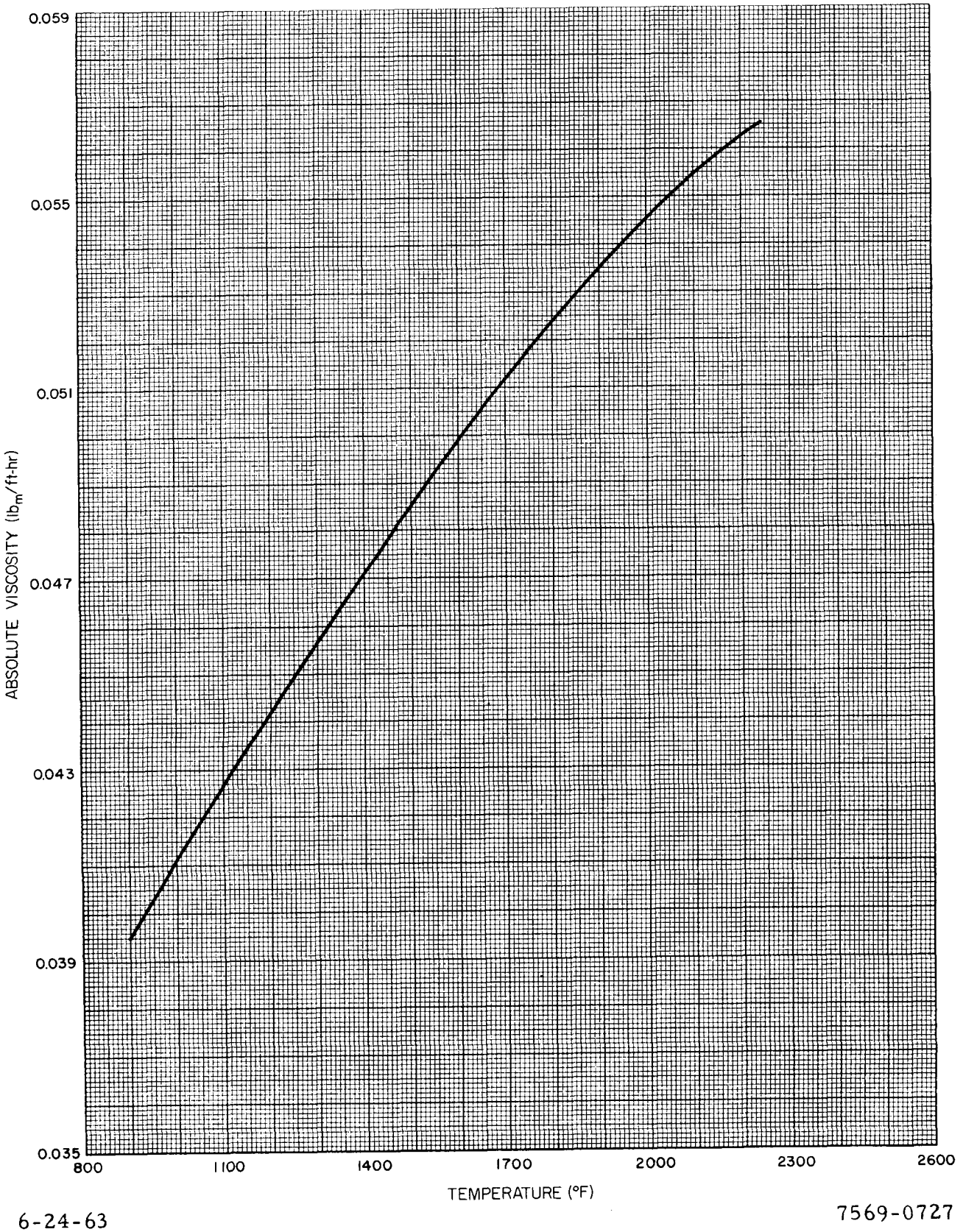

Figure 1.46 Absolute Viscosity of Saturated Potassium Vapor (Reference 2)

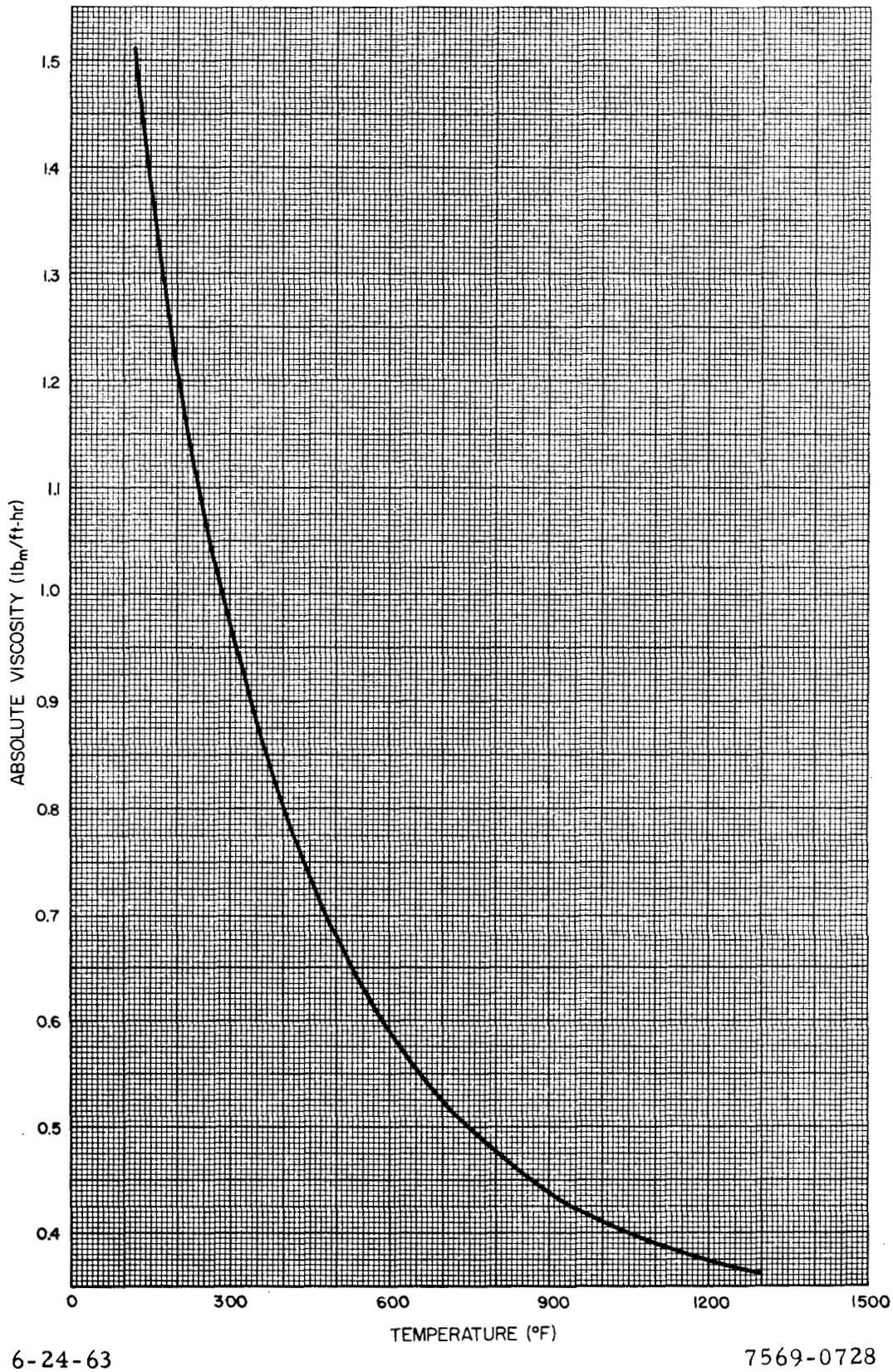

Figure 1.47 Absolute Viscosity of Liquid Rubidium (Reference 2)

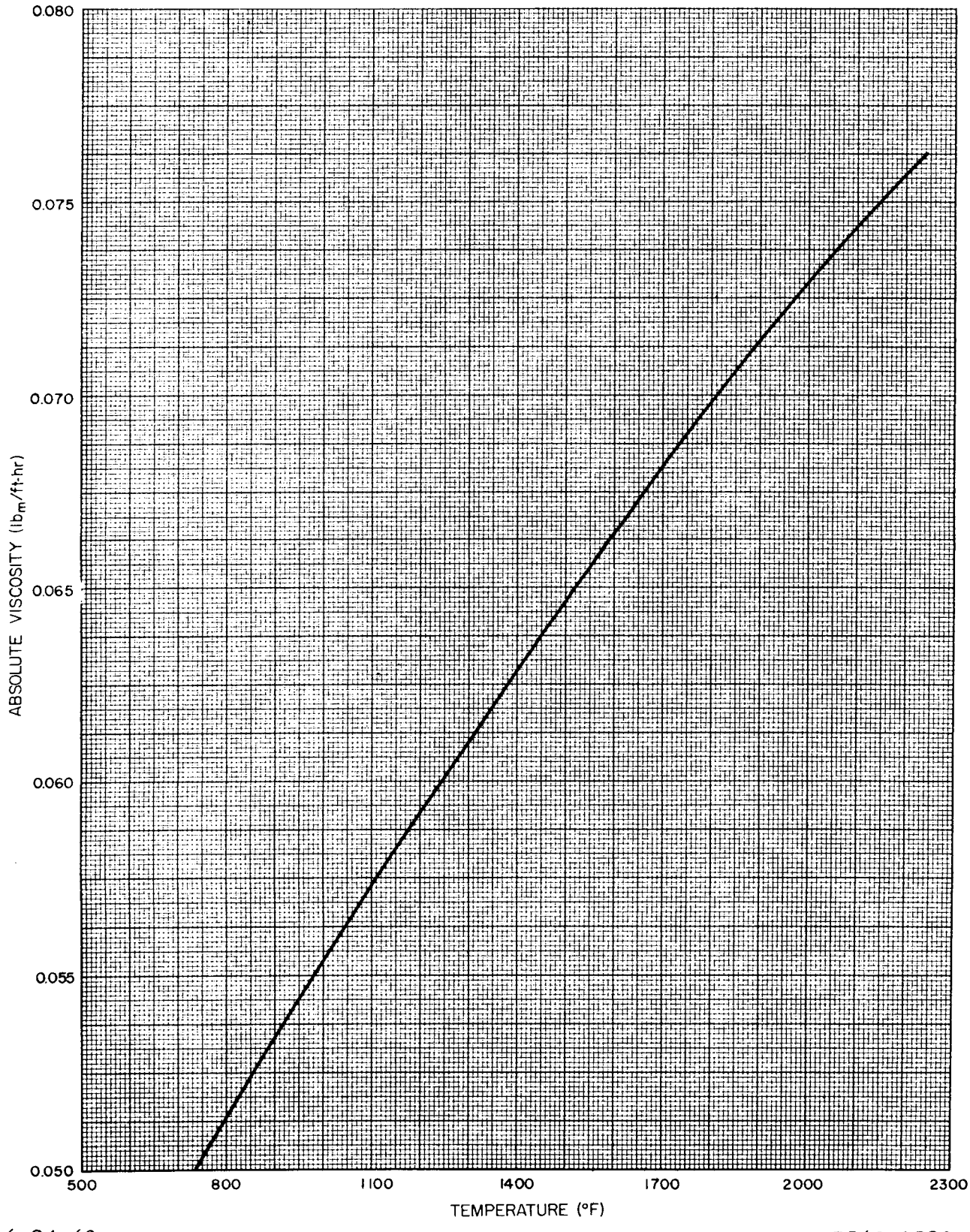

Figure 1.48 Absolute Viscosity of Saturated Rubidium Vapor (Reference 2)

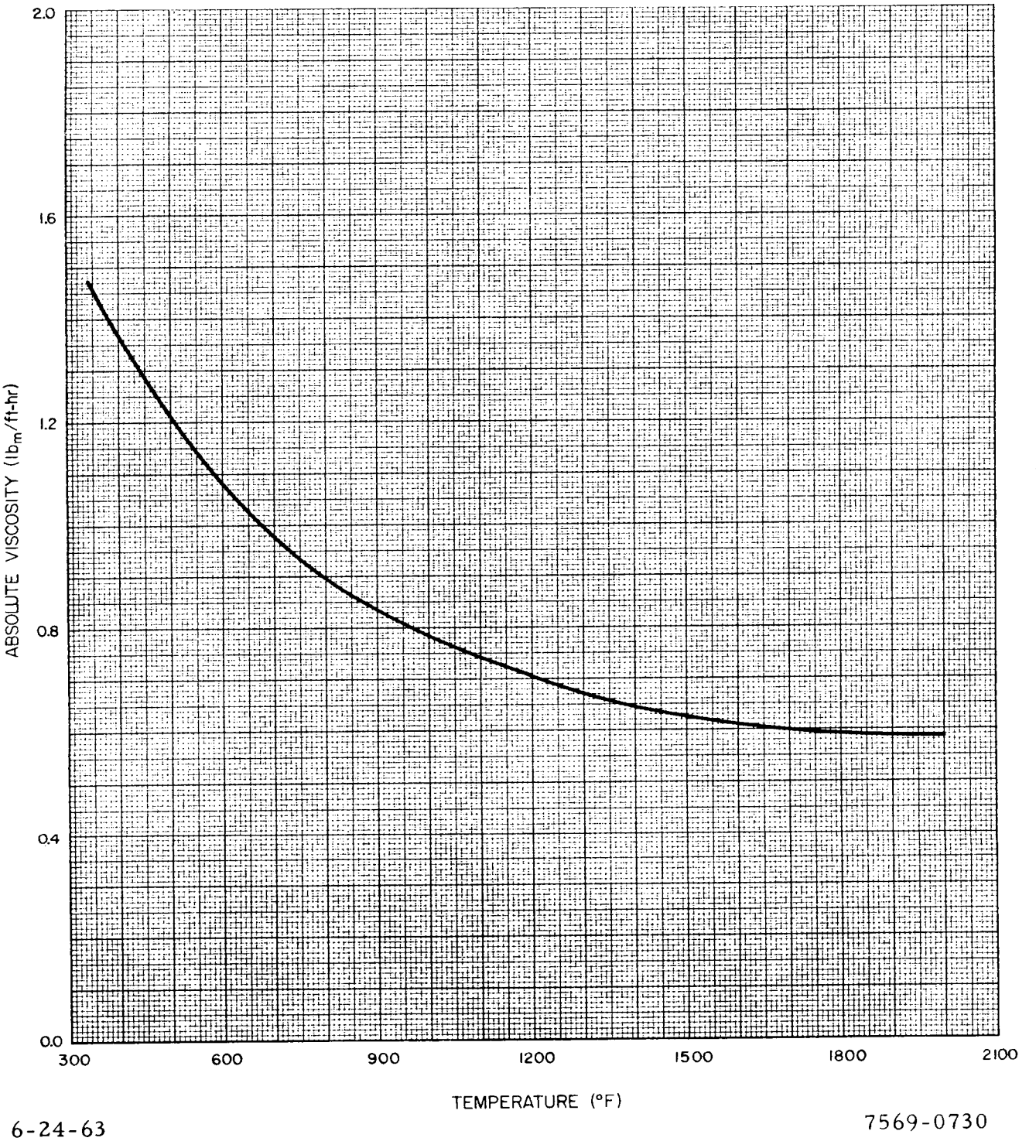

Figure 1.49 Absolute Viscosity of Liquid Lithium
(Reference 2, 12)

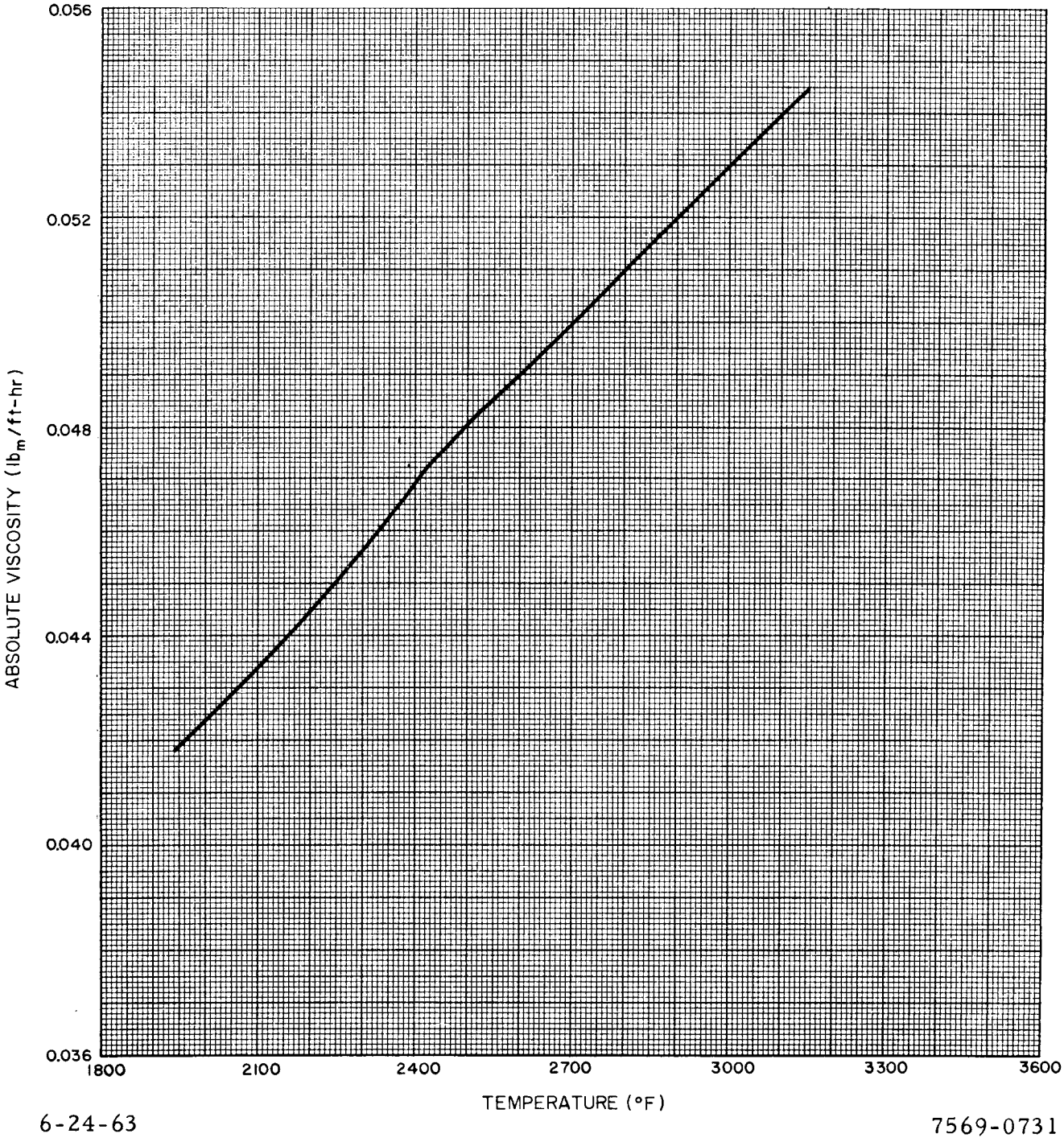

Figure 1.50 Absolute Viscosity of Saturated Lithium Vapor (Reference 2)

1.3 HAZARDOUS PROPERTIES[1,10,20]

This discussion is presented to briefly describe the hazards involved with liquid metals and should be used only as a guide.

The possibility of a leak in a nuclear-powered system presents many problems. For a mercury-coolant system the major hazard created due to leakage is the toxicity of mercury vapor. Even when the concentration of mercury vapor in air is low, over long periods of time chronic mercury poisoning will result. After absorption it circulates in the blood and is stored in the bone, liver, kidneys, and spleen. The chief effect is upon the central nervous system and upon the mouth and gums, similar to the effect caused by tetraethyl lead. There are several symptoms indicating the possibility of mercury poisoning; stomatitis, tremors, psychic disturbances, excessive salivation, and pain on chewing are among the common ones while gingivitis, loosening of the teeth, and a dark line on the gum margins (resembling the "lead line") are among the ones in severe cases.

Another important fact should be noted at this time. Less than one ounce of mercury compounds when swallowed can cause death; this indicates that mercury compounds formed with eating material and mercury can be more dangerous than metallic mercury if one is careless.

An even greater hazard is created when hot alkali metal leaks out of a system, because the alkali metals will ignite in air or water resulting in severe alkali burns to personnel if contacted with the liquid metal.* The oxide smoke produced by combustion is very irritating to the throat and lungs but is not poisonous. Injury to the throat and lungs will be largely due to the inhaling of the hydroxide mist produced by the alkali metal-water reaction. Armour Research Institute has indicated that NaK will react explosively at room temperature with certain fluorinated and chlorinated hydrocarbon compounds (such as stopcock grease and Teflon).[20]

It should also be noted that under some circumstances it has been reported that the products of the apparently innocuous reaction between the cleaning fluid trichloroethylene and alkali metals can explode violently without warning.

*Atomics International presently employs a company developed NaK loading cart which combines a purification, loading, and closure system for loading NaK into a system. NaK technology has progressed to the point where NaK loops are operated in an open laboratory utilizing only the usual chemical fire precautions.

2.0 HEAT TRANSFER

2.1 NATURAL CONVECTION

The problem may arise where a component in a reactor system needs to be cooled by natural convection, such as during shutdown. The cases considered in this section, unless otherwise specified, will be where the liquid metal flow in the assembly is not dependent on the hydraulic and thermal characteristics of the external circuit. The cooling characteristics will be dependent on the generation of heat in the element, or on the geometry of the cooling system, the properties of the cooling medium, and its constant temperature. Transient systems and boiling natural convection will not be considered here; however, transient calculations may be made with the data presented. The following subsection contains the best correlated heat transfer equations that are presently available.

Ostrach[21] presented an analysis which takes into consideration friction heating. His parameter which determines whether or not frictional heating is of any significance when analyzing convection heat transfer is

$$\overline{K} = Gr_L \frac{\beta f_i L}{c_p} \qquad \ldots (2.1)$$

If the quantity $[(\beta f_i L)/c_p] > 1.0$, the Nusselt number should be determined as a function of $\overline{K}$ in addition to Pr and Gr.

In order to determine whether natural of forced convection is the dominating heat transfer process, the ratio Gr/Re^2 should be examined. If $Gr/Re^2 << 1.0$, natural convection can be neglected; if $Gr/Re^2 >> 1.0$, natural convection will be the dominating heat transfer process; and if $Gr/Re^2 \cong 1.0$, natural convection should not be neglected.[21] The equations in the following sections are recommended for use in calculating Nusselt numbers for various geometries. Unless otherwise stated, the fluid properties should be evaluated at the film temperature $[T_f = (T_w + T_b)/2]$. Also the entrance region is usually neglected, because it is quite small ($L_e << 100D$); it is a function of the Reynolds number, which is small in natural convection.[22]

2.1.1 Vertical Plates and Cylinders

Eckert[22] derived the average Nusselt number equation for a vertical plate at constant temperatures in laminar natural convection flow, $Ra_L < 5 \times 10^8$, which is

$$\overline{Nu}_L = \frac{0.667 Pr^{1/2} Gr_L^{1/4}}{(0.952 + Pr)^{1/4}} \qquad \ldots(2.2)$$

using the characteristic dimension (L) as the height of the plate. Equation 2.2 agrees satisfactorily with Ostrach's[23] exact solution.

Siegel[24] obtained Equation 2.3 for a constant surface heat flux and laminar flow occurring

$$\overline{Nu}_L = \frac{0.727 Pr^{1/2} Gr_L^{1/4}}{(0.800 + Pr)^{1/4}} \; . \qquad \ldots(2.3)$$

Eckert and Jackson[25] developed an equation for turbulent flow ($Ra_L > 5 \times 10^8$) with the vertical plate held at constant temperature which is,

$$\overline{Nu}_L = \frac{0.0246 Pr^{7/15} Gr_L^{2/5}}{(1 + 0.494 Pr^{2/3})^{2/5}} \; . \qquad \ldots(2.4)$$

Equation 2.4 inherently is in error due to the assumption that the surface heat flux varies as $Pr^{-2/3}$ which is not always true at low Prandtl numbers, but because of the lack of experimental results, its usage is still recommended (Equation 2. 4 was developed only for liquids having a Prandtl number close to one; therefore its usage may not be valid for liquid metals, however no data are available to prove this hypothesis so that it is still useful as a last alternative for predicting the heat transfer coefficient).

For constant heat rate instead of constant wall temperature, Equation 2.4 becomes[24]

$$\overline{Nu}_L = \frac{0.0246 Gr_L^{2/5} Pr^{7/15}}{(1 + 0.444 Pr^{2/3})^{2/5}} \; . \qquad \ldots(2.5)$$

There seems to be a general consensus among various authors that the equations for vertical plates also hold true for vertical cylinders. This approximation is conservative because as the radius of an element becomes smaller, its Nusselt number increases[26] (the characteristic length is the height of the cylinder).

2.1.2 Horizontal Cylinders and Flat Plates

Hyman, Bonilla, and Ehrlich[27] did experimental work on the heat transfer about a horizontal circular cylinder – characteristic length (D) being the diameter of the cylinder – at constant wall temperature for laminar natural convection flow ($Ra<5 \times 10^8$) and they recommended the following average Nusselt equation for cylinders larger than 1/8 inch in diameter;

$$\overline{Nu}_D = \frac{0.53 Pr^{1/2} Gr_D^{1/4}}{(0.952 + Pr)^{1/4}} \quad . \qquad \ldots(2.6)$$

Levy,[28] using an integral method, obtained an equation for a constant wall temperature horizontal plate facing upwards with laminar natural convection flow occurring. The characteristic dimension (L) refers to the small side of the rectangular plate. The equation is

$$\overline{Nu}_L = 0.371 Pr^{2/5} Gr_L^{1/5} \frac{1}{(0.762 + Pr)^{1/5}} \quad . \qquad \ldots(2.7)$$

For turbulent flow in the above case, the Nusselt equation becomes[10]

$$\overline{Nu}_L = \frac{0.0727 Pr^{9/33} Gr^{4/11}}{(1 + 0.441 Pr^{2/3})^{4/11}} \quad . \qquad \ldots(2.8)$$

Equations 2.7 and 2.8 should be used with caution, because verification of these equations has not thus far been accomplished. Also, experimental data for cubes, spheres, etc., have not been obtained. Reference 28 gives the differential equations for such configurations, but Levy's equations need to be verified experimentally before they may be used with confidence.

2.1.3 Vertical Pipe or Parallel Plates

Shown below in Figure 2.1 are schemes[10] which were considered by various investigators.

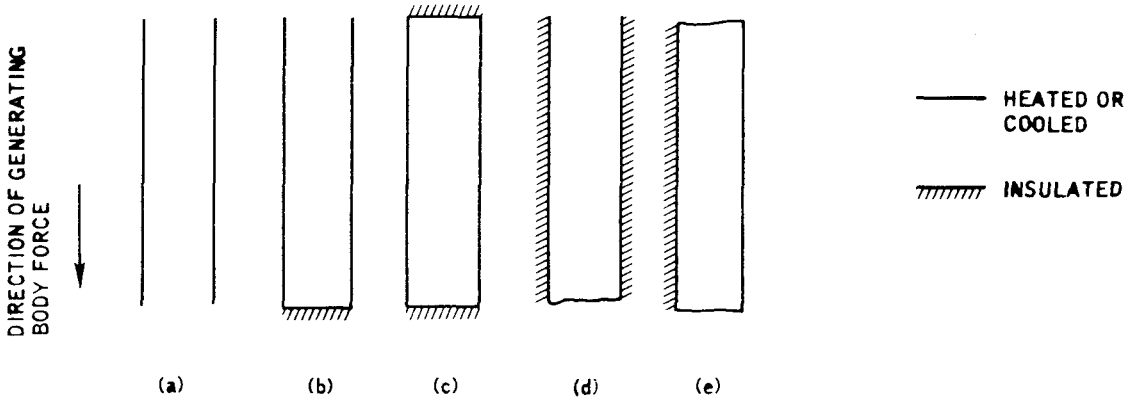

Figure 2.1. Schemes Considered in Natural Convection Flow

Ostrach[29] derived exact solutions for case (a) for fully developed laminar natural convection flow of fluids with and without heat sources and constant wall temperatures. Figure 2.2 shows his results for walls at equal temperatures as a function of a heat source parameter,

$$G = \frac{Qd^2}{k(T_w - T_b)} \quad , \qquad \ldots(2.9$$

where Q, d, and k are; respectively, the heat added by the heat sources, spacing between plates, and thermal conductivity of the fluid. Ostrach[30] and Lietzke,[31] whose results are shown in Figure 2.3, derived similar solutions when one wall was heated and the other cooled uniformly.

Solutions for case (b) were proposed by Lighthill[32] and Levy[28] for flow in a pipe or between parallel plates with either end assumed closed and with constant wall temperatures, but the results are not entirely valid for low Prandtl numbers. For estimation purposes their results may be extrapolated to include liquid metals.

Only special cases of case (c) can be analyzed. Ostrach[30] obtained results shown in Figure 2.4 for heat sources in a completely enclosed region

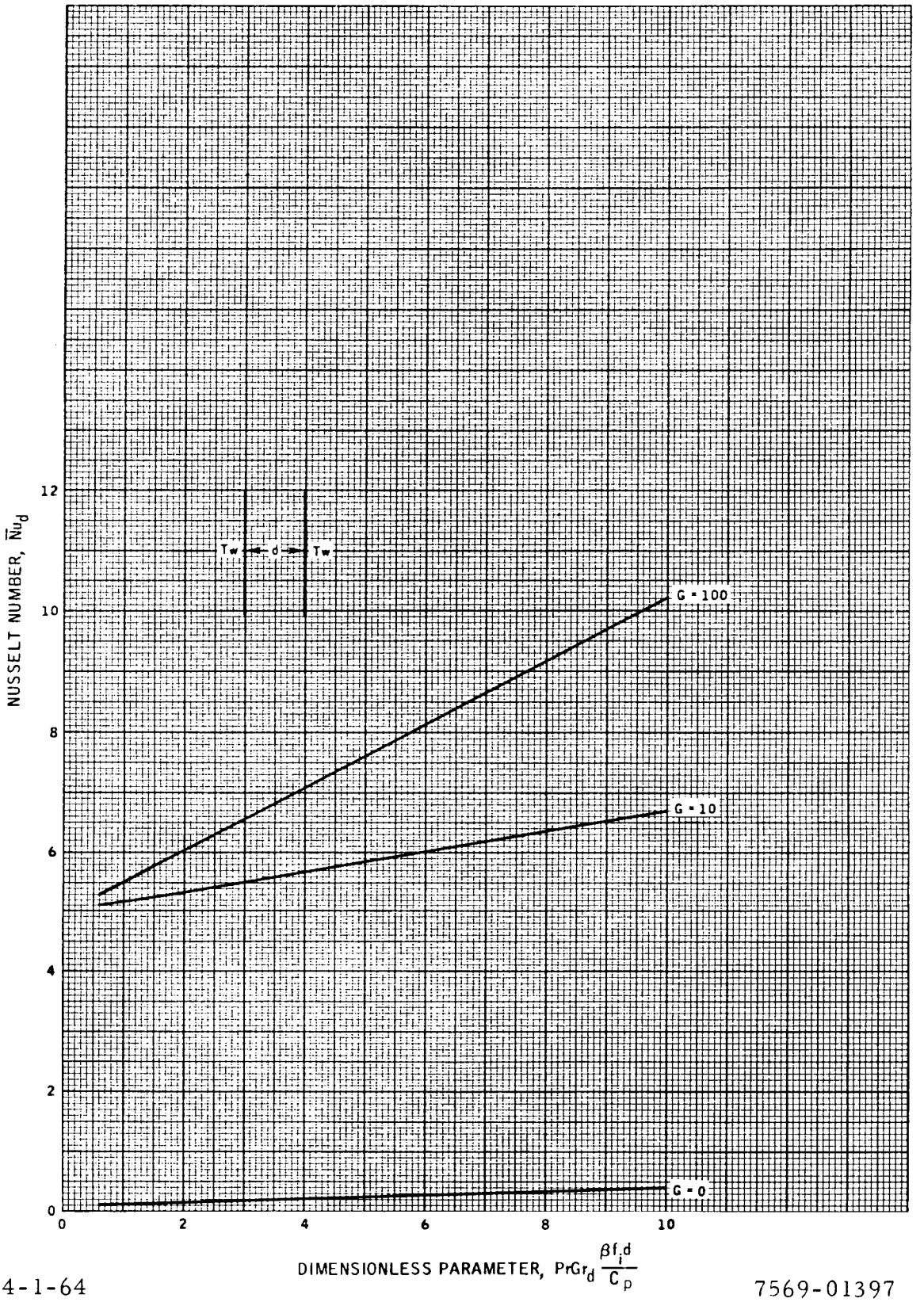

4-1-64 7569-01397

Figure 2.2. Fully Developed Laminar Natural Convection Flow Between Two Parallel Plates Maintained at the Same Temperature

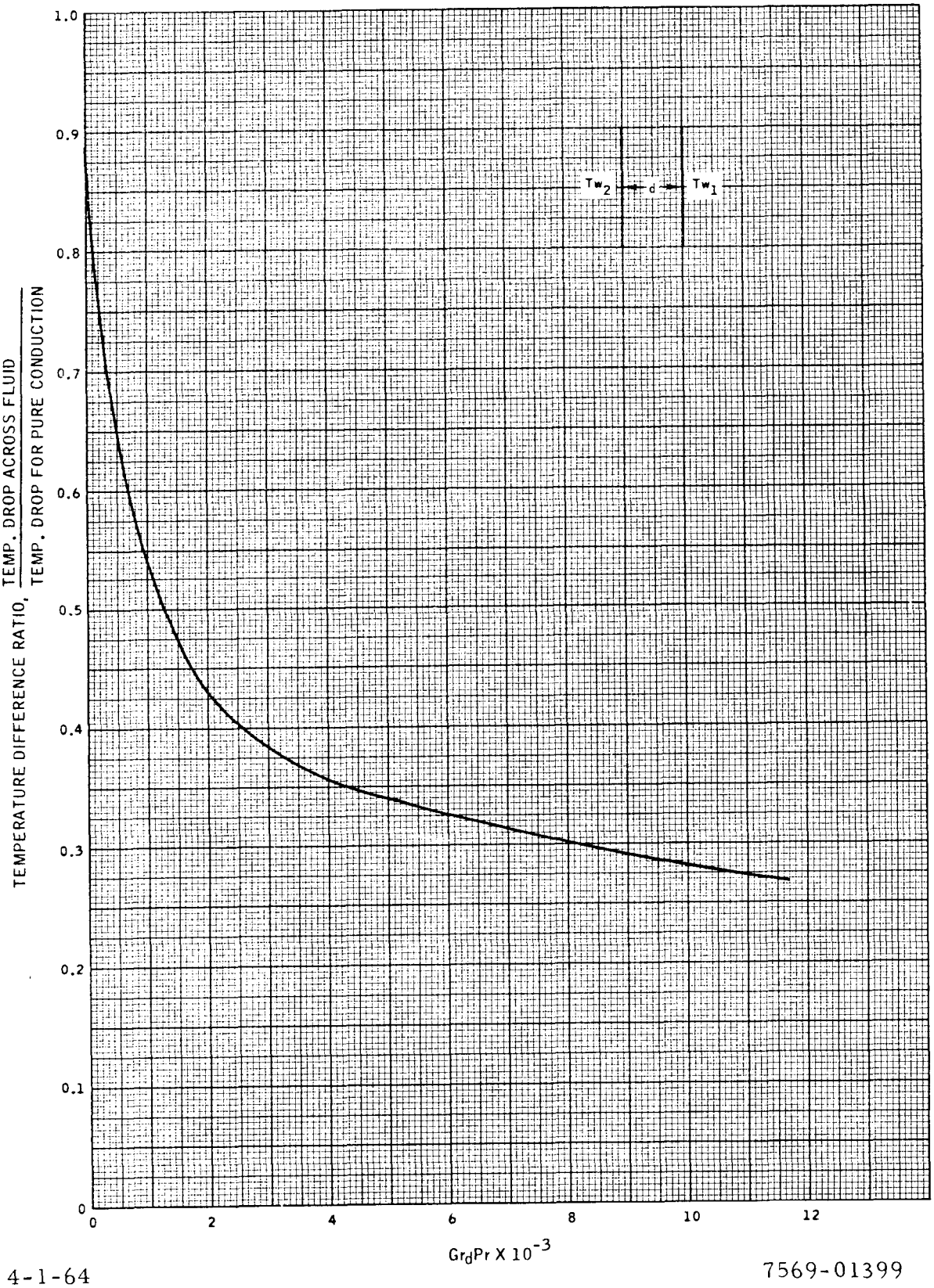

Figure 2.3. Streamline Flow Between Surfaces at Different Temperatures and with Uniform Heat Rate

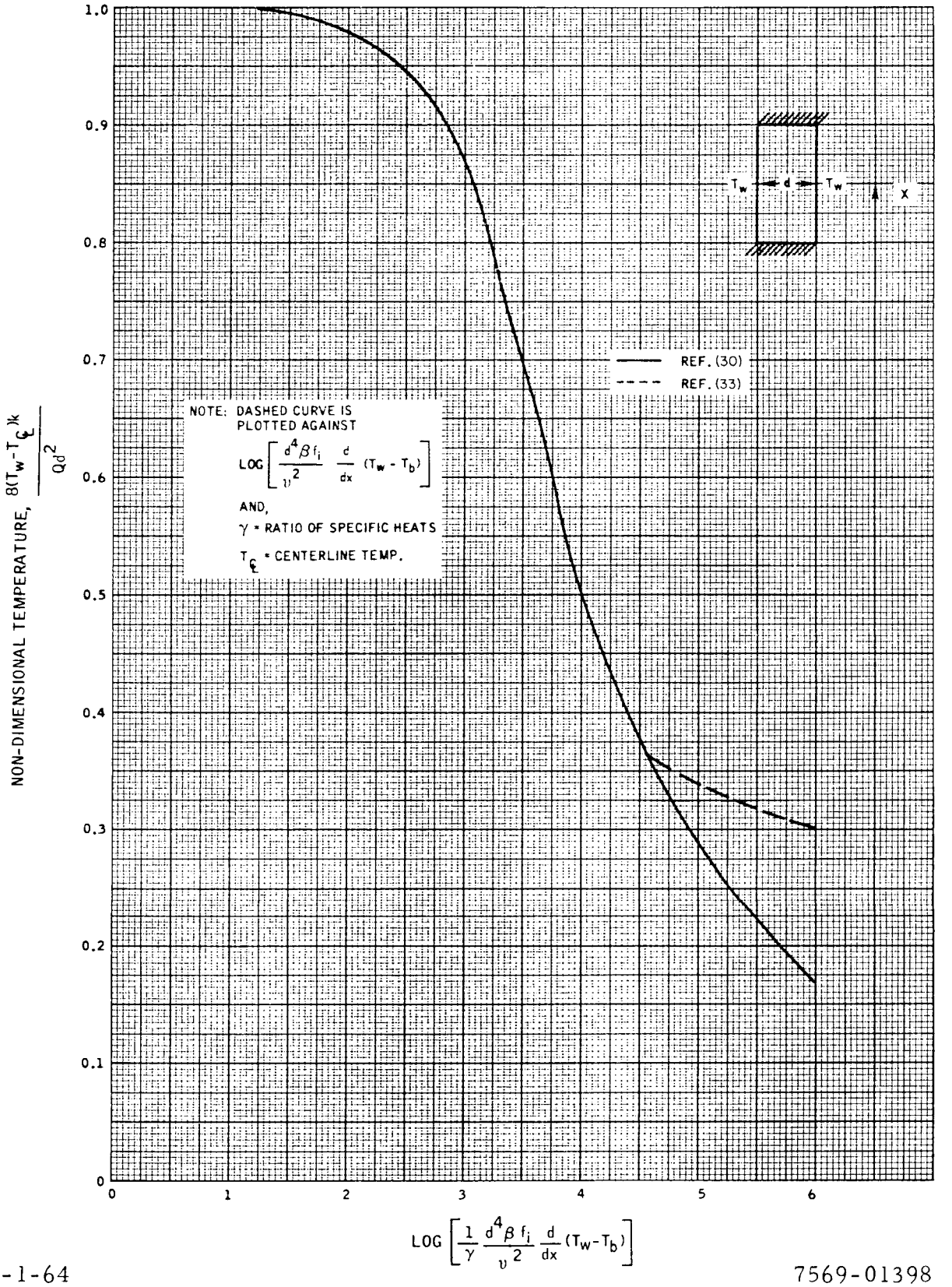

4-1-64

7569-01398

Figure 2.4. Laminar Natural Convection Flow in a Region Enclosed Between Two Parallel Plates with Equal and Linearly Varying Wall Temperature

with equal and constant wall temperatures. Also shown in Figure 2.4 are approximate results by Hamilton, Poppendiek, and Palmer[33] incorporating a simplified velocity distribution.

Cases (d) and (e) do not lend themselves readily to theoretical solutions. If the sidewall spacing is very small, solution for a thin vertical annuli by Timo, discussed in Section 2.1.5, may be used.[10]

2.1.4 Horizontal Pipe or Parallel Plates

Cases (c) and (e) in this section are identical to cases (e) and (c), respectively, of the previous section and need not be mentioned again. The rest of the cases have been considered only on the basis of melting or freezing a liquid metal. Steiner[34] and Tidball and Ciarlariello[35] have considered these problems.[12]

2.1.5 Thin Vertical and Horizontal Annuli

Experimental investigations by Timo,[36] Mausteller and McGoff,[37] and Powledge[38] on vertical annuli were correlated by Mausteller and McGoff on the conditions of convection and conduction heat transfer up the annulus, solid sodium at the top, and an open chamber of molten sodium at the bottom. The empirically correlated equation is

$$\overline{Nu}_{D_m} = 6.5 \times 10^{-6}\left(Gr_{D_m} Pr\right)^{0.73} , \qquad \ldots(2.10)$$

where D_m is the log mean diameter of the annulus (ft).

NOMENCLATURE

c_p = Specific heat at constant pressure, Btu/lb-°F

d = Spacing between parallel plates or annulus width

D = Diameter, ft

f_i = Acceleration component in the i direction (parallel to vertical plate or perpendicular to horizontal plate), ft/hr^2.

Gr = Grashof number $\left\{Gr_L = \left[\beta f_i (T_w - T_b) L^3\right]/\nu^2\right\}$, nondimensional. Subscripts D, L, etc., means that the Grashof number is based on this dimension.

G = Heat source parameter defined by Equation 2.9, nondimensional

h = Local heat transfer coefficient, $Btu/hr\text{-}ft^2\text{-}°F$

$\bar{h}$ = Averaged heat transfer coefficient over a length, $Btu/hr\text{-}ft^2\text{-}°F$

k = Thermal conductivity, Btu/hr-ft-°F

$\bar{K}$ = Frictional heating parameter defined by Equation 2.1, nondimensional

L = Length of plate, pipe, or annulus, ft

$\bar{Nu}$ = Average Nusselt number over a surface $[\bar{Nu}_L = (\bar{h}L/k)]$, nondimensional. Subscript D or L means that the Nusselt number is based upon this length.

Pr = Prandtl number $[Pr = (c_p\mu/k) = (\rho c_p \nu/k)]$, nondimensional

q = Heat transfer rate, Btu/hr

Ra = Rayleigh number (Ra = GrPr), nondimensional

Re = Reynolds number $[Re_D = (pvD/\mu)]$, nondimensional. Subscript L or D represents length used in definition of Reynolds number.

T = Temperature, °F. Subscripts w, b, or f represent wall, bulk fluid, or film temperature

v = Average velocity of fluid bulk, ft/hr

β = Coefficient of volumetric expansion, $°F^{-1}$

μ = Absolute viscosity, $lb_m/ft\text{-}hr$

ν = Kinematic viscosity, ft^2/hr

ρ = Density, lb_m/ft^3

2.2 FORCED CONVECTION

Externally caused fluid motion has three zones associated with it – laminar ($Re_D < 2100$), transitional ($2100 \leq Re_D \leq 10{,}000$), and turbulent ($Re_D > 10{,}000$). Most of the experimental results on liquid metals have been obtained within the turbulent regime. These results have been correlated by finding the average Nusselt number as a function of the Peclet number which has proven to be very satisfactory. In the following subsections the recommended and best presently available equations for finding the average Nusselt number and resulting heat transfer coefficients will be given for various geometrical environments with the fluid properties evaluated at the film temperature. The entrance region (amounting to 20 to 40 diameters in length) has been neglected in most cases, because it affects the average Nusselt number by only 0 to 5%.[39]

2.2.1 Circular Pipes

One of the most widely used of the semi-empirical equations for uniform wall heat flux and turbulent flow is Lyon's[40] equation (neglecting entrance effects):

$$\overline{Nu}_D = 7.0 + 0.025\ Pe_D^{0.8} \quad . \qquad \ldots(2.11)$$

Dwyer[41] proposed to modify Lyon's equation in order to bring it into better agreement with experimental results by obtaining an equation for the average effective value of the ratio of the eddy diffusivity of heat transfer to that for momentum transfer which was considered equal to one in Lyon's equation. Dwyer's relationships, which apply only for $Pe_D > 400$, are as follows:

$$\overline{Nu}_D = 7.0 + 0.025(\overline{\psi}\, Pe_D)^{0.8} \quad , \qquad \ldots(2.12)$$

$$\overline{\psi} = 1 - \frac{1.82}{Pr(\epsilon_M/\nu)^{1.4}_{max}} \quad . \qquad \ldots(2.13)$$

Values of $(\epsilon_M/\nu)_{max}$, $\overline{\psi}$, and $\overline{Nu}_D$ are given in Figures 2.5, 2.6, and 2.7 respectively. Note that in Figure 2.5 $(\epsilon_M/\nu)_{max}$ is given for pipes, annuli, and rod bundles. The latter two geometries will be discussed in later sections.

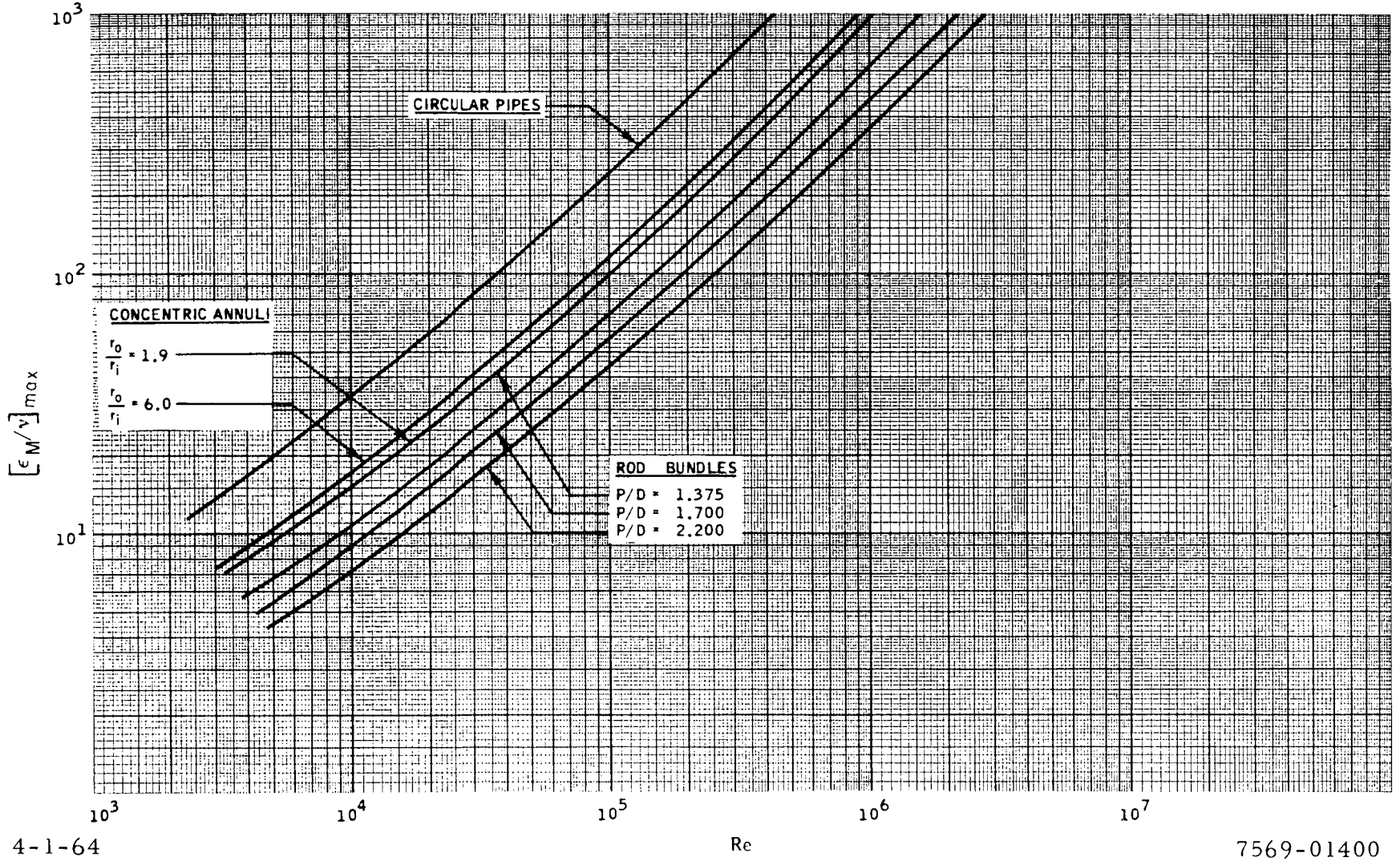

Figure 2.5 $[\epsilon_m/\nu]_{max}$ vs Reynolds No. for Fully-Established Turbulent Flow of Liquid Metals Through Circular Tubes, Concentric Annuli, and Rod Bundles with Equilateral Triangular Spacing

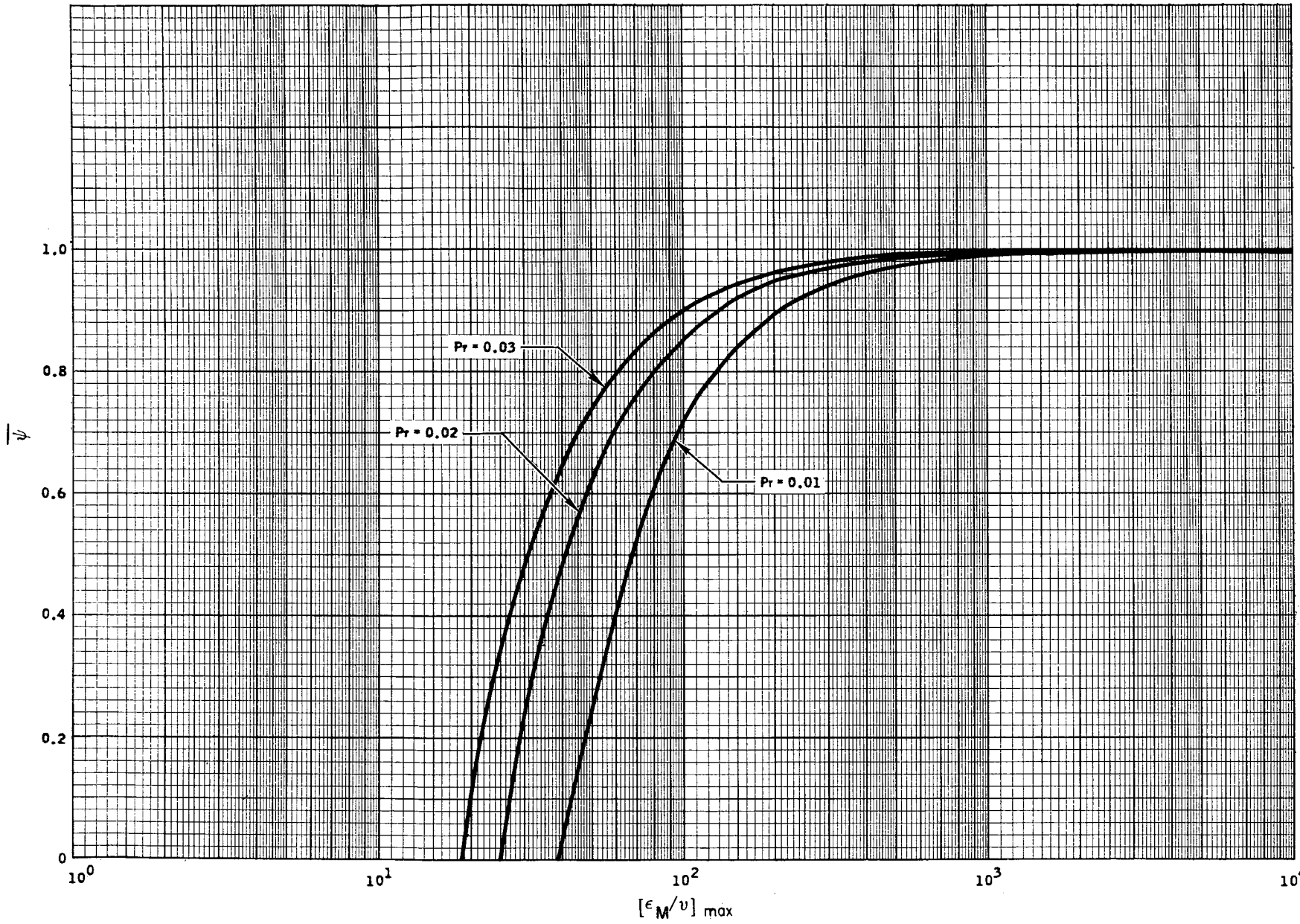

4-1-64

Figure 2.6 Graphical Representation of Equation 2.13

7569-01401

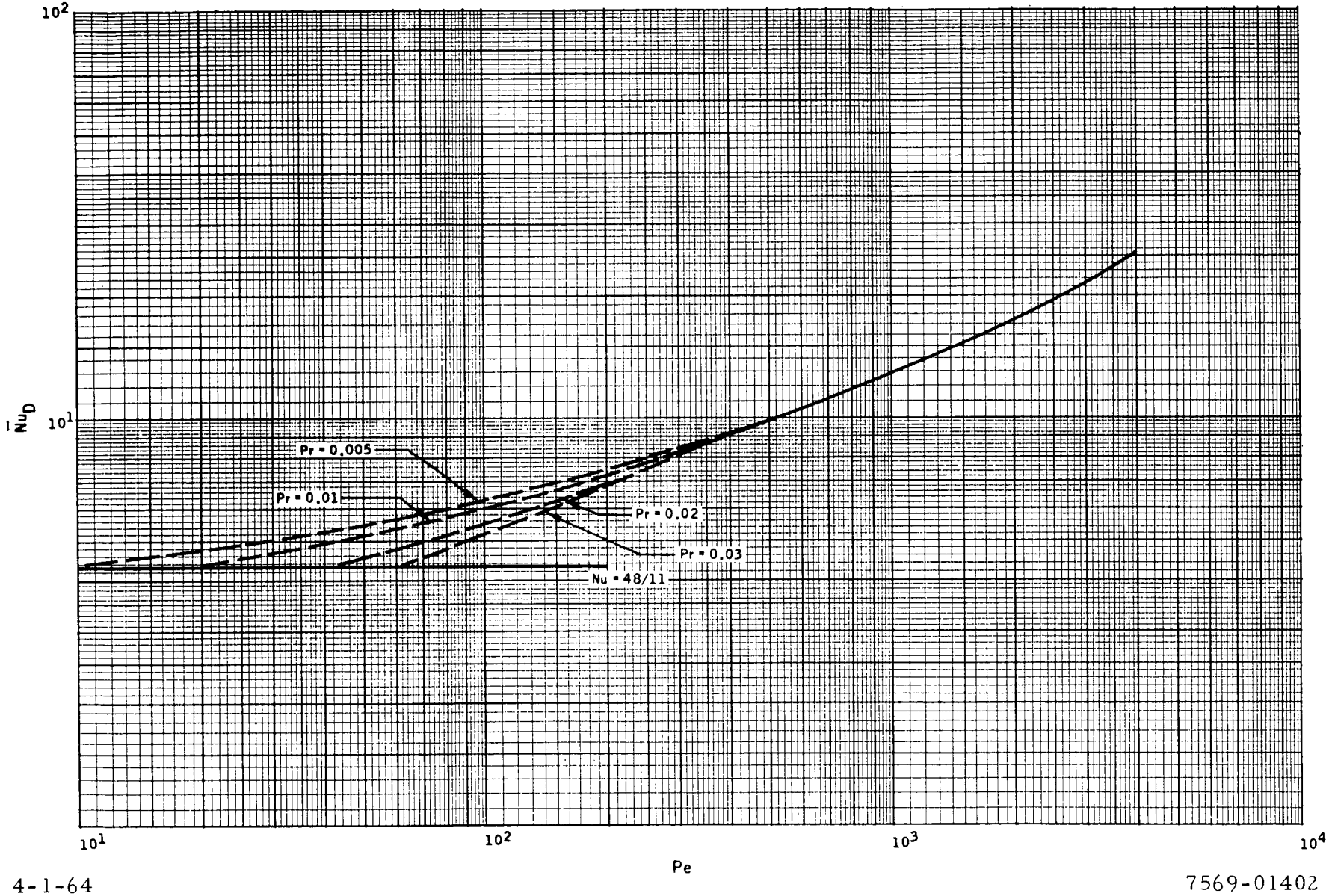

4-1-64

7569-01402

Figure 2.7 Average Nusselt No. vs Peclet No. for Liquid Metal Flowing in Circular Tubes Under Conditions of Constant Heat Flux and Fully-Established Flow

Dwyer compared his equation with the experimental results by Brown et al[42] and Kirillov et al[43] for mercury under "wetting" conditions in the high Peclet number range ($Pe_D > 10^3$) and found that good agreement was evident. In the intermediate Peclet number range Equation 2.12 was compared to the discrepant experimental results of Kirillov[43] and Khabakhpasheva[44] with NaK, and Novikov et al[45] with Na and was found to be a compromise between their results. The author compared Equation 2.12 with the results of Baker and Sesonske[39] for forced convection in a horizontal concentric tube in the Peclet number range, $300 < Pe < 2500$, with NaK-56 as the fluid and found that Equation 2.12 agreed quite well with their results. In the low Peclet number range, $10 < Pe < 600$, Dwyer compared a family (Pr as the variable) of extrapolated curves between Equation 2.12 and the known limiting laminar Nusselt number, $\overline{Nu}_D = 48/11$, with the disagreeing experimental results of Pirogov[46] with Na and Petukhov and Yushin[47] with Hg (lower results occurred with Hg than with Na) and found that his equation was again a compromise between the two different results. Additional experimental results are needed to properly evaluate the accuracy of the extrapolated Equation 2.12 in the low (laminar) Peclet number range, but its use in all ranges is recommended until such data are available to warrant the use of an improved equation.*

For the uniform wall temperature case with turbulent pipe flow, Segan and Shimazaki[48] obtained the equation,

$$\overline{Nu}_D = 5.0 + 0.025\, Pe_D^{0.8} \quad , \qquad \ldots(2.14)$$

which gives results about 5 to 10% lower than Equation 2.12, but Baker[39] found experimentally that there existed no difference between a Nusselt number for uniform wall temperature or for uniform wall heat flux. Therefore, Equation 2.12 may be used for both cases.

2.2.2 Parallel Plates

Seban[49] approximated a solution for turbulent flow between two wide parallel plates with heat transfer through one side only and obtained the equation,

$$\overline{Nu}_{D_e} = 5.8 + 0.02\left(Pe_{D_e}\right)^{0.8} \quad . \qquad \ldots(2.15)$$

*See B. Lubarsky and S. J. Kraufman's report (NACA-TN-3336) for older liquid metal work and R. Herrick's report (TRG Report 546R) for a recent heat transfer survey.

For the case of parallel plates with heat through both sides, Seban[49] obtains an approximation by the principle of superposition which is best understood by reviewing his paper.

2.2.3 Concentric Annuli

Dwyer and Tu[50] obtained a semiempirical equation for constant wall heat flux through the inner wall only and fully established turbulent flow which is:

$$\overline{Nu}_{ann,D_e} = A + B\left(\psi Pe_{D_e}\right)^C \qquad \ldots(2.16)$$

where,

$$A = 4.63 + 0.686\left(\frac{r_o}{r_i}\right) , \qquad \ldots(2.16a)$$

$$B = 0.02154 - 0.000043\left(\frac{r_o}{r_i}\right), \text{ and} \qquad \ldots(2.16b)$$

$$C = 0.752 + 0.01657\left(\frac{r_o}{r_i}\right) - 0.000883\left(\frac{r_o}{r_i}\right)^2 . \qquad \ldots(2.16c)$$

Values of ϵ_M/ν and ψ are obtained from Figures 2.5 and 2.6, respectively. Dwyer compared Equation 2.16 with the experimental results of Subbotin et al[51] for mercury flowing through an annulus of $r_o/r_i = 1.09$ and of Petrovichev[52] for mercury flowing through annuli of $r_o/r_i = 1.55$ and $r_o/r_i = 1.67$ and found that Equation 2.16 agreed quite well with the data. Figure 2.8 contains a plot of Equation 2.16 for various r_o/r_i values.

2.2.4 Noncircular Ducts

Hartnett and Irvine[53] proposed an equation for finding the Nusselt number in turbulent flow for various geometries and boundary conditions by using a slug Nusselt number given by various experimenters, which is;

$$\overline{Nu}_{D_e} = (2/3)\overline{Nu}_s + 0.015\ Pe_{D_e}^{0.8} , \qquad \ldots(2.17$$

where the various boundary conditions are given in Figure 2.9 and the slug Nusselt numbers for simple geometries are given in Table 2.1 (see original paper for more complex geometries).

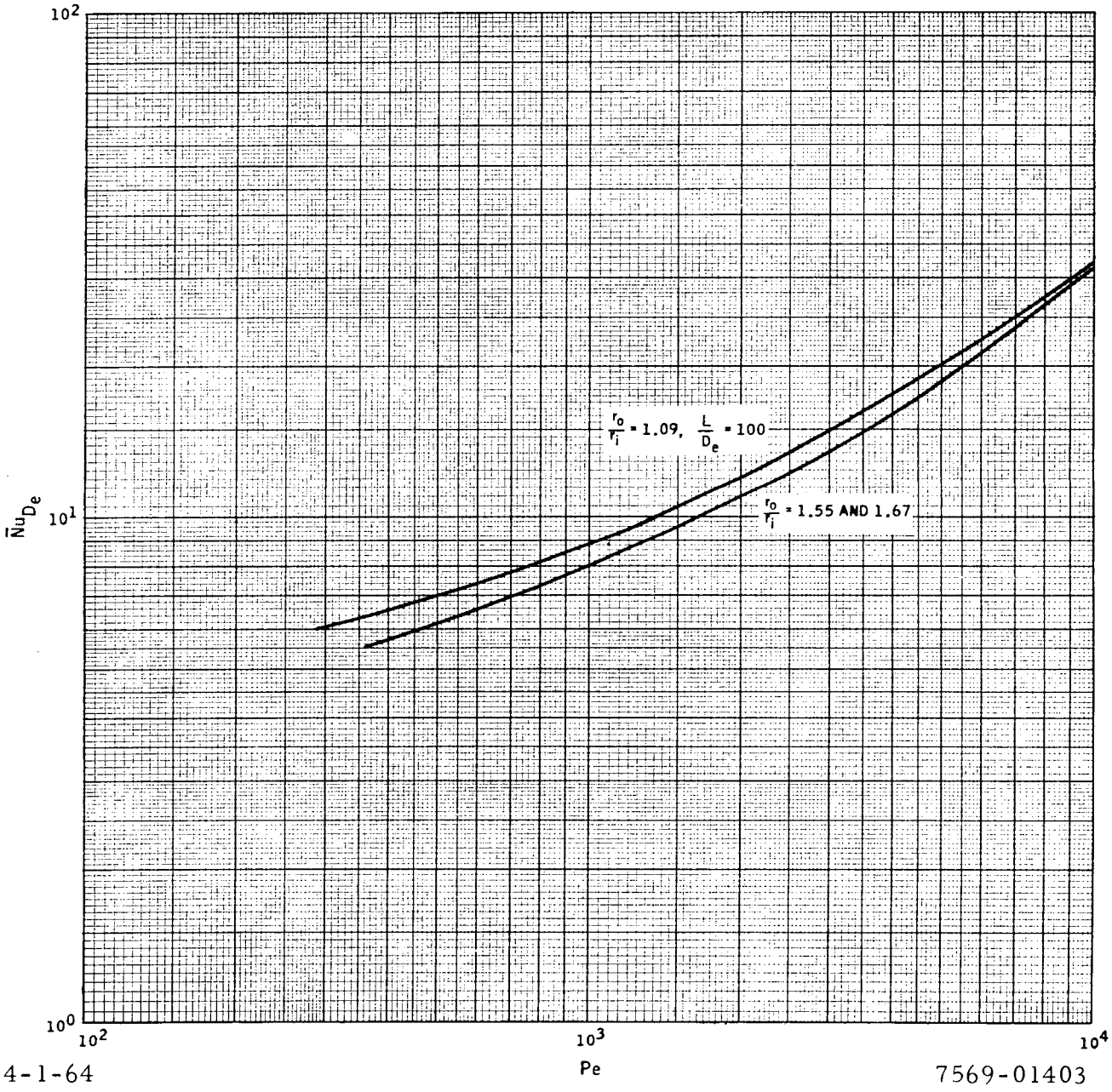

Figure 2.8 Nusselt Number vs Peclet Number for Mercury Flowing in Concentric Annuli Under Conditions of Constant Heat Flux and Heat Transfer Through Inner Wall Only

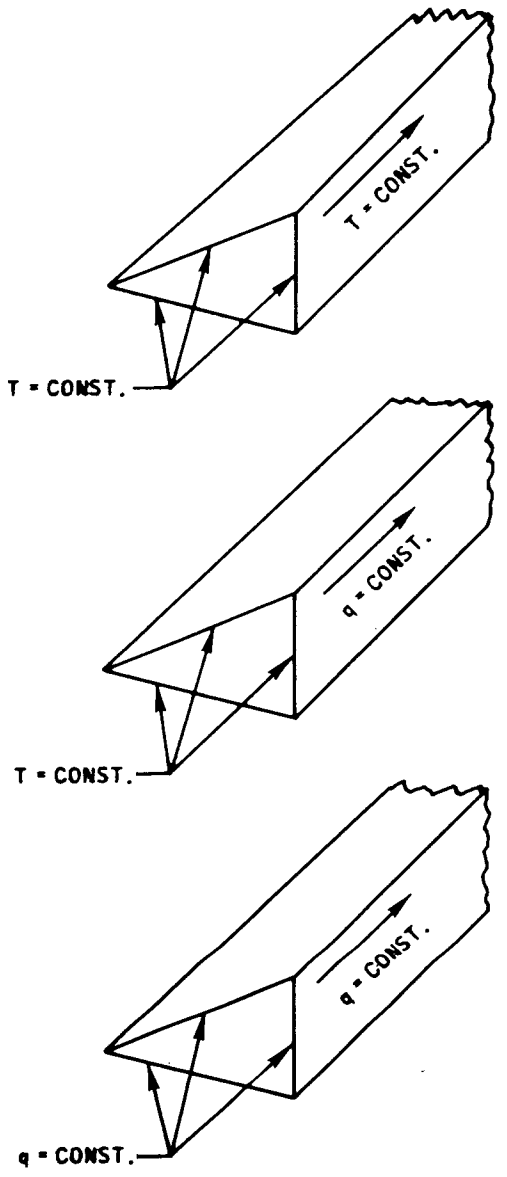

A. WALL TEMPERATURE CONSTANT IN FLOW DIRECTION AND AROUND PERIPHERY

B. CONSTANT HEAT INPUT PER UNIT LENGTH AND CONSTANT PERIPHERAL WALL TEMPERATURE AT A GIVEN AXIAL POSITION

C. CONSTANT HEAT INPUT PER UNIT LENGTH AND PER UNIT PERIPHERAL DISTANCE

4-1-64 7569-01404

Figure 2.9 Boundary Conditions of Importance For Noncircular Ducts

TABLE 2.1

SLUG NUSSELT NUMBERS FOR SIMPLE GEOMETRIES

Geometry	Boundary* Conditions	Slug Nusselt Number
Circle	A	5.80
	B	8.0
Square	A	$(\pi)^2/2 = 4.93$
	B	7.03
Equilateral triangle	A	?
	B	6.67
Infinite slot	A	$(\pi)^2 = 9.87$
	B	12
Infinite slot with one wall insulated	A	$(\pi)^2/2 = 4.93$
	B	6
90° isosceles triangle	A	?
	B	6.55

*See Figure 2.8

2.2.5 Shell Side Heat Transfer

Very few experiments have been conducted with liquid metals flowing parallel through equilateral triangular tube bundles. In fact Friedland et al[54] and Dwyer and Tu[55] seem to be the only experimenters that have published reproducible results for the above case. Dwyer[41] modified Dwyer and Tu's equation ($1.375 \leq P/D \leq 2.20$),

$$\overline{Nu}_D = 0.93 + 10.81\left(\frac{P}{D}\right) - 2.01\left(\frac{P}{D}\right)^2 + 0.0252\left(\frac{P}{D}\right)^{0.273} (\overline{\psi}\, Pe_D)^{0.8} \qquad \ldots (2.18)$$

which was for full-established turbulent flow ($10^2 \leq Pe \leq 10^4$) and constant heat flux, by using Figures 2.5 and 2.6 to obtain a value for ψ other than 1.0. Comparison of Equation 2.18 by Dwyer with the results of Friedland et al for mercury not wetting the tubes (no difference was found between wetted and unwetted walls if no entrained gas is present) showed excellent agreement between the two. Figure 2.10 gives a plot of Equation 2.18, for various P/D values, extrapolated into the streamline zone by Dwyer. Since Equation 2.18 was found only for mercury, it may also be used for the alkali metals (in other geometries the correlations hold for alkali metals as well as for mercury) until such data are available to warrant the use of a different equation.

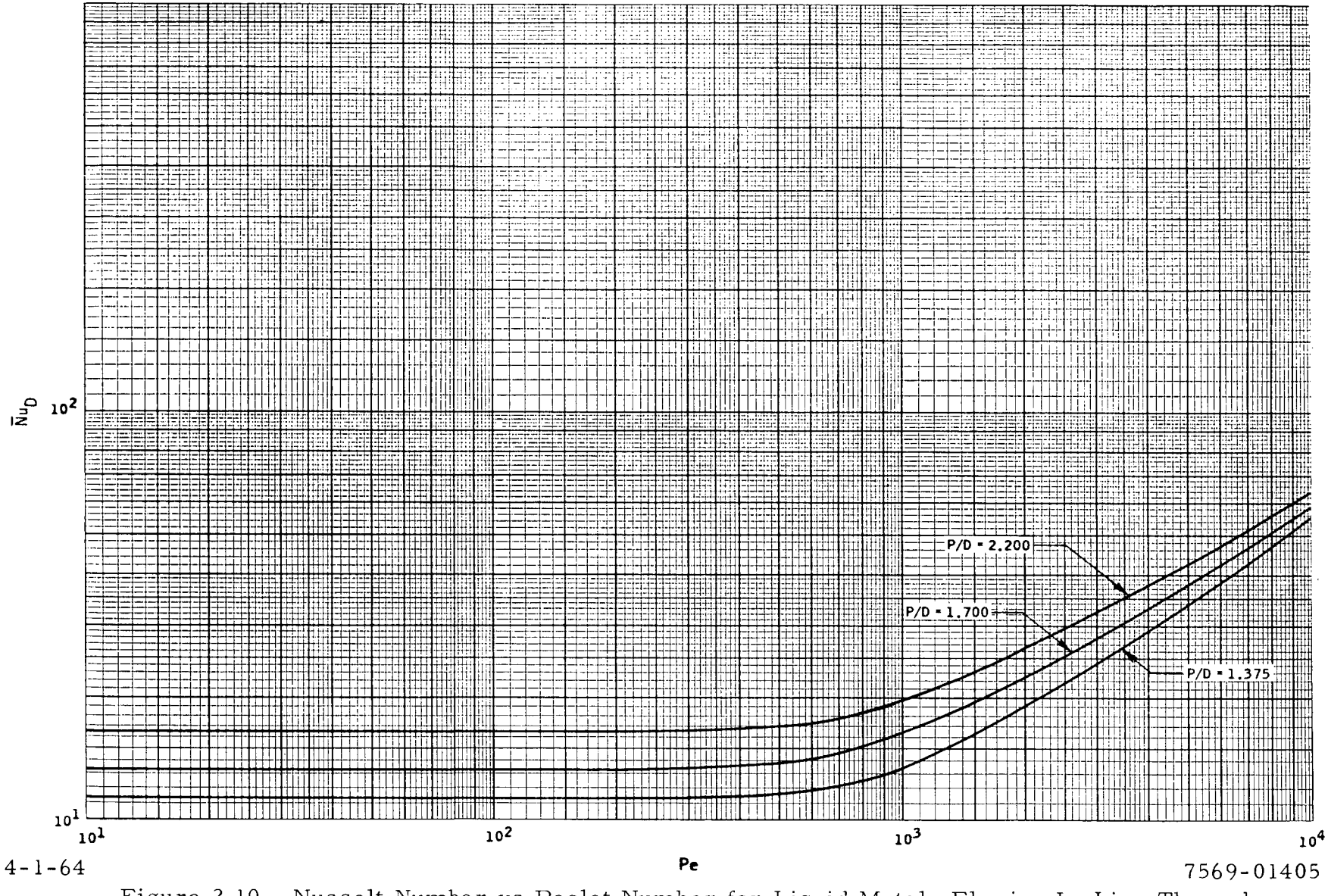

Figure 2.10. Nusselt Number vs Peclet Number for Liquid Metals Flowing In-Line Through Unbaffled Rod Bundles Under Constant Heat Flux and Fully Established Flow (Ref. 41)

Some work has also been done on cross-flowing liquid metals in equilateral triangular tube banks. Rickard, Dwyer, and Dropkin[56] obtained results with nonwetting and wetting mercury (no gas entrainment) under conditions of constant axial, not angular, heat flux (electrically heated tubes), and P/D equal to 1.37 and published the following equation:

$$\overline{Nu}_D = 4.03 + 0.228\ Pe_D^{0.67} \quad . \qquad \ldots(2.19)$$

McGoff and Mausteller[57] obtained results for NaK-56 heating the tubes on the inside and cooling by crossflow on the outside for a P/D ratio of 1.25. The author correlated their results into the following equation:

$$\overline{Nu}_D = 0.068 + 0.25\ Pe_D^{0.8} \quad . \qquad \ldots(2.20)$$

Equations 2.19 and 2.20 are plotted in Figure 2.11. Since Rickard, Dwyer, and Dropkin could not explain why the mercury results varied according to the 0.67 power of the Reynolds number as compared to McGoff and Mausteller's results, which varied according to the 0.8 power and because the mercury results differ to such a great extent from the NaK results, Equation 2.19 is recommended for mercury systems and Equation 2.20 for alkali metal systems until further experimental results are available to prove otherwise.

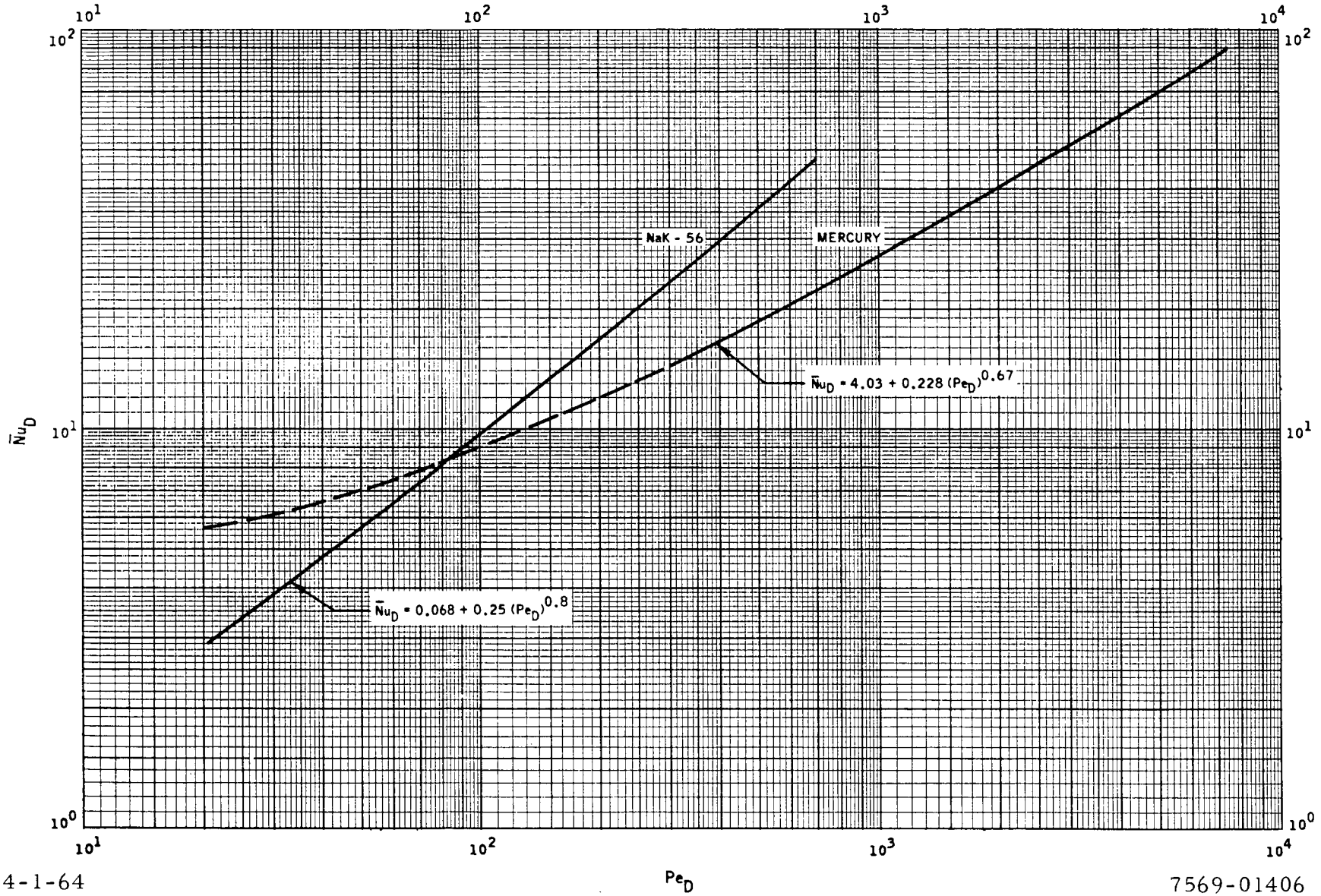

Figure 2.11 Average Nusselt Number vs Peclet Number for Cross-Flowing Through Equilateral Triangular Tube Bundles

NOMENCLATURE

c_p = Specific heat at constant pressure, Btu/lb-°F

D = Diameter of tube, ft

D_e = Equivalent diameter of a conduit other than a tube [D_e = 4 (cross sectional area/wetted perimeter)], ft. For two wide parallel plates close to each other, D_e equals two times the width of one plate.

h = Local heat transfer coefficient, Btu/hr-ft^2-°F

$\overline{h}$ = Averaged heat transfer coefficient over a length, Btu/hr-ft^2-°F

k = Thermal conductivity of fluid, Btu/hr-ft-°F

$\overline{Nu}$ = Average Nusselt number over a surface [$\overline{Nu}_D = (\overline{h}D/k)$], dimensionless. Subscript s will indicate the Nusselt number is for slug flow.

P = Tube pitch, i.e., distance between tube centers in a bundle, ft

Pe = Peclet number (Pe = RePr), dimensionless

Pr = Prandtl number [$Pr = (c_p \mu/k)$], dimensionless

r = Radius, ft

r_i = Inner radius of annulus, ft

r_o = Outer radius of annulus, ft

Re = Reynolds number [$Re_D = (\rho vD/\mu)$], dimensionless. Subscript D represents the geometrical dimension used in the definition of the Reynolds number.

v = Average velocity of fluid bulk, ft/hr

ϵ_H = Eddy diffusivity for heat transfer, ft^2/hr

ϵ_M = Eddy diffusivity for mass transfer, ft^2/hr

μ = Absolute viscosity, lb$_m$/hr-ft

ν = Kinematic viscosity, ft^2/hr

ρ = Density, lb$_m$/ft^3

$\overline{\psi}$ = Average value of ϵ_H/ϵ_M ratio, dimensionless

2.3 BOILING

Considerable attention has been given to boiling liquid metal heat transfer within the last few years. There exist only limited amounts of data on this mode of heat transfer. Recently several authors[58, 59, 60] have published literature surveys, while others[61, 62, 63, 64, 65, 66] have presented results on boiling liquid metal heat transfer. However, no adequate correlation has been developed to predict the local boiling heat transfer coefficient, mainly because programs were conducted to produce data for specific projects and conditions. What is needed to break through the barrier produced by the many variables – increased surface roughness, boiler pressure, or exit quality (for $x_e < 50\%$) increases the heat flux at a fixed temperature difference – in boiling heat transfer is an extensive experimental program conducted with the sole purpose of developing correlations that will adequately predict local heat transfer coefficients in two-phase flow. The following subsections contain information and conclusions formed by the author from the known available data on boiling heat transfer.

2.3.1 Pool and Forced Convection Boiling

Figure 2.12 contains all the known pool, nucleate boiling, heat flux data on liquid metals that are available. Lyon[67] performed a pool boiling experiment with pure mercury and mercury containing additives to promote wetting in order to obtain pool boiling heat flux data, which are shown in Figure 2.12 as a line to within ±10%. Lyon used a 3/4-in. diameter, horizontal, stainless steel cylinder to boil mercury over the outside surface at a saturation pressure of one atmosphere. The sodium data were obtained from Shulman[63] and Noyes[68] where sodium was pool boiled over a 1/4-in. diameter horizontal cylinder at various saturation pressures. Shulman used stainless steel heaters, while Noyes used both stainless steel and molybdenum heaters, and found a difference in heat fluxes existing at a given temperature difference which could not be explained. The potassium data were obtained from Reference 60 where potassium was pool boiled over a lapped and polished nickel plate at various saturation pressures. No significant spread in data existed over the range of pressures used, resulting in the data being represented in Figure 2.12 as one line to within ±15%. No boiling data were available for rubidium or lithium; however, a company-sponsored program on boiling rubidium is being conducted at Atomics International with the sole purpose of obtaining local heat transfer coefficients

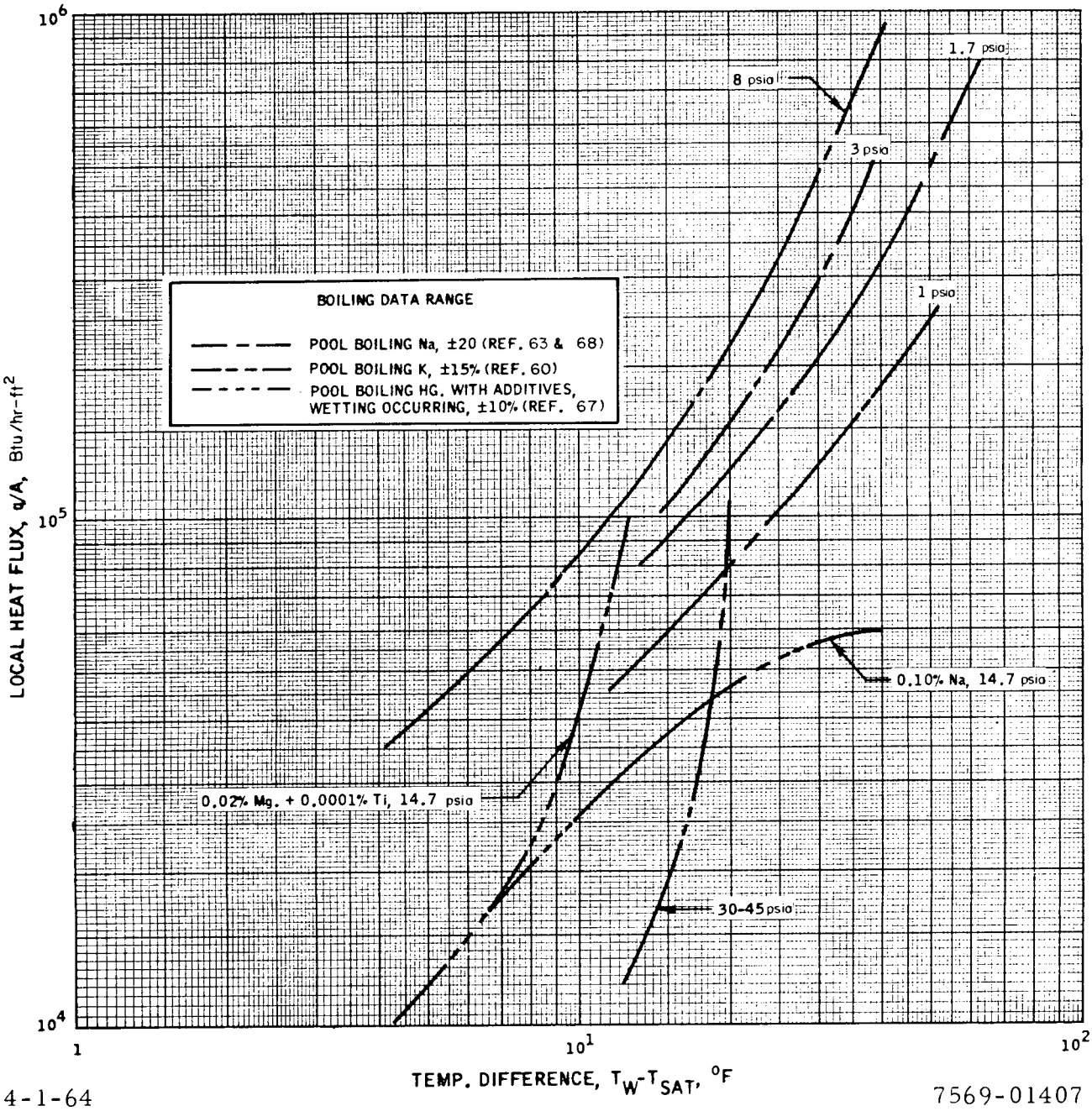

4-1-64 7569-01407

Figure 2.12. Saturated Pool Boiling Heat Flux vs ΔT, Wall Temperature Minus Saturation Temperature

as a function of pressure and quality in single and multirod flow channels. The range of variables are as follows: boiling temperature ranging from 1200 to 1800°F; heat fluxes up to 500,000 Btu/hr-ft^2; and quality ranging from 0 to 50%.[69]

Figures 2.13 to 2.15 represent a proposed method (formerly presented by Forster and Grief[65]) of determining saturated, forced convection, nucleate boiling heat fluxes in liquid metals for which saturated, pool boiling data are available (only mercury with additives, sodium, and potassium data were currently available). The major assumption involved in this method is that there exists a point along the pool boiling curve beyond which force convection has no effect on the existing heat flux; therefore, beyond this point the forced convection boiling heat flux is exactly equal to the pool boiling heat flux. This point can be determined by extending a constant Reynolds number forced convection curve (Figure 2.15) until it intersects the pool boiling curve. The heat flux at the intersection point (q_o in Figure 2.15) is multiplied by the factor, 1.3, resulting in a heat flux of q_1 which is the minimum heat flux for which pool boiling controls and determines the forced convection boiling heat flux.[65] At some finite amount below this point the forced convection boiling heat flux is exactly equal to the heat flux produced by forced convection only. A transition exists between these two heat flux producing mechanisms where both processes, forced convection and pool boiling, produce the forced convection boiling heat flux (Figures 2.14 and 2.15). Of course, if the forced convection Reynolds number is low enough so that it never intersects the pool boiling curve, as shown in Figure 2.13, the forced convection boiling heat flux will be controlled entirely by the pool boiling mechanism.

Essentially, the above method inplies that at small temperature differences the bubble activity is so low that negligible heat is transferred by this mechanism as compared to the forced convection mechanism. As the temperature difference increases, a transition is reached where the pool boiling mechanism begins to overcome the forced convection mechanism. At still larger temperature differences, the bubble activity is so great that it completely nullifies the forced convection mechanism. The author feels that this method of predicting forced convection boiling heat fluxes can not be used at high qualities ($x_e > 50\%$); slug or mist flow might exist thereby preventing a liquid film, by which bubbles transfer energy, from contacting the entire heat transfer surface.

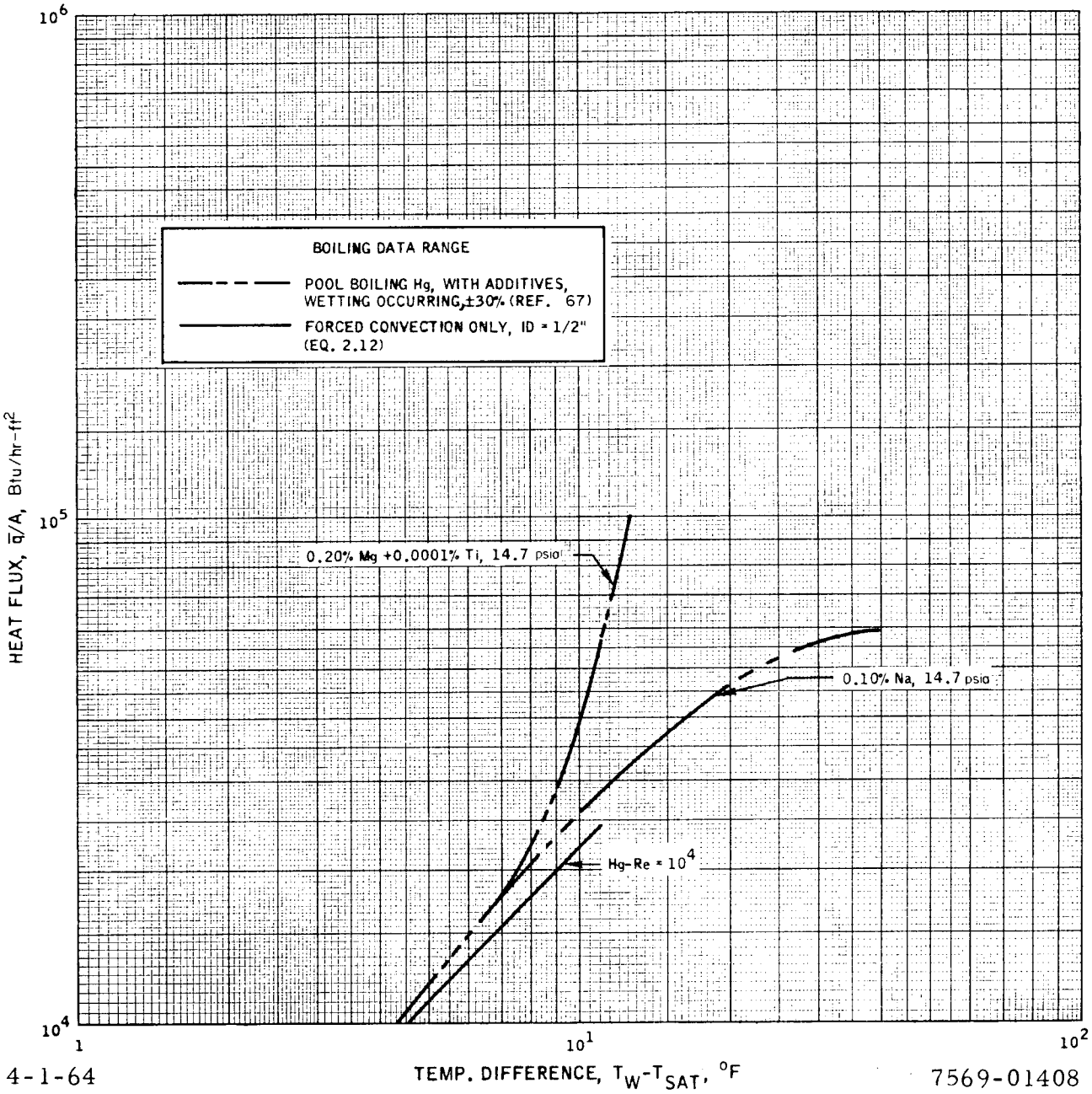

Figure 2.13. Superimposed Forced Convection Heat Flux and Pool Boiling Heat Flux Data For Prediction of Forced Convection Boiling Heat Fluxes in Mercury With Additives

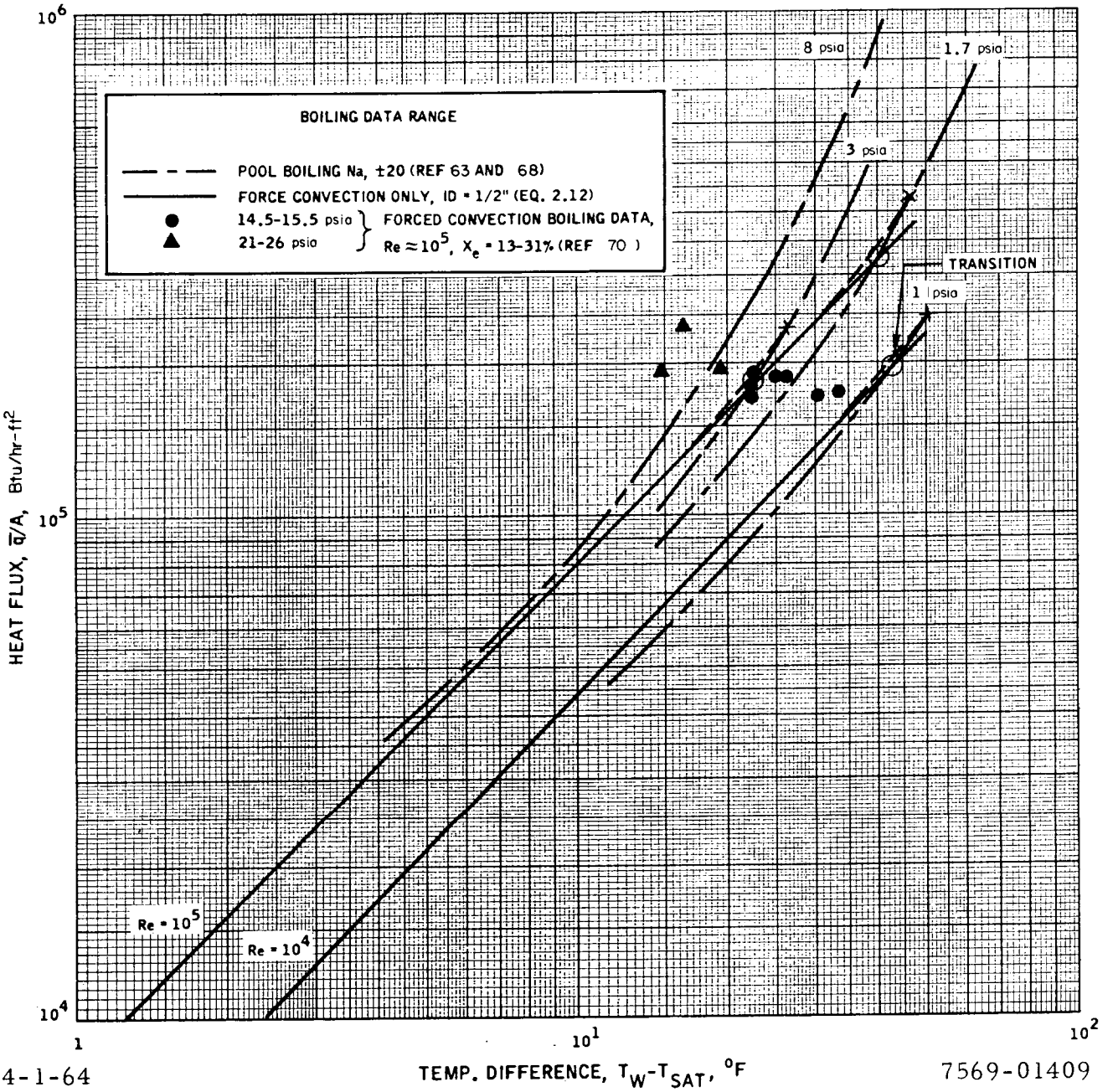

Figure 2.14. Superimposed Forced Convection Heat Flux and Pool Boiling Heat Flux Data For Prediction of Force Convection Boiling Heat Fluxes in Sodium

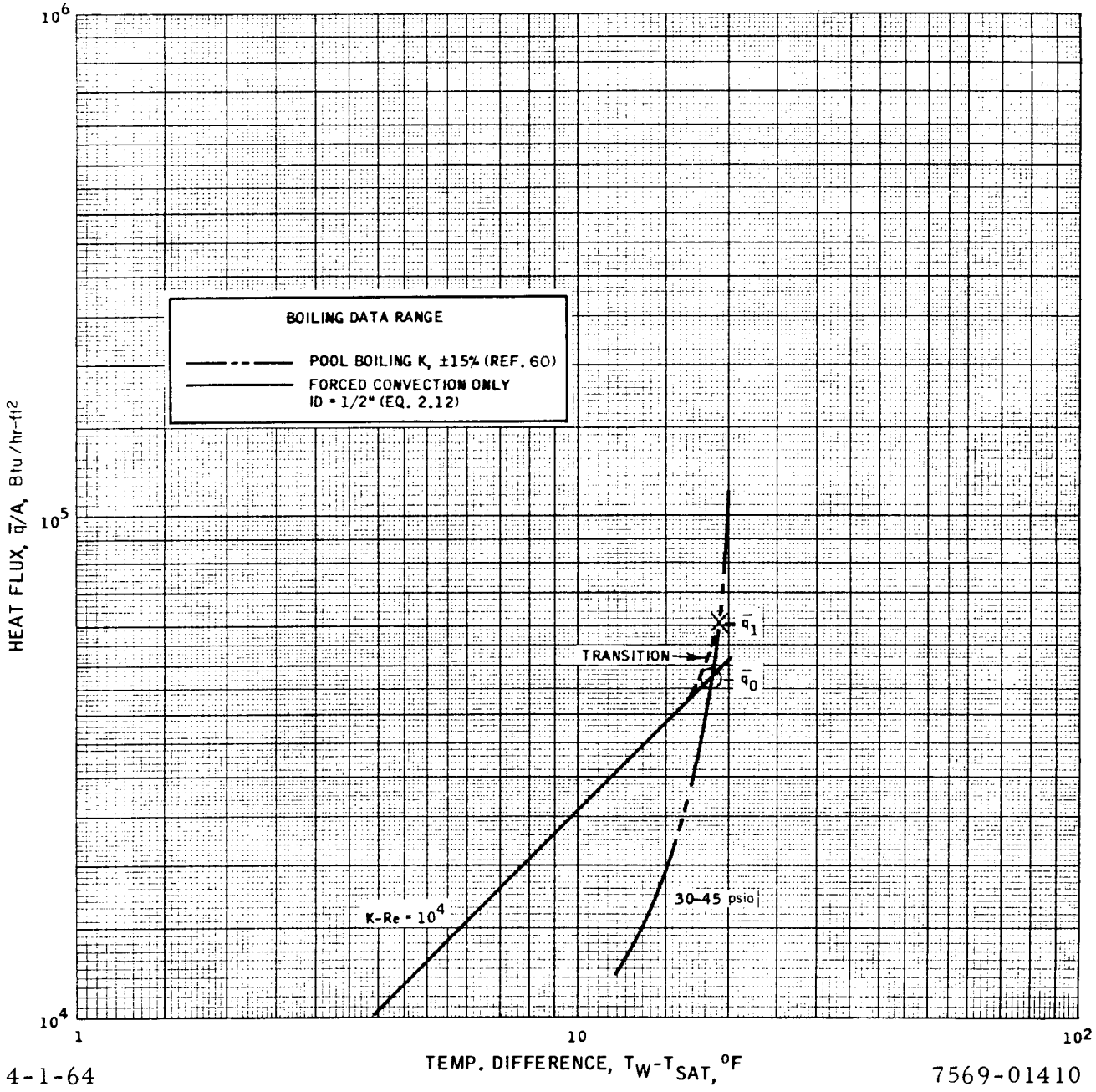

Figure 2.15. Superimposed Forced Convection Heat Flux and Pool Boiling Heat Flux Data For Prediction of Forced Convected Boiling Heat Fluxes in Potassium

Very little data on forced convection boiling heat transfer are available for comparison to the above hypothesis. Longo[70] presented some forced convection boiling results (x_e = 13 to 31%; Re $\cong 10^5$) on sodium which are presented in Figure 2.14 for comparison. One can see that Longo's results are somewhat lower than would be expected for forced convection boiling, since the boiler pressures are higher than the pool boiling results. But at least the results do indicate that the proposed method predicts saturated, forced convection, boiling heat fluxes to within experimental accuracy; as more data are obtained this conclusion will be proven more precisely.

The pressure and quality effects on the forced convection boiling heat transfer coefficient are shown in Figure 2.16 for informative purposes. The data shown are from the preliminary results of Longo[70] on sodium. One can see that at low pressures the boiling heat transfer coefficient is affected very little by quality. It is generally known that at high qualities the heat transfer coefficient decreases with increasing quality; therefore, as more data are generated the curves in Figure 2.16 can be completed for sodium as well as other liquid metals. It should be further noted that the data in Figure 2.16 were obtained as a specific pressure by fixing the heat flux and varying the flow rate which indicates that the quality and flow effects are compounded. Certain plans are being made in future tests to eliminate the compounded effect.[70]

Bersenson and Killackey[71] presented some film boiling results with potassium; however, their results were not included in this handbook, because their temperature differences were much too low for film boiling to occur.

Because of the complexity of designing a compact liquid metal boiler for space applications, a brief description of the SNAP 2 boiler (being used in a nuclear-powered Rankine cycle space system[72]) heat transfer characteristics is in order. However, such a description from References 73 and 74 is classified. The reader is referred to NAA-SR-8617 Vol I, Addendum I, which contains the classified portion of this handbook.

Zero gravity effects were also studied under the SNAP 2 program. Due to the high gravity force produced by the swirl wire insert, no noticeable change in the boiler performance occurred under zero gravity conditions.

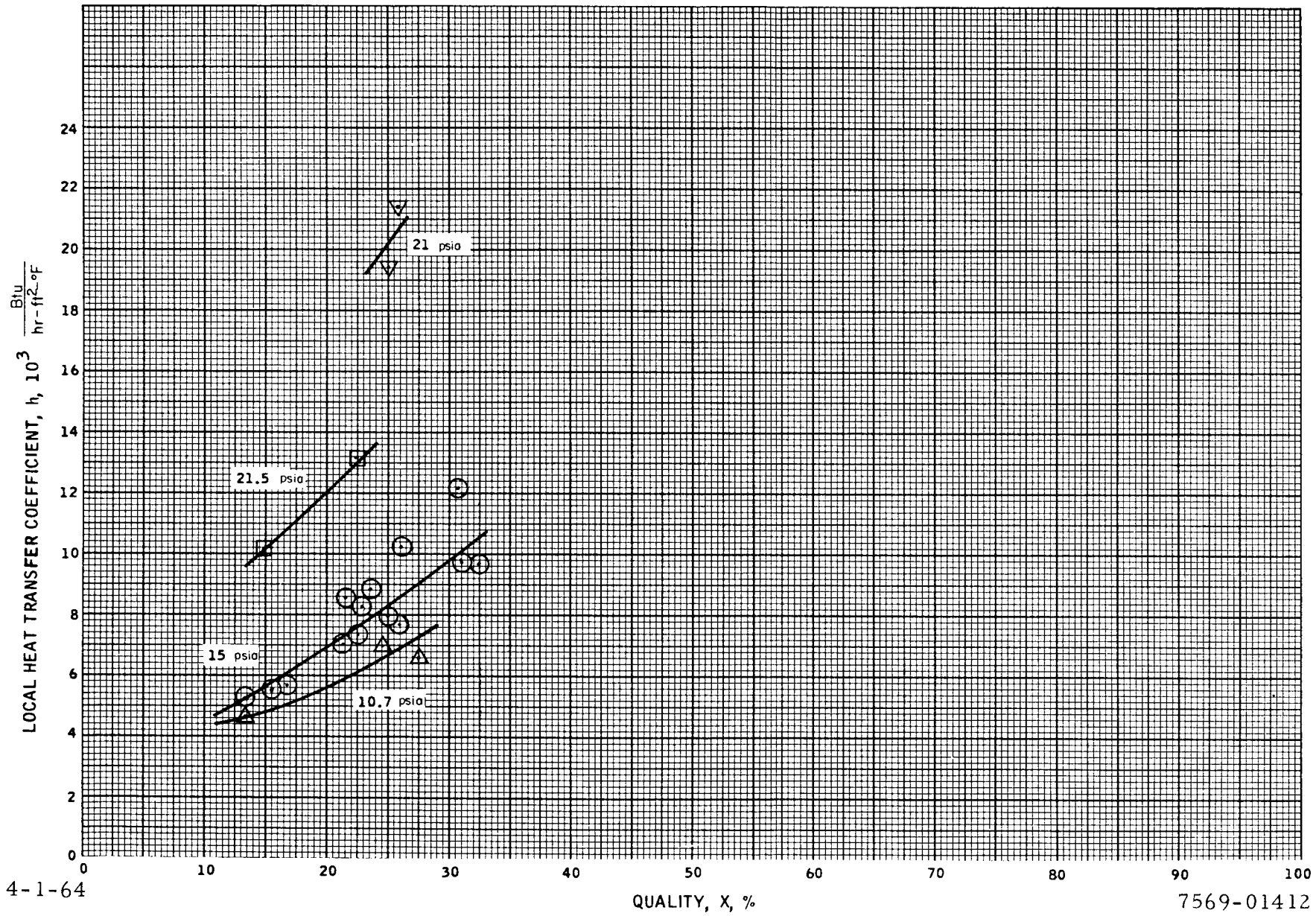

Figure 2.16. Sodium Forced Convection Boiling Heat Transfer Coefficient vs Quality and Pressure (Reference 70)

2.3.2 Critical Heat Flux

Many investigators have proposed analytical expressions for predicting the burnout (critical) heat flux in saturated, pool boiling water, while a few investigators[75, 76, 77] have extended their generalized correlation to boiling liquid metal. However, these correlations predict burnout heat fluxes approximately 75% below the experimental results.[68, 78] One of the most recent and somewhat successful burnout correlation for liquid metals was presented by Noyes,[68] who modified Addoms' correlation[79] in order to correlate the sodium, sulphur, liquefied gas, and "high-g" data with water and organic data. Noyes' correlation is as follows:

$$\left(\frac{q}{A}\right)_{C,P,sat} = 1.325\,\lambda\rho_v\left(\frac{\rho_\ell - \rho_v}{\rho_v}\right)^{0.545} \cdot (g\alpha)^{1/3} \cdot \left(\frac{Pr}{n}\right)^{1/12} \qquad \ldots(2.21)$$

Figure 2.17 contains plots of Equation 2.21 made by the author using the liquid metal properties from Section 1.2 of this handbook and Reference 2. Noyes' results[68] on saturated pool boiling sodium are represented in Figure 2.17 by the Na curve to within ±30%. Also contained in Figure 2.17 are preliminary burnout results on saturated, pool boiling potassium, which were recently published by Balzhiser.[78] Some agreement can be seen to exist between Equation 2.21 and Balzhiser's preliminary results. While more burnout results on liquid metals are needed to determine if Equation 2.21 is general enough to predict the saturated, pool boiling, critical heat flux for all wetting liquid metals, it shall be used until results are made available which tend to prove whether or not Equation 2.21 predicts erroneous burnout heat fluxes. In order to obtain a conservative estimation of potassium burnout heat fluxes which is normally used for design purposes, the following equation developed by the author and based on Balzhiser's data in Figure 2.17, should be used until Equation 2.21 is proven to be correct for all liquid metals:

$$\left(\frac{q}{A}\right)_{C,P,sat} = (3.962 \times 10^5)p^{0.173} \quad . \qquad \ldots(2.22)$$

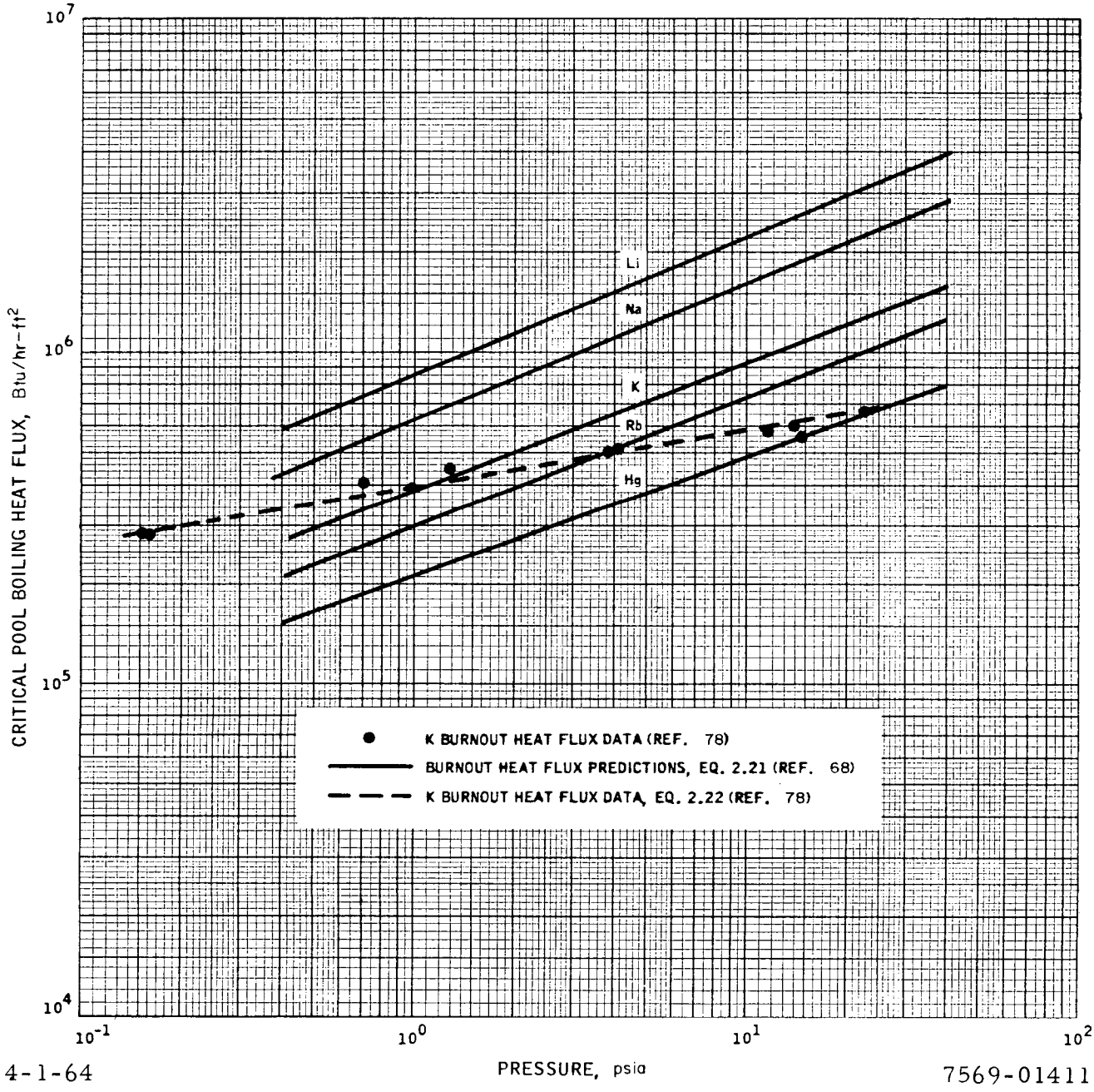

Figure 2.17. Pool Boiling Burnout Heat Flux vs Saturation Pressure For Liquid Metals

It should also be noted that the author compared the burnout predictions of Zuber and Tribus[64] with Equation 2.21 resulting in 75% lower values. It was concluded that Equation 2.21 was the best general correlation available.

The presence of forced convection and subcooling greatly complicates the problem of predicting the burnout heat flux, which is ~20 to 150% higher, depending upon the amount of subcooling and forced convection, than the saturated, pool boiling, critical heat flux. Very little advancement has been made in this area since experimental data are not readily available. Gambill[80] proposed an additive method for the forced convection contribution and a multiplying factor to take into account subcooling. Hoffman[61] proposed to compare critical heat fluxes in liquid metals to Lowdermilk's results[81] on water. Some results were obtained with potassium and compared favorably (within 10%)[82] to Lowdermilk's correlations, which are as follows:

In the low-velocity high-exit-quality region, for $G/(L/D)^2 < 150$,

$$\left(\frac{q}{A}\right)_{C,F,sub} = 270G^{0.85}D^{-0.2}\left(\frac{L}{D}\right)^{-0.85}, \qquad \ldots(2.23)$$

and in the high-velocity low-exit-quality region, for $G/(L/D)^2 > 150$,

$$\left(\frac{q}{A}\right)_{C,F,sub} = 1400G^{0.5}D^{-0.2}\left(\frac{L}{D}\right)^{-0.15} \qquad \ldots(2.24)$$

The range of variables used in Lowdermilk's experiment are as follows: stable flow occurred; velocity ranged from 0.1 to 98 ft/sec; pressure ranged from atmospheric to 100 psi; subcooling ranged from 0 to 140°F; tube diameter ranged from 0.051 to 0.188 in.; and length-to-diameter ratio ranged from 25 to 250. Until more experimental data becomes available, Equations 2.23 and 2.24 should be used to predict forced convection, subcooled, critical, boil-heat fluxes with caution.

NOMENCLATURE

c_p = Specific heat at constant pressure, $Btu/lb_m\text{-}°F$

D = Diameter, ft

g = Local acceleration, ft/hr^2

G = Mass velocity, $lb_m/hr\text{-}ft^2$

h = Local heat transfer coefficient, $Btu/hr\text{-}ft^2\text{-}°F$

$\bar{h}$ = Average heat transfer coefficient, $Btu/hr\text{-}ft^2\text{-}°F$

k = Thermal conductivity, $Btu/hr\text{-}ft\text{-}°F$

L = Length, ft

n = Number of local accelerations (g's), nondimensional

p = Pressure, psia

Pr = Liquid Prandtl number $[Pr = (\mu c_p/k)]$, nondimensional

q = Local heat transfer rate, Btu/hr

$\bar{q}$ = Average heat transfer rate, Btu/hr

$q/A, \bar{q}/A$ = Heat flux, $Btu/hr\text{-}ft^2$. Subscripts C, P, sat, F, and sub indicate critical, pool, saturated, forced, and subcooled, respectively.

Re = Reynolds number $[Re_D = (\rho vD/\mu)]$, nondimensional

T = Temperature, °F. Subscripts w, b, f, sat, and v indicate wall, bulk, film, saturation, and vapor, respectively.

v = Average velocity of fluid bulk, ft/hr

x = Quality, vapor wt %. Subscripts e and i indicate exit and inlet, respectively.

α = Liquid thermal diffusivity $[\alpha = (k/\rho c_p)]$, ft^2/hr

λ = Latent heat of vaporization, Btu/lb_m

μ = Absolute viscosity, $lb_m/ft\text{-}hr$

ρ = Density, lb_m/ft^3. Subscripts ℓ and v indicate liquid and vapor, respectively.

2.4 CONDENSING

There exists, basically, two types of condensation – dropwise and filmwise – by which vapor transfers heat to a wall. If a liquid metal wets the wall, a film of liquid metal forms, resulting in filmwise condensation. Dropwise condensation exists when the liquid metal is unable to wet the surface; the vapor condenses in drops rather than as a continuous film. Somewhat higher heat transfer coefficients are obtained in dropwise condensation as compared to filmwise condensation, because the vapor transfers its energy directly to the surface instead of through a film. Due to the high thermal conductivity of a liquid metal, the advantage of dropwise condensation is somewhat suppressed as compared to dropwise condensation for steam, which results in four to eight times higher heat transfer coefficients than in filmwise condensation. However, dropwise condensation rarely exists with liquid metals, except with mercury which has the property of not wetting most metallic surfaces.

While very little data have been published on boiling heat transfer, still smaller amounts have been published on condensing heat transfer. Cohn[58] performed a literature survey on the heat transfer properties of mercury which summarizes all work conducted prior to the year 1960. Bonilla and Misra[83,84] obtained results for mercury and sodium condensing in a vertical, natural convection tube (Figure 2.18)(sodium was condensed in a 45° inclined tube). No explanation was given as to why the low-heat flux, air-cooled condenser gave lower heat transfer coefficients than the high-heat flux, water-cooled condenser, except that filmwise condensation may have existed in the air-cooled condenser. Cohn[85] obtained results for pure mercury and mercury with a sodium additive condensing is a vertical, natural convection, air-cooled condenser which almost matched Bonilla and Misra's results.[84] Filmwise condensation was assumed to exist. No effect on the heat transfer coefficient was observed when the additive was used; this is probably due to the sodium additive not being volatile enough in the mercury vapor. Cohn's results are presented in Figure 2.18. Reed and Noyes[86] condensed sodium underneath a horizontal, natural convection, water-cooled plate; their results are presented in Figure 2.18. No statement was made as to whether the condensation was filmwise or dropwise, but it probably was filmwise, since sodium does eventually wet most surfaces. Brooks[87] presented some preliminary results, which are shown in Figure 2.18, on potassium

condensing in a vertical, downward forced convection flow, sodium-cooled tube. No correlations have been developed from the data to accurately predict condensing heat transfer coefficients in liquid metals.

Reed and Noyes[86] and Misra and Bonilla[84] studied the effects of noncondensable gases being present in the condenser for sodium and mercury, respectively. It can be concluded from their work that the condensing heat transfer coefficient drastically decreasing (somewhat exponentially) as the amount of noncondensibles increases. Figure 2.19 contains the results of Reed and Noyes. The independent variable (effective noncondensable gas layer) is defined by the following equation:

$$t \equiv \frac{L(p_t - \bar{p}_2)}{p_t} = \frac{\rho_2 \bar{D}_{12}}{G_2}\left(\frac{p_t - p_{20}}{p_t}\right)\left[1 - \exp\left(-\frac{G_2 L}{\rho_2 \bar{D}_{12}}\right)\right]. \qquad \ldots(2.25)$$

This method of correlation was used so that a gas heat transfer resistance could be defined in terms of the effective thickness of the noncondensable gas. However, the author feels that more work is needed in this field in order to better understand and predict condensing heat transfer coefficients in a system containing noncondensables.

It should be briefly noted that in forced convection systems zero gravity has no effect on the condensing process, due to the dynamic force from forced convection overriding the effect of gravity.

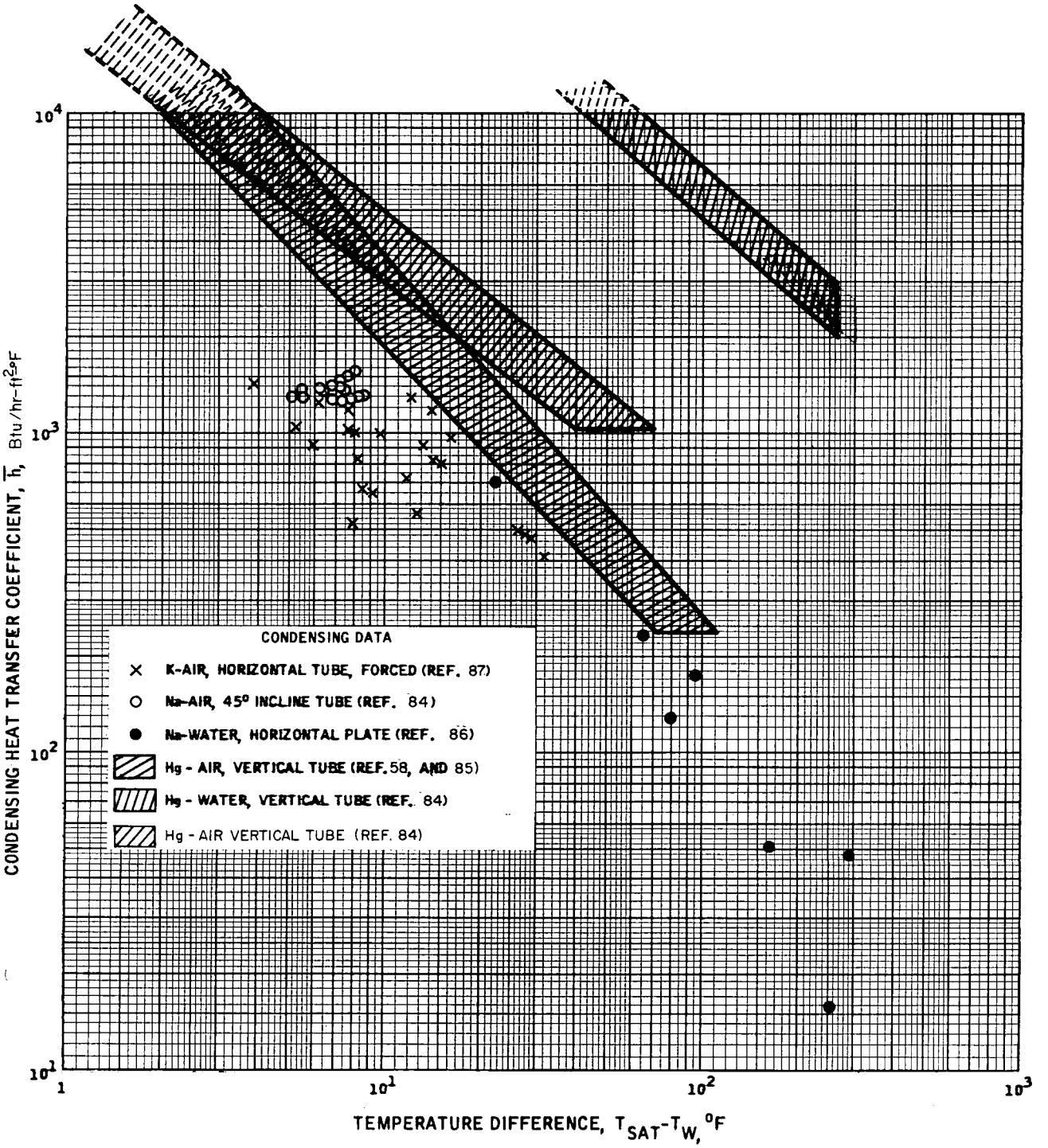

4-1-64 7569-01413

Figure 2.18. Condensing Heat Transfer Coefficients vs $T_{sat} - T_w$

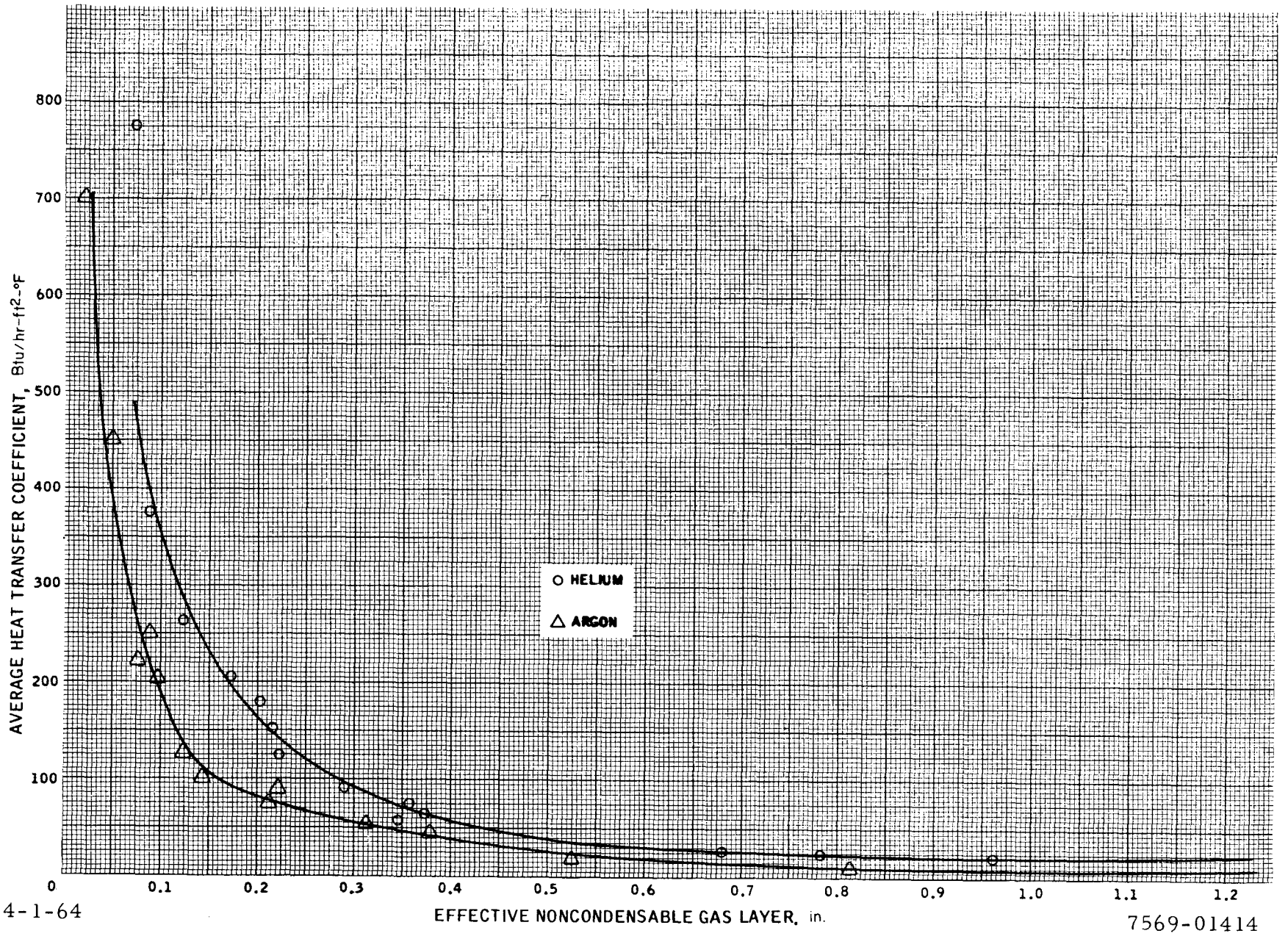

Figure 2.19 Effect of Noncondensable Gas on Sodium Condensing Heat Transfer (Reference 86)

NOMENCLATURE

C_1 = Constant dependent on the noncondensable gas (0.0079 for helium and 0.00223 for argon)

$\overline{D}_{12}$ = Average binary diffusion coefficient, ft^2/hr

G = Mass velocity, $lb_m/hr\text{-}ft^2$. Subscript 2 indicates liquid metal vapor.

$\overline{h}$ = Average heat transfer coefficient, $Btu/hr\text{-}ft^2\text{-}°F$

L = Distance between condensing surface and liquid metal vapor-liquid interface, ft

M = Molecular weight. Subscript 2 indicates liquid metal vapor.

p = Partical pressure, lb_f/ft^2. Subscripts t, 1, 2, and 20 indicate total system, noncondensable gas, liquid metal vapor, and liquid metal vapor partial pressure at condensing surface, respectively.

T = Temperature, °R. Subscript t indicates mean system temperature of gas mixture.

t = Effective noncondensable gas layer thickness, ft

$\overline{R}$ = Universal gas constant; = 1545 $ft\text{-}lb_f/lb\ mol\text{-}°R$

ρ_2 = Density of liquid metal vapor $[\rho_2 = (p_t M_2/\overline{R}T_t)]$, lb_m/ft^3

$\rho_2\overline{D}_{12}$ = Pressure independent effective diffusion coefficient $(\rho_2\overline{D}_{12} = C_1\sqrt{T_t})$, $lb_m/ft\text{-}hr$

3.0 MATERIAL TRANSFER

3.1 MATERIAL COMPATIBILITY

Because of the ever increasing use of liquid metals in heat transfer systems, the problem of corrosion has reached a point where research and development on corrosion resistant materials is needed prior to system construction. Materials must be found which will be compatible at high temperatures and for long periods of time. Unfortunately, no model has been developed to predict corrosion rates, probably because of the many variables and types of corrosion that are present in a system. Allowable corrosion rates should not be formulated, since the allowable corrosion will depend entirely upon the component's location in the system. It should also be pointed out that extensive mass transport of the corrosion products to the colder portions of the system may result in "plugging." The measured corrosion rate at the hotter portions may not give a good indication of how much precipitation develops at the colder region; because as the corrosion products precipitate out chemically or physically, bonded materials from the coolant stream may accompany the precipitation. Therefore, the possibility of "plugging" must also be considered, in addition to corrosion rates, when designing a dynamic system.

The following three sections will briefly outline the mechanisms and prevention of corrosion and a summary of dynamic corrosion data using mercury, sodium, NaK, potassium, rubidium, or lithium. These sections are by no means complete since there is currently much research being done in this field.

3.1.1 Corrosion[3,88,89,90]

Corrosion will be defined in the broad sense as the destruction of a metal by chemical, electrochemical, or physical (such as erosion, solution, and cavitation) means. There are in general two types of attack, intergranular (metal is attached along the grain boundaries) and transgranular (metal is attacked within the grains); these are controlled by four mechanisms of corrosion, which will be discussed in the following paragraphs.

Dissolution of solid metal in liquid metal is the first mechanism which is influenced by the chemical potential of "A" in the solid metal relative to "A" in the liquid metal. Its rate is controlled by the diffusion rate of the solute and the rate of reaction between the liquid and the solid. High energy regions, such

as twinned regions (produced by the application of stress) and grain boundaries, greatly accelerate the dissolution rate. The reader is referred to other authors [91,92] for a detailed description of the process and variables involved. The presence of impurities, such as oxygen, carbon, etc., in the grain and grain boundaries greatly control the depth of penetration by the liquid metal by precipitating out at the grain boundaries and reacting with the liquid metal. Decarburization of low alloy steel by a liquid metal is an example of this leaching type of corrosion mechanism.

Dissolution of liquid metals in solids is the second mechanism of corrosion where the liquid metal, or its impurities, diffuse into the solid and form compounds. This phenomenon can reduce the stability of a metal phase or even change phases. The presence of nitrogen in the liquid metal can either stabilize a metal (stainless steel) or produce a nitride as in a lithium system, which is corrosive to most metal or ceramic containers.[88]

Diffusion welding is another mechanism of corrosion which occurs due to the presence of a liquid metal acting as a bridge between the two metals tending to weld together. The presence of pressure holding the metals together, or increases in system temperature, greatly increase diffusion welding. In fact, the presence of valves, pumps, etc., may determine the upper temperature limit due to the occurrence of diffusion welding in these components.

Erosion is another mechanism of corrosion. This mechanism is exceedingly important in orifices and nozzles. It results from the flowing liquid metal mechanically removing scale or particles from the metal and may create cavities under extreme erosion.

The amount of corrosion is usually measured in two ways — depth of penetration per exposed time and amount of material transport per exposed time. There are two mechanisms that control the amount of transport through the liquid metal; thermal-gradient mass transfer (also called solubility-gradient mass transfer) and concentration-gradient mass transfer (also called activity-gradient or dissimilar-metal mass transfer). Liquid metal systems automatically satisfy the requirements of mass transfer, since the system cannot be isothermal, if heat is to be obtained from it; and it seldom occurs that the metal loops are constructed entirely from the same material.

Temperature-gradient mass transfer occurs due to a finite solubility of one or more components of the structural material in the liquid metal, a temperature effect on solubility, and an anisothermal liquid metal coolant. Material that is being transferred dissolves into the liquid metal (usually in the "hot" zone), is transported to another part of the system (usually the "cold" zone), and "plates out" onto the metal surface. The process is controlled by either the rate of solution or deposition or by the diffusion rate of the transported material through the metal to the liquid-metal interface. "Plugging" is an excellent example of this type of material transfer.

Concentration-gradient mass transfer will occur when different materials with different concentrations, which act as the driving force or potential, of at least one constituent, are present. A constituent having the lower affinity for a metal will dissolve into the liquid metal and be carried along until it "sees" a metal having a higher affinity. The constituent then leaves the coolant and diffuses into this metal, thus completing the cycle, which continues until the affinity for this constituent in both metals are equal. The rate of material transfer may be controlled by the diffusion rates through each metal, by the rate of transfer through the liquid metal coolant, or/and by the rate of solution or depletion at the metal surface. An excellent example of this type of material transfer is the transfer of carbon from low alloy steel to stainless steel in sodium systems.[89]

3.1.2 Inhibition of Corrosion

There are only a few methods by which corrosion in a dynamic, anisothermal system can be reduced. The use of inhibitors (scavenging type or diffusion-barrier type) may effectively reduce corrosion.[93] The scavenging-type of inhibitor acts by removing the impurities (oxides, nitrides, hydrides, etc.) from the liquid metal that are responsible for accelerating corrosion, by either increasing the rate of mass transfer or reacting with the container material, thus depleting the container of its constitutents. In order for this type of inhibitor to be successful, its thermodynamic stability with the impurity must be much greater than that of the impurity with the container. The scavenger may be present as either dissolved atoms in the liquid metal or a solid suspended in the stream of liquid metal, both methods of location having its advantages and disadvantages.[93] Examples of the scavenging type of inhibitors are magnesium, titanium, and zirconium which are used to deoxidize liquid sodium.[94] Hot trapping would also be an example of this method of corrosion reduction.

The diffusion-barrier type of inhibitor acts by forming a protective surface film on the container, which prevents the container from coming into contact with the liquid metal; which in turn decreases the rate of solution of the container material, thus reducing corrosion. For successful reduction of corcorion by a diffusion-barrier type of inhibitor, certain requirements must be met as follows: (1) large negative free energy of formation of the film layer must exist; (2) the film must be chemically inert to all components of the system, including impurities that may come into contact with the inhibiting layer; (3) stability of the film must exist; and (4) the container's solubility and diffusion rate in the film must be low.[93] Examples of the diffusion-barrier type of inhibitor is calcium plus titanium or zirconium which is used to reduce mass transfer of iron in liquid mercury.[95]

Heat treatment may be used to reduce corrosion on materials containing carbon. If carbides exist along the grain boundaries of the solid, spheriodizing heat treatment can effectively reduce intergranular attack by removing these carbides from the grain boundaries.[88]

Purification during operation by either cold trapping or hot trapping (discussed earlier) can effectively reduce corrosion, if impurities are the cause of such corrosion. Unfortunately in some systems, the impurity concentration can not be reduced sufficiently to prevent excessive mass transfer (corrosion). Davis and Draycott[94] demonstrated that the oxide concentration could not be reduced to a tolerable level by cold trapping in a niobium or vanadium loop. Hot trapping had to be incorporated into the system.

3.1.3 Choice of Material

Many authors [2,3,88,96] have attempted to summarize the corrosion results of other experimenters. Unfortunately test times, temperatures, and metal surface conditions were in most cases not clearly reported. Because of the numerous static tests conducted and reported elsewhere, only recent dynamic and semistatic tests will be summarized in this report. The reader is referred to References 2, 3, 88, 96, and 97 that summarize the early static and dynamic tests. The following sections contain corrosion data on the six liquid metals considered in this handbook.

3.1.3.1 Mercury

Most of the material compatibility investigations with mercury have been done for SNAP 2 program. One of the most extensive corrosion tests[98] conducted was done by first screening materials using bent reflex tubes at 900°F or 1100°F and then using two-phase, natural circulation loops constructed from the materials that proved satisfactory in the bent reflex tube (BRT) tests. The reader is referred to Reference 98 for the discussion and results of the materials tested (low- and high-alloy steels, 300 and 400 series stainless steels, precipitation hardening steels, nickel- and cobalt-base alloys, and nonmetallics). Figure 3.1 somewhat summarizes very briefly the results of Reference 98.

Ellis[99] reported some bent reflux tube tests using mercury with nickel-base braze alloys, which also was done under the SNAP 2 program. Brazing was done in a vacuum and for 10 min at temperature. Table 3.1 summarizes these scattered tests, from which no conclusions were drawn. Reference 100 is an extension of the work by Ellis and presents corrosion and subsequent mass transfer results on materials that are being considered for use in the SNAP 2 system. The reader is referred to NAA-SR-8617 Vol I, Addendum I for the discussion on Reference 100, since it is classified.

3.1.3.2 Sodium

Davis and Draycott[94] reported on some extensive forced convection loop tests conducted to determine the effect of sodium on material specimens, such as stainless steel, various ferritic steels, nickel, titanium, zirconium and alloys, niobium, vanadium, uranium and fission products, thorium, and beryllium. The largest part of their work was conducted to determine the effect of oxygen in the liquid metal on niobium (columbium) and vanadium which resulted in concluding that the mechanism of excessive attack was oxide controlled.

Some tests were conducted using NaK instead of sodium which seemed to pose no problem, since sodium is oxidized preferentially to potassium; however, some potassium oxide might exist, because some kind of equilibrium would seem likely to occur. Therefore, the corrosion results will have to be verified before it can be definitely stated that the oxide causing the corrosion is sodium oxide only. However, it can be stated that misleading results are obtained if

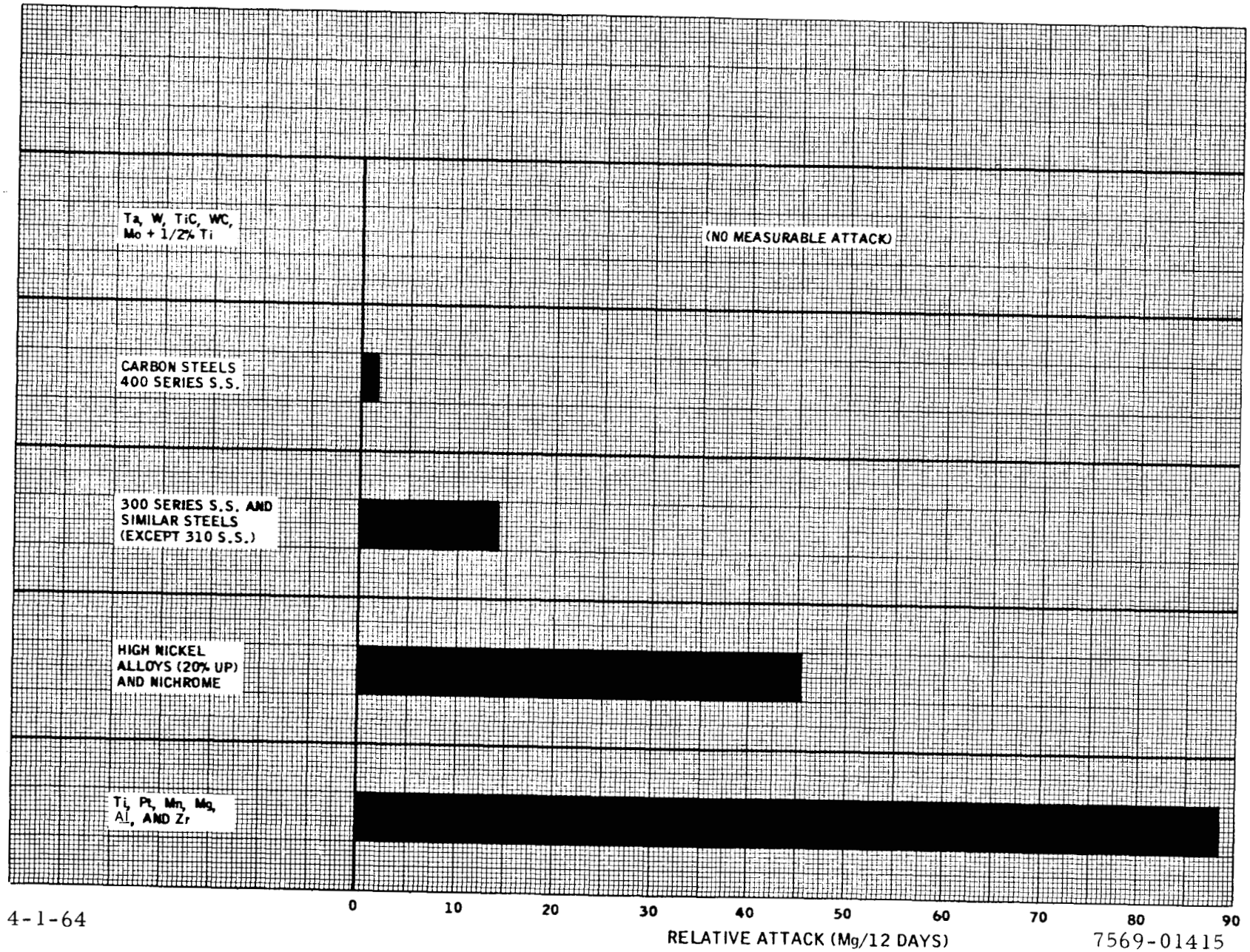

Figure 3.1 Relative Corrosion of Some Material in Mercury at 900°F (Reference 98, 102)

TABLE 3.1

Hg CORROSION RESULTS OF NICKEL-BRAZED SPECIMENS (PH15-7 Mo)
TESTED IN BRT FOR 30 DAYS AT 900°F (REF. 99)

Braze Alloy (wt %)	Braze Temperature (°F)	Weight Change (mg)	Penetration* (in.)
Nicrobraze No. LC (Ni + 13.5 Cr + 4.5 Fe + 3.5 B + 0.15 C + 4.5 Si)	2150	+0.2	0.0014
Repeated	2075	-10.6	0.0104
Repeated	2075	-5.0	0.0016
Nicrobraze No. LM (Ni + 65 Cr + 2.5 Fe + 3.0 B + 0.15 C + 4.5 Si)	1900	-9.3	0.0144
Repeated	1900	-5.6	0.0014
Nicrobraze No. 150 (Ni + 15.0 Cr + 3.5 B + 0.15 C)	2150	-13.2	0.0076
Repeated	2150	-6.7	0.0094
Repeated	2075	-10.0	0.0063
Repeated	2075	-9.3	0.0076
Nicrobraze No. 130 (Ni + 3.0 B + 0.15 C + 4.5 Si)	1875	-1.4	0.0055
Nicrobraze No. 30 (Ni + 19.0 Cr + 0.15 C + 10.0 Si)	2175	-7.6	0.0041
Repeated	2175	-3.6	0.0096

*Penetration is defined as the maximum local surface recession due to the mercury test environment.

the corrosion is dependent upon the formation of alloys or solutions with either sodium or potassium; this does not seem to be the case with niobium, vanadium, uranium, zirconium, and nickel materials. A summary of some of the corrosion results of Reference 94 is given in Tables 3.2 through 3.12.

Hoffman and Manly[101,102] also summarized some results which are worth presenting for the sake of a very brief outlook upon the materials problem with sodium. Figure 3.2 is a representation of Hoffman and Manly's conclusions.

Wagner and Kline[103] tested some zirconium alloys in natural convection, cold trapped (O_2 at 10 ppm) sodium for various lengths of time. Their results are summarized in Table 3.13.

3.1.3.3 NaK

The eutectic sodium-potassium alloy has received considerable attention due to the SNAP 2 program. Perlow[104] presented results from corrosion studies conducted with NaK-78 which are presented in Tables 3.14 and 3.15.

Page[89] made a literature search and presented results from the tab- corrosion studies at Atomics International and mass transfer studies at the Oak Ridge National Laboratory. From the data available, the conclusion was formed that NaK corrosion with metals other than refractory materials was by carbon transfer above 800°F, intergranular penetration between 1000 and 1400°F induced by oxygen, and nickel and chromium transfer above 1400°F.

3.1.3.4 Potassium

Jansen and Hoffman[105] have conducted some compatibility tests using natural circulated, boiling potassium loops with two different materials. Their results are classified; therefore, refer to NAA-SR-8617, Vol I, Addendum 1 for this information. Tests with a Cb + 1% Zr alloy are being conducted, but as yet have not been reported.

Hammond and Littman[106] presented some corrosion results using refractory material specimens inserted in a forced convection, boiling potassium loop. Table 3.16 summarizes their results, which are very misleading

TABLE 3.2

NIOBIUM CORROSION IN COLD TRAPPED CIRCUITS
(Reference 94)

Test Number	Duration of Test (hr)	Temperature of Specimen (°C)	Velocity (ft/sec)	Cold Trap Temperature (°C)	Weight Change ($g/dm^2/mo$)	Penetration Rate (mil/mo)
1	500	370	1.31	140	-0.093	0.042
2	500	370	2.07	140	-0.086	0.039
3	500	370	3.58	140	-0.099	0.045
4	500	370	5.86	140	-0.079	0.035
5	500	370	11.32	140	-0.090	0.040
6	500	405	1.32	140	-1.57	0.71
7	500	405	2.09	140	-1.83	0.82
8	500	405	3.62	140	-2.44	1.09
9	500	405	5.93	140	-2.70	1.22
10	500	405	11.42	140	-5.21	2.34
11	500	456	1.35	140	-7.77	3.49
12	500	456	2.13	140	-8.83	3.75
13	500	456	3.69	140	-15.7	7.07
14	500	456	6.04	140	-21.2	9.54
15	500	456	11.65	140	-49.2	22.11
16	500	500	1.36	140	-17.5	7.86
17	500	500	2.15	140	-25.9	11.68
18	500	500	3.73	140	-36.3	16.64
19	500	500	6.12	140	-47.4	21.37
20	500	500	11.79	140	Completely corroded	30
21	350	600	5.5	120	-1.60	0.74
22	350	600	5.5	240	-2.92	1.34
23	336	600	16.2	125	-33.34	15.35
24	336	600	24.2	125	-42.75	19.63
25	336	600	27.1	125	-55.5	25.60
26	336	600	29.5	125	-71.6	32.90

NOTE: Liquid metal Tests 1 to 20, NaK-78; Tests 21 to 26, NaK-30.
Material Tests 1 to 20, tubes; Tests 21 to 26, sheets.

TABLE 3.3

NIOBIUM – REDUCTIONS OF CORROSION RATE EFFECTED BY INCORPORATION OF DEOXIDANTS INTO THE CIRCUIT
(Reference 94)

Test No.	Duration of Test (hr)	Temperature of Specimen (°C)	Velocity (ft/sec)	Method of Oxide Control	Measured O Level (ppm)	Weight Change ($g/dm^2/mo$)	Penetration Rate (mils/mo)
Deoxidant-Magnesium*							
1	250	500	1.34	120°C cold trapped for 72 hr. Specimens then raised to test condition – 10% of flow passed through Mg dispenser at 400°C.	-	-0.0347	0.0155
2	250	500	2.10		-	-0.278	0.1239
3	250	500	3.64		-	-0.138	0.0618
4	250	500	5.96		-	-0.352	0.1571
5	250	500	11.46		-	-0.145	0.0646
				Preclean Conditions			
6	176	600	30	110°C CT§ 4 hr Mg dispenser 185°C 24 hr	-	-0.0358	0.016
7	357	600	25	120°C CT§ 35 hr Mg dispenser 200°C 35 hr	-	+0.048	No loss
8	350	600	25	130°C CT§ 124 hr Mg dispenser 200°C 29 hr	-	+0.040	No loss
Deoxidant-Titanium†							
				Preclean Conditions			
1	12	550	30	120°C CT§ 6 hr Ti HT** 650°C 12 hr	10	-10.72	5.24
2	72	540	30	120°C CT§ 24 hr Ti HT** 650°C 48 hr	3	-0.7	0.33
3	302	550	30	120°C CT§ 24 hr Ti HT** 650°C 48 hr	3	-0.116	0.054
Deoxidant-Zirconium†							
				Preclean Conditions			
1	168	600	30	120°C CT§ 24 hr 600°C Zr HT** 48 hr	49	-0.1334	0.061
2	163	600	30	120°C CT§ 24 hr 600°C Zr HT** 48 hr	63	-6.34	2.92
3	168	500/600	30	120°C CT§ 48 hr 500°C Zr HT** 72 hr	4	-0.099	0.045
4	256	600	30	120°C CT§ 48 hr 600°C Zr HT** 72 hr	28	-0.0575	0.025
5	162	600	30	120°C CT§ 48 hr 600°C Zr HT** 72 hr	5	-0.161	0.074

*Liquid metal 1 to 5 NaK-78, 6 to 8 NaK-30
†Liquid metal Na
§CT = cold trapped
**HT = hot trapped
All material, tubes

TABLE 3.4

VANADIUM CORROSION IN COLD TRAPPED CIRCUITS
(Reference 94)

Test No.	Temperature of Specimen (°C)	Velocity (ft/sec)	Weight Change ($g/dm^2/mo$)	Penetration Rate (mils/mo)
1	350	1.845	-0.828	0.53
2	350	2.91	-1.635	1.06
3	350	5.04	-2.670	1.74
4	350	8.24	-3.280	2.12
5	350	15.89	-5.230	3.38
6	394	0.85	-2.78	1.79
7	394	1.34	-3.31	2.13
8	394	2.33	-5.37	3.46
9	394	3.81	-7.51	4.84
10	394	7.31	-9.42	6.07
11	406	1.878	-5.46	3.52
12	406	2.96	-8.49	5.47
13	406	5.13	-12.82	8.27
14	406	8.38	-16.45	10.62
15	406	16.15	-21.94	14.12
16	460	0.875	-7.71	4.98
17	460	1.37	-11.52	7.58
18	460	2.38	-15.89	10.26
19	460	3.90	-20.30	13.20
20	460	7.57	-23.10	14.70
21	600	5.5	-9.12	5.8

NOTE: Duration of test 500 hr except for Test 21 (350 hr)
Cold trap temperature 141°C except for Test 21 (120°C)
Liquid metal NaK-78 except for Test 21 (NaK-30)
Material all tube except Test 21 which was sheet

TABLE 3.5

VANADIUM REDUCTIONS OF CORROSION RATE EFFECTED BY INCORPORATION OF DEOXIDANTS INTO THE CIRCUIT
(Reference 94)

Test No.	Duration of Test (hr)	Temperature of Specimen (°C)	Velocity (ft/sec)	Method of Oxide Control	Measured O Level (ppm)	Weight Change ($g/dm^2/mo$)	Penetration Rate (mils/mo)
Deoxidant-Magnesium							
1	350	600	5.5	120°C CT 24 hr 0.01% Mg added	-	-0.072	0.046
Deoxidant-Titanium							
2	350	550	5.5	120°C CT 48 hr HT 700° - 24 hr	-	-0.019	0.012
3	136	600	25	120°C CT 48 hr HT 700° - 72 hr	8	-0.047	0.3
Deoxidant-Zirconium							
4	127	600	25	120°C CT 48 hr HT 600° - 72 hr	8	-0.298	0.190
5	216	550	25	120°C CT 48 hr HT 600° - 72 hr	5	-0.036	0.023
6	393	580	25	120°C CT 48 hr HT 600° - 72 hr	-	-0.033	0.021

NOTE: Penetration rate at same temperature and velocity under CT conditions 5.8 for Test 1.
Liquid metal NaK-30 for Test 1, Na for other tests.
Material Tests 1 and 2, sheet; Tests 3 to 6, tube.

TABLE 3.6

STAINLESS STEEL 18-1-1
CORROSION IN COLD TRAPPED CIRCUITS
(Reference 94)

Test No.	Temperature of Specimen (°C)	Velocity (ft/sec)	Weight Change ($g/dm^2/mo$)	Penetration Rate (mils/mo)
1	400	4	+0.0028	-
2	400	8	+0.0003	-
3	400	10	-0.0032	0.0017
4	600	5.5	+0.0022	-
5	600	0.1	-0.0138	0.0068

NOTE: Form of material for all tests, 18-8-1 SS sheet, except Test 5 which was tube. Cold trap temperature for all tests 130°C, except Test 5 (100°C). Liquid metal for all tests, Na, except Test 5 (NaK-78). Duration of Tests 1 to 4, 350 hr, Test 5, 500 hr.

TABLE 3.7

URANIUM CORROSION IN COLD TRAPPED CIRCUITS
(Reference 94)

Test Number	Temperature of Specimen (°C)	Velocity (ft/sec)	Weight Change ($g/dm^2/mo$)	Penetration Rate (mil/mo)
1	511	1.02	-6.53	1.33
2	511	1.67	-9.04	1.84
3	581	1.67	-13.95	2.85
4	581	3.21	-22.2	4.33

NOTES:
Form of material – quadrant of 1.5 in. disc, pickled.
Duration of test, 500 hr
Cold trap temperature, 180°C
Liquid metal, NaK-78

TABLE 3.8

ZIRCONIUM CORROSION IN COLD TRAPPED CIRCUITS
(Reference 94)

Test No.	Material	Temperature of Specimen (°C)	Velocity (ft/sec)	Cold Trap Temperature (°C)	Weight Change (g/dm^2)
1	Tube-pickled	393	1.0	120	-0.012
2	Tube-pickled	393	1.6	120	-0.016
3	Tube-pickled	393	2.8	120	-0.013
4	Tube-pickled	393	4.6	120	-0.022
5	Tube-pickled	393	8.8	120	+0.006
6	Tube-pickled	467	1.05	120	+0.008
7	Tube-pickled	467	1.7	120	+0.015
8	Tube-pickled	467	2.9	120	+0.021
9	Tube-pickled	467	4.7	120	+0.013
10	Tube-pickled	467	9.0	120	+0.062
11	Tube-pickled	550	1.08	120	+0.028
12	Tube-pickled	550	1.7	120	+0.042
13	Tube-pickled	550	3.0	120	+0.046
14	Tube-pickled	550	4.8	120	+0.039
15	Tube-pickled	550	9.3	120	+0.006
16	Tube-pickled	481	2.1	180	+0.0563
17	Tube-pickled	481	3.4	180	+0.0527
18	Tube	481	3.4	180	+0.0461
19	Tube-pickled	523	2.2	180	+0.0727
20	Tube-pickled	523	3.5	180	+0.0725
21	Tube	523	3.5	180	+0.0593
22	Arc melted-pickled	550	3.5	150	+0.0463
23	Arc melted-pickled	550	2	150	+0.0500
24	Carbon melted as received	600	4.8	145	+0.225
25	Carbon melted-pickled	600	4.8	145	+0.156
26	Arc melted as received	600	4.8	145	+0.163
27	Arc melted-pickled	600	4.8	145	+0.162
28	Arc melted-pickled	650	4.8	160	+0.309
29	Arc melted-pickled	650	3.5	160	+0.300
30	Arc melted-pickled	650	2.0	160	+0.294
31	Arc melted-pickled + 200 ppm N_2	650	4.8	160	+0.339
32	Arc melted-pickled + 100 ppm N_2	650	4.8	160	+0.329
33	Arc melted-pickled	650	3.5	160	+0.344
34	Arc melted-pickled + 50 ppm N_2	650	4.8	160	+0.352
35	Arc melted-pickled	650	2.0	160	+0.325

NOTE: Liquid metal for Tests 1 to 21 (NaK-78), Tests 22 to 35 (Na)
Duration of Tests 1 to 5, 500 hr; Tests 6 to 15, 250 hr; Tests 16 to 21, 2288 hr, Tests 22 to 27, 350 hr; Tests 28 to 35, 700 hr.

TABLE 3.9

FERRITIC STEELS CORROSION IN COLD TRAPPED SODIUM
(Reference 94)

Test No.	Type of Material and Preparation	Velocity (ft/sec)	Weight Change ($g/cm^2/mo$)	
			400°C	550°C
1	Hitem: 1/2% Cu steel	5.5	-0.01302	-0.0826
2	Hitem: 1/2% Cu normalized	2.0	-0.0127	-0.0746
3	Hitem: 1/2% Cu normalized and stress relieved	5.5	-0.00496	-0.0816
4	C - 1% Mn steel	5.5	-0.0124	-0.1068
5	C - 1% Mn steel normalized	2.0	-0.0093	-0.0988
6	C - 1% Mn steel normalized and stress relieved	5.5	-0.00404	-0.0510
7	1% Cr - 1/2% Mo	5.5	-0.0149	-0.047
8	1% Cr - 1/2% Mo normalized	2.2	-0.01304	-0.0476
9	1% Cr - 1/2% Mo normalized and stress relieved	5.5	-0.00404	-0.051
10	1/2% Mo - 1/4% V	5.5	-0.00558	-0.0498
11	1/2% Mo - 1/4% V normalized and tempered	4.0	-0.0059	-0.0542
12	1/2% Mo - 1/4% V normalized, tempered, and stress relieved	5.5	-0.00992	-0.0506

NOTE: Unless otherwise stated, experiments were carried out to 18-8-1 SS loops, and all in sodium. As decarburization occurred in most cases at 550°C, conversions of weight losses to penetration rates are worthless and are not given. Duration of all tests 350 hr. Cold trap temperature all tests 120°C.

TABLE 3.10

2-1/4% Cr - 1/2% Mo STEEL CORROSION IN COLD TRAPPED CIRCUITS
(Reference 94)

Test No.	Material Preparation	Velocity (ft/sec)	Weight Change ($g/dm^2/mo$)	Metallographic Examination
1	As received	5.5	-0.00532	No decarburization
2	As received	5.5	-0.03974	Slight evidence of decarburization, the edge grains being mainly ferritic.
3	Annealed	4.8	-0.0358	Each end of the specimen showed an area 0.012 in. deep of diminished pearlite intensity
5	Normalized and tempered	4.8	-0.0358	
6	Annealed and stress-relieved	4.8	-0.0282	
7	Annealed and stress-relieved	2.2	-0.0290	
8	Normalized, tempered, and stress-relieved	4.8	-0.0239	
9	Normalized, tempered, and stress-relieved	2.2	-0.0172	
10	Annealed and spot welds	3.5	-0.0276	
11	Normalized, tempered, and spot welds	3.5	-0.0231	
12	Annealed, spot welds, and stress-relieved	2.2	-0.0304	Each end of the specimen showed an area 0.012 in. deep of diminished pearlite content.
13	Annealed, spot welds, and stress-relieved	4.8	-0.0342	
14	Normalized, tempered, spot welds, and stress-relieved	4.8	-0.0307	
15	Normalized, tempered, spot welds, and stress-relieved	2.2	-0.0169	

NOTE: Tests carried out in 18-8-1 SS rigs and in sodium. Penetration rates are not quoted because of the possibility of occurrence of decarburization. Duration of Test 1 and 2, 350 hr; Tests 3 to 15 700 hr. Temperature of specimens – Test 1, 400°C, other tests 550°C. Temperature of cold trap – Tests 1 and 2, 120°C, other tests 150°C.

TABLE 3.11

NICKEL CORROSION IN NaK-78, COLD TRAPPED AT 120°C
(Reference 94)

Test No.	Temperature of Specimen (°C)	Velocity (ft/sec)	Weight Change ($g/dm^2/mo$)	Penetration Rate (mils/mo)
1	464	1.57	+0.0028	-
2	464	2.52	-0.0576	0.00258
3	464	4.28	-0.01585	0.00071
4	499	1.57	+0.00865	-
5	499	2.52	+0.0072	-
6	499	4.28	+0.0153	-
7	542	0.92	-0.104	0.00465
8	542	1.48	+0.0048	-
9	542	2.52	+0.0176	-
10	590	0.92	+0.0272	-
11	590	1.48	+0.0208	-
12	590	2.52	+0.0176	-

NOTE: Material, all tube.
Duration of test — Test 1 to 6, 500 hr; Tests 7 to 12, 450 hr.

TABLE 3.12

TITANIUM CORROSION IN SODIUM,
COLD TRAPPED AT 120°C
(Reference 94)

Test No.	Duration of Test (hr)	Temperature (°C)	Weight Change ($g/dm^2/mo$)
1	440	400	+0.0012
2	6.7	500	-12.0
	16.7		-15.0
	33		-16.4
	83		-11.7
	167		-9.1
3	6.7	650	-47.0
	16.7		-42.8
	33		-40.0
	83		-54.4
	167		-40.8

NOTE: Na velocity; 5.5 ft/sec.

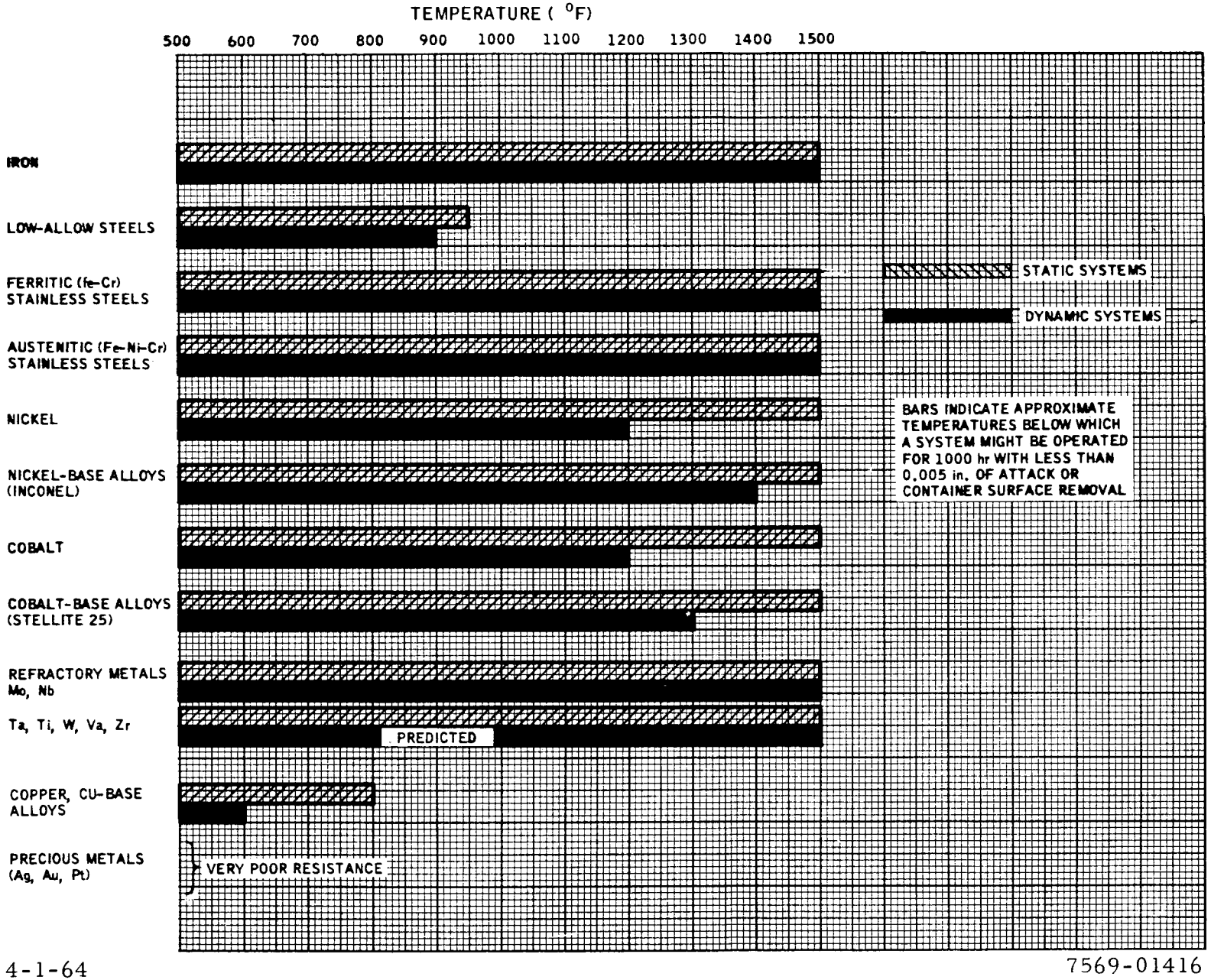

Figure 3.2 Corrosion Resistance of Various Metals and Alloys in Sodium (Reference 101)

TABLE 3.13

CORROSION OF ZIRCONIUM AND ZIRCONIUM ALLOYS IN 1000°F NATURAL CIRCULATED SODIUM
(Reference 103)

Alloy (wt %)	Average Weight Gain (mg/cm^2)						
	Hours						
	75	163	303	500	1000	1500	2500
Zr	0.14	0.23	0.33	0.30	0.55	0.50	0.56
Zr + 1.5 Al	0.16	0.26	0.37	-	-	-	-
Zr + 1.5 Al + 1.5 Sn	0.14	0.24	0.36	-	-	-	-
Zr + 1.5 Al + 3 Sn	0.15	0.21	0.27	0.27	0.49	0.38	0.41
Zr + 1.5 Al + 1.5 Mo	0.22	0.35	0.44	0.46	0.73	0.61	0.59
Zr + 1.5 Al + 1.5 Sn + 1.5 Mo	0.18	0.33	0.40	-	-	-	-
Zr + 3 Al	0.18	0.25	0.31	-	-	-	-
Zr + 3 Al + 1.5 Sn	0.17	0.25	0.29	0.30	0.45	0.39	0.39
Zr + 3 Al + 3 Sn	0.17	0.22	0.27	0.26	0.45	0.35	0.35
Zr + 3 Al + 1.5 Sn + 1.5 Mo	0.23	0.31	0.36	0.35	0.56	0.43	0.52
Zr + 2 Al	0.17	0.26	0.39	-	-	-	-

TABLE 3.14

1200°F NaK-78 CORROSION DATA
(Reference 104)

Specimen	Duration (hr)	Type and Rate of Attack
304 SS*	1500	No apparent attack
	2500	0.0014 in. intergranular corrosion
	3500	Evidence of general corrosion
	4500	0.0015 in. pitting
316 SS*	1000	0.0026 in. general corrosion
	2000	0.0025 in. intergranular corrosion
	3000	0.0010 in. general corrosion
347 SS*	1500	0.0007 in. intergranular corrosion
	2500	0.0020 in. general corrosion
	3500	0.0019 in. intergranular corrosion
	4500	0.0020 in. pitting
Hastelloy N	1500	Slight evidence of general corrosion
	2500	No apparent attack
	3500	No apparent attack
	4500	0.0014 in. intergranular corrosion
Columbium†	1000	No evidence of intergranular attack or general corrosion

*Stainless steel
†This specimen at 1300°F

TABLE 3.15

1400°F NaK-78 CORROSION DATA
(Reference 104)

Specimen	Duration (hr)	Type and Rate of Attack
304 SS*	1500	No apparent attack, slight evidence of decarburization
	2500	0.0014 in. pitting
	3500	0.0013 in. intergranular corrosion
	4500	0.0023 in. decarburization
316 SS*	1000	Slight evidence of general corrosion
	2000	0.0004 in. decarburization
	3000	0.0008 in. decarburization
347 SS*	1500	0.0006 in. intergranular corrosion
	2500	0.0004 in. pitting
	3500	General corrosion to a depth of 0.0006 in.
	4500	0.0025 in. decarburization
Hastelloy N	1500	Slight evidence of intergranular attack
	2500	General corrosion to a depth of 0.0005 in.
	3500	No apparent attack
	4500	Very slight surface attack
Haynes 25	1000	0.0002 in. pitting
	2000	Very slight evidence of general corrosion
	3000	0.0011 in. decarburization
Molybdenum	1000	No apparent attack
	2000	No apparent attack
	3000	Slight pitting, no depth
Inconel X	1000	No apparent attack
	2000	Very slight general corrosion
	3000	Very slight pitting, no depth
Hastelloy C	1000	0.0010 in. pitting
	2000	0.0017 in. decarburization

*Stainless Steel

TABLE 3.16

REFRACTORY MATERIAL CORROSION RESULTS WITH POTASSIUM
(Reference 106)

Sample Location	Conditions	Specimen Material	Weight Loss (mg/cm^2)
Purification Loop	Liquid velocity 10 ft/sec 11 hr at 1000 to 1150 °F	Cb	2.1
		Cb + 1% Zr	1.7
		Ta	1.9
		Mo	0.6
Boiler Discharge	Liquid velocity 1 ft/sec 4.5 hr at 1200 to 1700°F	Cb	24.4
		Cb + 1% Zr (weld)	23.0
	Vapor velocity 20 ft/sec 5 hr at 1700 to 1780°F	Ta	69.2
		Mo	3.0
Nozzle Outlet	Liquid velocity 32 ft/sec 4.5 hr at 1200 to 1700°F	Mo	9.0
	Vapor velocity 1800 ft/sec 5 hr at 1700 to 1780°F	Cb	141

because of the tremendous amount of erosion that occurred. Unpurified potassium was also used again resulting in misleading results. The results are presented here to give an indication of what will happen in an unpurified system.

Semmel[97] presented results on Haynes 25 alloy and formed the conclusion that Haynes 25 (L-605) is highly resistant to transgranular and intergranular attack to as high as 1850°F potassium for 1000 hr. He hypothesized that carbon and nitrogen in L-605 could cause local carburization and nitriding of the alloy, thus changing its mechanical properties. However, his tests were not conducted to prove this statement. Loops made of Type 316 SS and Cb + 1% Zr were tested, but the results were not presented in Semmel's presentation.

3.1.3.5 Rubidium

There exists a scarcity of information on the compatibility of rubidium with various materials. The reader is referred to References 2, 88, and 107 for a summary of static compatibility tests with various materials. Simons[96] concluded after performing some static capsule tests using Type 316 SS, Inconel X, KE-7 (WC + 6% Co), beryllium, and DiMax M-19 silicon steel materials at temperatures between 900 and 1400°F for 500 hr that these materials, with the exception of beryllium, would be suitable for liquid metal loop materials.

Whitman and Stockton[11] performed static and thermal convection boiling loop tests with Inconel at temperatures ranging from 160 to 1520°F and concluded that Inconel is quite suitable for use in a boiling rubidium system.

3.1.3.6 Lithium

The majority of this subsection is classified. The reader is referred to NAA-SR-8617 Vol I, Addendum I for the classified discussion of References 108, 61, 105, 109, 110, 111, and 112.

NAA-SR-8617 Vol I, Addendum I presents calculated results of corrosion tests of seven refractory metals in static lithium at elevated temperatures.[112] Hoffman[113] did an extensive study on the corrosion of materials by lithium. His conclusions are presented in Figure 3.3 which are valid for systems with the following conditions: the surface-to-volume ratio is approximately 13:1; and in dynamic systems the flow rate is less than 10 ft/min and the pipe is approximately 0.7 in. ID with a temperature gradient approximately 200°F.

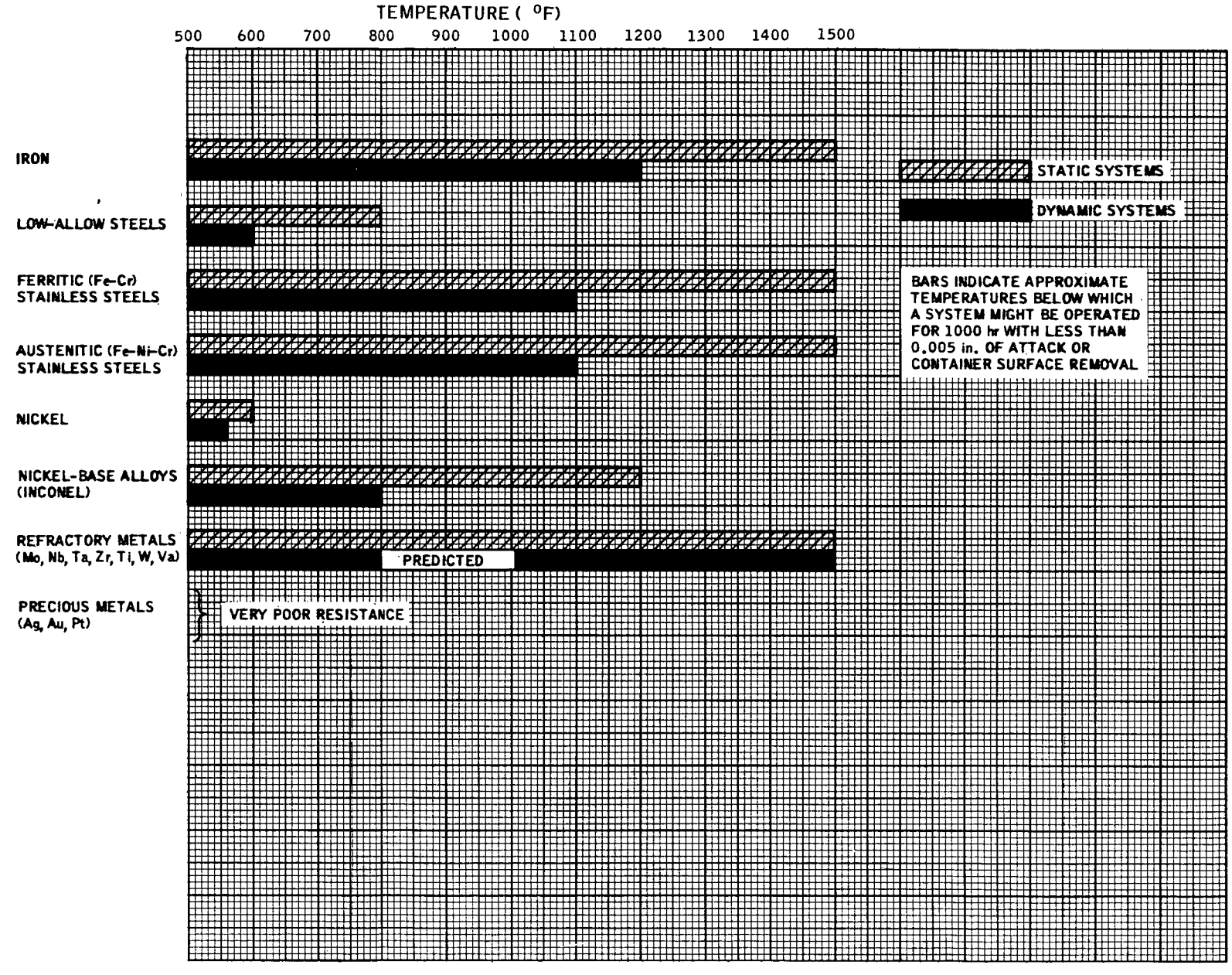

Figure 3.3 Corrosion Resistance of Various Metals and Alloys in Lithium (Reference 113)

3.2 HANDLING OF LIQUID METALS

The following sections will contain brief, general information on liquid metals regarding the storage, fire prevention, and personnel safety. These sections do not necessarily constitute the policies of any one company or organization, and should be used only as a guide. The information is presented in order to alert the reader to the hazards associated with liquid metals.

3.2.1 Storage[1, 9, 114, 115, 116]

Liquid metals should be stored in a dry, unsprinklered, fire resistant, ventilated building. The containers should be raised above the ground to prevent contact with water. Metal storm covers extending down the sides of the container should be used, in addition to drip pans in order to prevent liquid metal from coming into contact with a concrete floor, causing detrimental effects (for example, burning sodium reacts with concrete, releasing heat which spalls the concrete and scatters burning sodium over a wide area).[9] Usually inert gas is used as a cover gas in the container. Petroleum ether and hexane was used by McCoy and Hoffman[116] for storing rubidium, but a few disadvantages existed; the low flash points of the liquids presented a hazard when handling rubidium, and the rubidium had to be purified in order to remove the impurities associated with these liquids. Hill[115] indicates that only helium or argon is suitable for blanketing lithium, while in addition nitrogen may be used with sodium or NaK.

3.2.2 Fire and Personnel Safety[9, 114, 115, 117, 118]

Proper planning, maintenance, and personnel education will prevent most fires. To extinguish a fire special agents must be used; dry calcium carbonate applied with shovels and Met-L-X pressurized extinguishers are used at Atomics International on sodium, NaK, potassium, rubidium, and lithium fires. Graphite was used initially as a fire extinguishing agent, but it proved to be too messy to handle. Under no circumstances should ordinary extinguishing agents (water, CO_2, carbon tetrachloride, etc.) be applied. Another word of caution is that liquid metals do not burn like most materials; for example, sodium seldom burns with an open flame, instead there are many bright, yellow, glowing spots covering the surface of the liquid metal exposed to air. Sodium will ignite in air at temperatures greater than 257°F, and due to the large heat generation, will reach very quickly a temperature of 1500°F. No information is available on the burning characteristics of other liquid metals.

Policies at Atomics International regarding minimum personnel safety equipment have been established by Eggen[114, 117] and may be summarized in the following way (small liquid metal setups are usually completely enclosed to absolutely prevent personnel from coming into contact with the liquid metal, so that the following precautions may be eliminated). Personnel engaged in activities near or on the component test towers shall wear hard hats, gloves, and leather-soled shoes, with safety glasses (cup type) being optional, and shall raise and lower all tools and loose equipment by hand line. Personnel present around liquid metal systems shall wear fireproof coveralls and leather shoes, with hard hats having plastic face shields and plastic gloves being optional. All personnel involved in transferring or handling exposed liquid metal below 250°F shall wear flameproof coveralls, leather shoes, plastic gloves, and hard hats with plastic face shields. When the liquid metal is at a temperature greater than 250°F, all personnel shall wear welding helmets with canvas or leather snood, flameproof coveralls, asbestos or chrome leather gloves, chrome leather leggings, and leather shoes or rubber boots inside trouser legs. In general, all liquid metal spills shall be picked up and disposed of in dry calcium carbonate filled buckets or pans and wiped clean with flameproof rags. Clothing that has been exposed to liquid metal should be removed and the body should be flooded with water immediately. Low pressure water should be used for flushing the eyes. (Personnel working with liquid metals should know the location and use of safety showers). No matter how minor a liquid metal burn seems, it should be brought to the attention of the first aid station immediately.

4.0 HYDRAULICS

4.1 TWO-PHASE PRESSURE DROP

The following presentation will mainly consist of a method presented by Baroczy and Sanders[119] for calculating the local two-phase friction pressure drop in a two-phase, one- or two-component fluid-flow system. The total friction pressure change during condensing or boiling is obtained by numerically integrating the local two-phase pressure drop gradient over the range of condensation or boiling. A method for calculating the momentum pressure change during boiling or condensing in a horizontal pipe which was initiated by Martinelli and Nelson[120] will also be presented.

4.1.1 Friction Losses

The work of Baroczy and Sanders is actually an extension of work by previous authors[120, 121, 122] and uses an additional parameter (local gas Reynolds number) with the Lockhart-Martinelli two-phase flow modulus (X) to correlate two-phase pressure drop data. The following relationships are used to calculate the two-phase friction pressure change:

$$\Delta p_{TPF} = \int_o^L \left(\frac{\Delta p}{\Delta z}\right)_{TPF} dz \quad , \qquad \ldots(4.1)$$

$$\left(\frac{\Delta p}{\Delta z}\right)_{TPF} = \Phi_g^2 \left(\frac{\Delta p}{\Delta z}\right)_{gF} \quad . \qquad \ldots(4.2)$$

Figures 4.1 and 4.2 contain curves which give experimental values for Φ_g^2 as a function of the two-phase flow modulus; however, the local flow regimes for the liquid and the gas (vapor) flowing alone must be determined before one knows which curve to use. Thus, if the liquid and gas Reynold numbers are larger or smaller than 2000, the flows are turbulent or laminar (viscous), respectively. Therefore, X_{vv}, X_{vt}, X_{tt}, and X_{tv} indicate the two-phase flow modulus for viscous liquid-viscous gas, viscous liquid-turbulent gas, turbulent liquid-turbulent gas, and turbulent liquid-viscous gas, respectively, and the following equations are used to obtain values for the two-phase flow modulus:

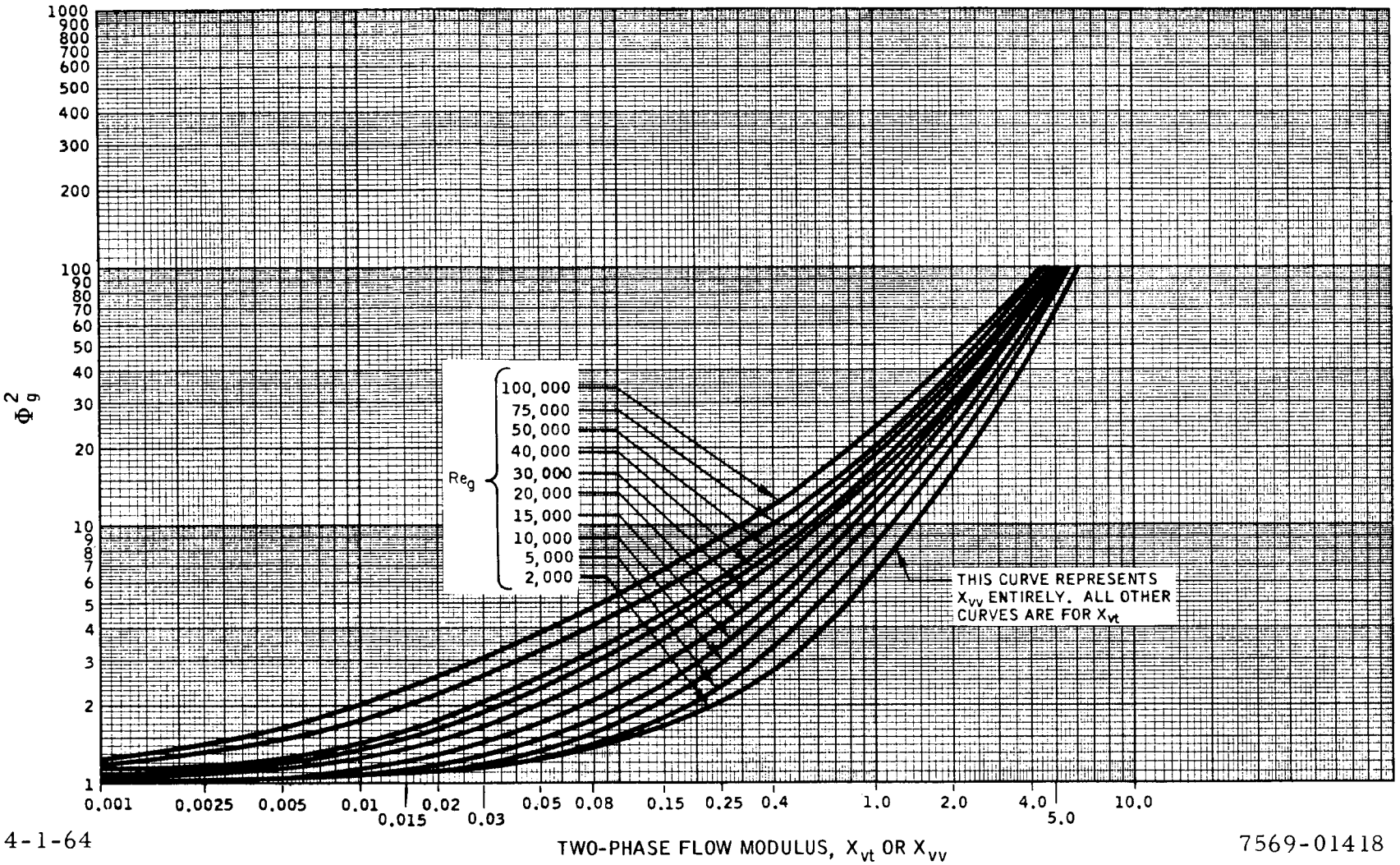

Figure 4.1 Correlation of Test Data From Reference 124 (using mercury-nitrogen) for Use With Two-Phase, One- or Two-Component Friction Pressure Change (Reference 119)

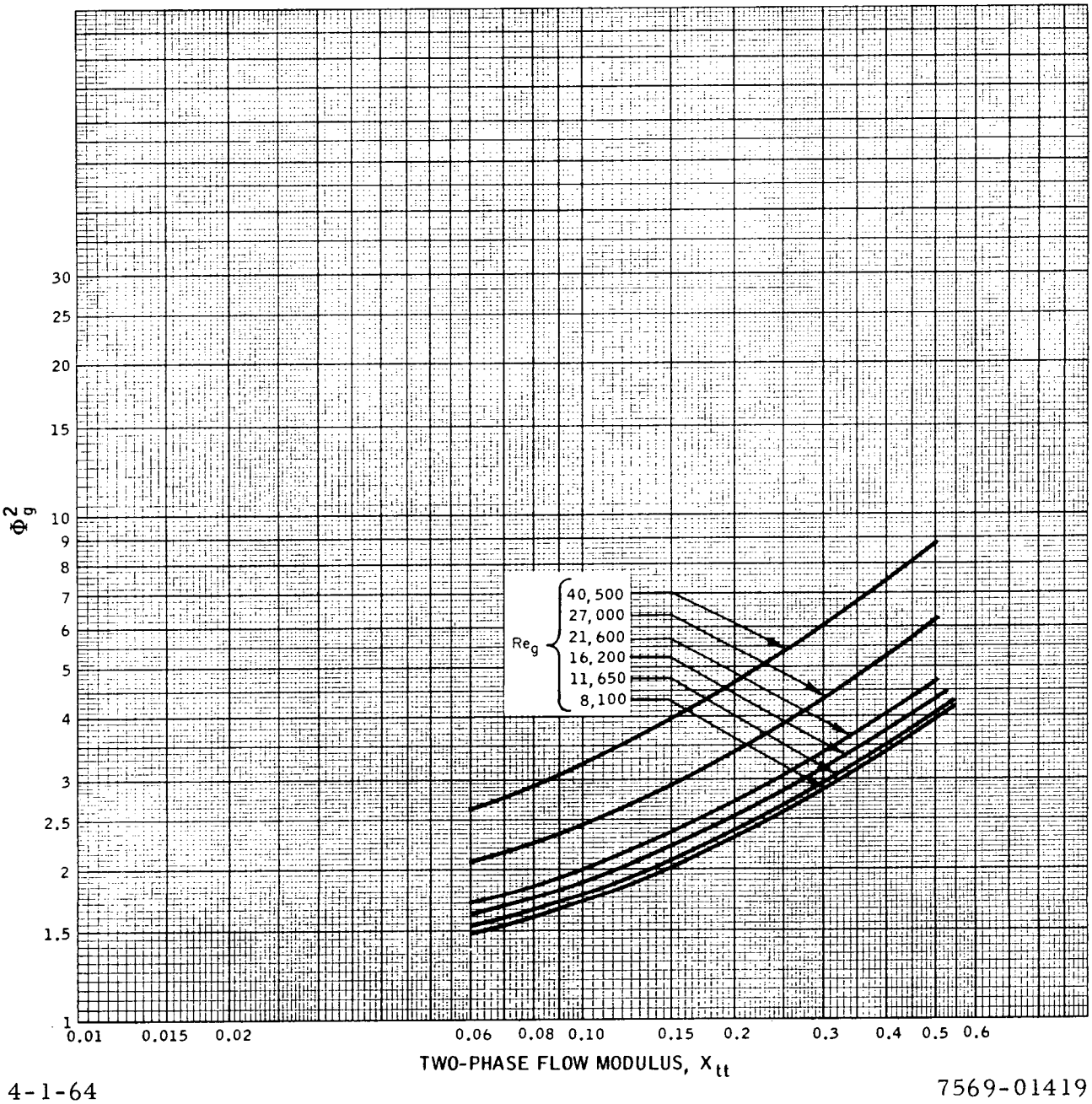

Figure 4.2 Correlation of Turbulent – Turbulent Test Data From Reference 124 (using mercury-nitrogen) for Use for Two-Phase, One- or Two-Component Friction Pressure Change (Reference 119)

$$X_{vv} = \left(\frac{W_\ell}{W_g}\frac{\rho_g}{\rho_\ell}\frac{\mu_\ell}{\mu_g}\right)^{0.5} , \qquad \ldots(4.3)$$

$$X_{vt} = \left(\frac{C_\ell}{C_g}\frac{W_\ell}{W_g}\frac{\rho_g}{\rho_\ell}\frac{\mu_\ell}{\mu_g}\right)^{0.5} Re_g^{-0.4} , \qquad \ldots(4.4)$$

$$X_{tt} = \left(\frac{W_\ell}{W_g}\right)^{0.9}\left(\frac{\rho_g}{\rho_\ell}\right)^{0.5}\left(\frac{\mu_\ell}{\mu_g}\right)^{0.1} , \qquad \ldots(4.5)$$

$$X_{tv} = \left(\frac{C_\ell}{C_g}\frac{W_\ell}{W_g}\frac{\rho_g}{\rho_\ell}\frac{\mu_\ell}{\mu_g}\right)^{0.5} Re_\ell^{0.4} . \qquad \ldots(4.6)$$

No data are presented for the turbulent liquid-viscous gas flow regime because of its scarcity. Since this type of flow, whenever it does exist, will exist over a short length at the entrance region of a boiler or at the exit region of a condenser, the turbulent liquid-turbulent gas flow regime is usually assumed to exist over this region. However, since the end points of the turbulent liquid-viscous gas flow regime are known, the pressure drop gradient may be extrapolated through this region. It should also be pointed out that the Lockhart-Martinelli parameter implicitly takes into account the different flow patterns (except slug or stratified flow) so that an investigation need not be made in order to determine the kind of flow pattern.

In order to calculate the local pressure drop gradient in Equation 4.2 for gas (vapor) flowing alone through a pipe, the following equation should be used (assuming specific weight and density are equal):

$$\left(\frac{\Delta p}{\Delta z}\right)_g = -2f_g\frac{\gamma_g V_g^2}{gD} = -2f_g\frac{G_g^2}{gD\rho_g} . \qquad \ldots(4.7)$$

Thus by using Equations 4.2 to 4.7 and Figures 4.1 and 4.2, the two-phase friction pressure change, $(p_e - p_i)_{TPF}$, can be obtained by numerically integrating Equation 4.1.

4.1.2 Momentum Changes

When vapor is generated or condensed during forced circulation, the momentum of the fluid stream changes resulting in a pressure drop or gain in addition to the pressure drop that is occurring due to friction. The pressure drop (denoted by a negative value for Δp_M) caused by the increase in momentum of the fluid stream during boiling can be expressed[120] as follows (assuming all liquid exists at the inlet):

$$(p_e - p_i)_M = \Delta p_M = \frac{W_T}{gA}\left[(V_\ell)_i - (1 - x_e)(V_\ell)_e - (x_e)(V_g)_e\right] \quad . \quad \ldots(4.8)$$

Using Equations 4.14 and 4.15 from the next section, one obtains (assuming that the liquid inlet and exit densities are not equal; however, they are usually assumed to be equal) the following equations in terms of known parameters:

$$\Delta p_M = \left[\frac{G_T^2}{g(\rho_\ell)_e}\frac{(\rho_\ell)_e}{(\rho_\ell)_i} - \frac{(1 - x_e)^2}{(R_\ell)_e} - \frac{\rho_\ell}{\rho_g}_e \frac{x_e^2}{(R_g)_e}\right] \quad . \quad \ldots(4.9)$$

The pressure gain (denoted by a positive value for Δp_M) caused by the decrease in momentum of the fluid stream during condensing can be expressed, similarly to Equation 4.8, as follows (assuming all liquid exists at the exit):

$$\Delta p_M = \frac{W_T}{gA}\left[(1 - x_i)(V_\ell)_i + (x_i)(V_g)_i - (V_\ell)_e\right] \quad . \quad \ldots(4.10)$$

Using again Equations 4.14 and 4.15, one obtains (assuming liquid inlet and exit densities are not equal) the following equation in terms of known parameters:

$$\Delta p_M = \frac{G_T^2}{g(\rho_\ell)_i}\left[\frac{(1 - x_i)^2}{(R_\ell)_i} + \left(\frac{\rho_\ell}{\rho_g}\right)_i \frac{x_i^2}{(R_g)_i} - \frac{(\rho_\ell)_i}{(\rho_\ell)_e}\right] \quad . \qquad \ldots(4.11)$$

Discussion on the local liquid and gas fractions is given in the next section.

In the above momentum discussion the liquid and vapor were assumed to be flowing completely separated (giving approximately $\Delta p_M \propto x^2$). This results in obtaining a somewhat lower pressure gain during condensing and a lower pressure loss during boiling than is actually occurring. The other extreme flow pattern that could be assumed is that the liquid and vapor are completely mixed (giving approximately $\Delta p_M \propto x$), i. e., fog flow exists ($V_g = V_\ell$). The real pressure gain or drop will actually be between the two extremes mentioned (found by comparing the multiplier curves of Reference 111 to the two extreme limits). However, since experimentally obtained liquid fraction data are used in determining the momentum pressure change, the values obtained from Equation 4.9 and 4.11 actually lie between the two extremes mentioned above and should be used with confidence.

The overall or total two-phase pressure change, $(p_e - p_i)_T$, through a horizontal boiler or condenser is obtained by using the following equation:

$$\Delta p_T = \Delta p_{TPF} + \Delta p_M \quad . \qquad \ldots(4.12)$$

By using Equation 4.1 and 4.9 or 4.11 the total two-phase pressure change over a given length can be obtained. One word of caution might be mentioned at this point. When attempting to find the overall two-phase pressure change gradient, the following equation should be used:[119]

$$\left(\frac{\Delta p}{\Delta z}\right)_T = \frac{\Delta p_{TPF} + \Delta p_M}{\Delta z} \quad . \qquad \ldots(4.13)$$

An error occurs if one attempts to obtain the overall pressure change gradient at $z = 0$ by adding the two-phase friction pressure change gradient to the momentum pressure change gradient, because at $z = 0$ the overall pressure change is due entirely to two phase friction. Therefore, the overall pressure change gradient

must be due only to the two-phase friction change gradient. Since the momentum pressure change is zero at $z = 0$ and the momentum change gradient is not zero at $z = 0$, Equation 4.13 must be used for calculating the overall pressure change gradient. Usually the heat flux is constant and the condensing or boiling rate is assumed linear in order to ease the calculating work needed to obtain point by point pressure changes and gradients.

NOMENCLATURE

A = Cross sectional area of pipe, ft^2

C = Constant in friction factor equation = 16 (laminar flow); = 0.046 (turbulent flow), dimensionless

D = Hydraulic diameter of pipe, ft

f = Fanning friction factor = 16/Re (laminar flow); $= \frac{0.046}{Re^{0.2}}$ (turbulent flow), dimensionless

Φ = Function of X utilized in calculating two-phase friction pressure drop $\left[\Phi_g^2 \equiv \frac{(\Delta p/\Delta z)TPF}{(\Delta p/\Delta z)_g}\right]$, dimensionless

g = Gravitational acceleration = 4.18×10^8 ft/hr^2

G = Mass velocity ($G = \rho V$) $lb_m/hr\text{-}ft^2$

γ = Specific weight, lb_f/ft^3

p = Pressure, psf

Δp = Pressure change ($\Delta p = p_e - p_i$), psf

$(\Delta p/\Delta z)$ = Pressure change gradient in separated flow, psf/ft

R_g = Fraction of pipe flow cross section occupied by gas ($R_g = 1 - R_\ell$), dimensionless

R_ℓ = Fraction of pipe flow cross section occupied by liquid, dimensionless

Re = Reynolds number based on single-phase flow $\left(Re = \frac{\rho VD}{\mu}\right)$, dimensionless

V = Velocity, ft/hr

W = Mass flow rate, lb_m/hr

X = Two-phase flow modulus, dimensionless

x = Quality $\left(x = \frac{Wg}{W_T}\right)$, dimensionless

z = Length along boiler or condenser, ft

ρ = Density, lb_m/ft^3

μ = Absolute viscosity, $lb_m/hr\text{-}ft$

SUBSCRIPTS

e = Exit

F = Friction

g = Gas

i = Inlet

ℓ = Liquid

M = Momentum

t = Turbulent

T = Total

TP = Two-phase

tt = Turbulent liquid-turbulent gas

tv = Turbulent liquid-viscous gas

v = Viscous

vt = Viscous liquid-turbulent gas

vv = Viscous liquid-viscous gas

4.2 LIQUID HOLDUP

Liquid holdup is very important in SNAP systems because of the weight requirements set forth in space systems. It has become necessary to be able to predict the amount of liquid contained in a boiler or a condenser. Pressure changes in two-phase fluids flowing through ducts are also affected by the amount of liquid contained in a boiler or a condenser. Therefore the term, local liquid fraction, has been devised and is defined as the fraction of fluid flow area occupied by the liquid at a given cross section. The local gas fraction is the remaining cross sectional area which is unoccupied by liquid.

Baroczy[123] extended the work of other authors[120, 90, 122] by correlating local liquid fraction data with the Martinelli two-phase flow modulus parameter plus an additional parameter, $(\mu_\ell/\mu_g)^{0.2}/(\rho_\ell/\rho_g)$. The additional variable was needed, because when the liquid mercury-nitrogen data[124] were compared to the Lockhart-Martinelli correlation,[121] the liquid fraction data represented only 10% of the Lockhart-Martinelli values.[123] Therefore, by correlating the data of other workers[121, 124, 125, 126] for various liquids and gases, a generalized correlation of data was developed and is represented by Figure 4.3. The turbulent liquid-turbulent gas flow regime was the only one investigated by Baroczy; the problem becomes more complex when other flow regimes are investigated, since a family of Reynolds number curves results for each two-phase flow modulus value. However, work by Baroczy[69] and Martinelli and Nelson[120] indicated that the momentum pressure change is only slightly affected by the different flow regimes. Therefore, it seems advisable to use Figure 4.3 for all flow regimes for the time being.

An end result of the local liquid fraction curves is the ability to be able to determine the slip ratio (V_g/V_ℓ) in two-phase flow. The respective liquid and gas velocities are defined as follows:

$$V_\ell = \frac{W_\ell}{\rho_\ell A R_\ell} \quad , \qquad \ldots(4.14)$$

$$V_g = \frac{W_g}{\rho_g A R_g} \quad . \qquad \ldots(4.15)$$

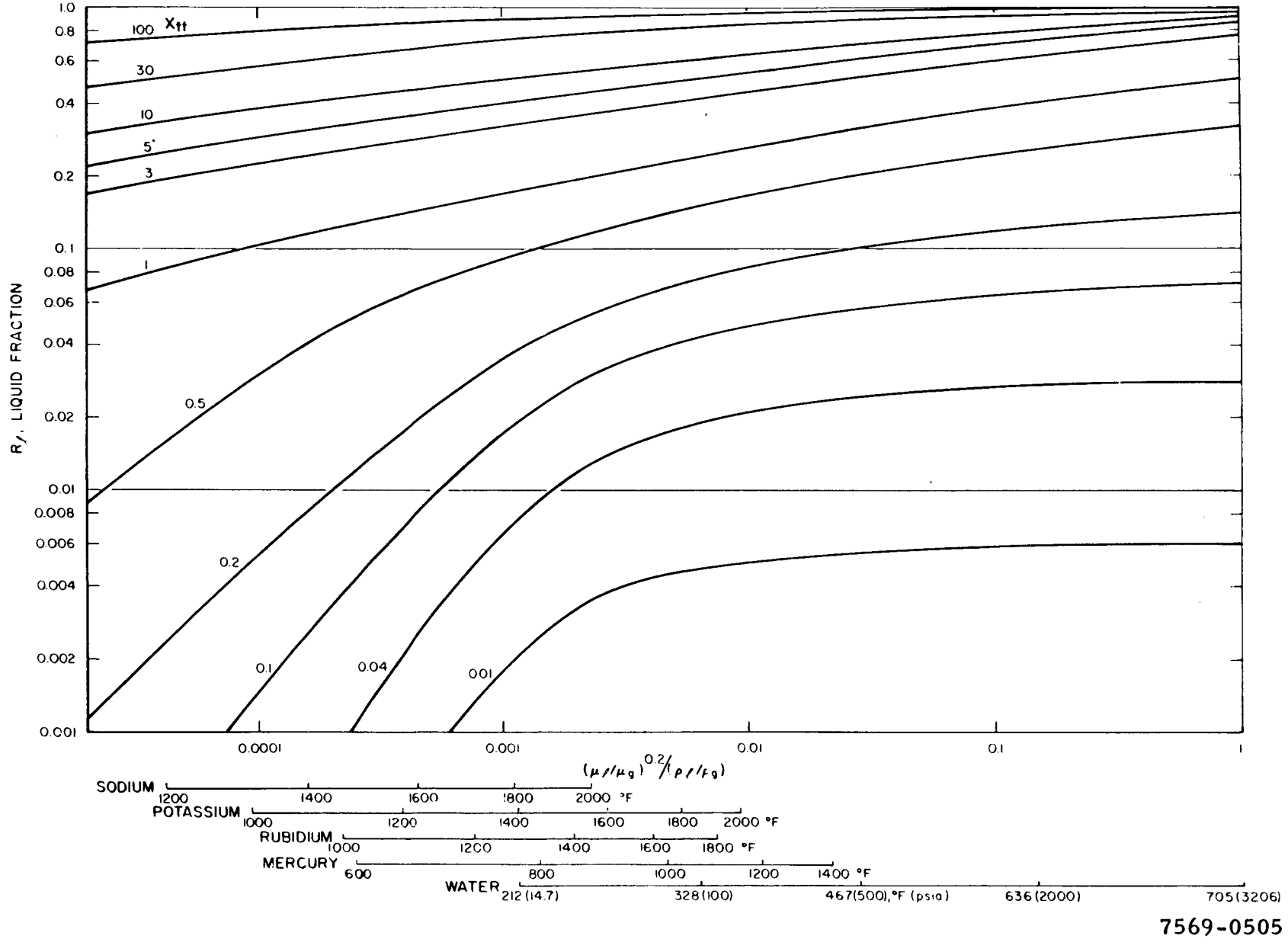

Figure 4.3. Generalized Local Liquid Fraction Correlation (Reference 123)

Therefore, the slip ratio becomes,

$$\frac{V_g}{V_\ell} = \frac{W_g \rho_\ell R_\ell}{W_\ell \rho_g (1 - R_\ell)} \quad , \qquad \ldots(4.16)$$

since,

$$R_g = 1 - R_\ell \quad . \qquad \ldots(4.17)$$

REFERENCES

1. "Liquid Metals Safety Manual for Mercury and Sodium-Potassium (NaK)," Report 0390-Sd-3, Aerojet-General Corp. (January 1961)

2. "Properties of Inorganic Energy-Conversion and Heat Transfer Fluids for Space Applications," WADD-TR-61-96 (November 1961)

3. NAVEXOS P-733, Liquid Metals Handbook, 2nd ed. (June 1952)

4. "Drainage and Disposal of NaK in the S-2-PSM-1 System Test," IOL, May 24, 1962, S. Sudar to I. W. Harper, Internal Communication, Atomics International, A Division of North American Aviation, Canoga Park, California

5. "Drainage and Disposal of Mercury in the S-2-PSM-1 System Test," June 1, 1962, S. Sudar to I. W. Harper, Internal Communication, Atomics International, A Division of North American Aviation, Canoga Park, California

6. C. R. Tipton, Jr. (ed.), Reactor Handbook, Volume I — Materials, Interscience Publishers, Inc., New York (1960)

7. "NaK and Potassium," MSAR 59-120, Technical Bulletin, MSA Research Corporation (1963).

8. "Table of Reactor Coolant Properties," BNL 661 (T-215), Reactor Technology, TID-4500 16th edition (March 10, 1961)

9. "Cesium and Rubidium Metals," Bulletin No. TD-CS-Rb, American Potash and Chemical Corporation (December 1961)

10. TID-5277, Liquid Metals Handbook, Sodium NaK Supplement, 3rd ed. (July 1955)

11. M. J. Whitman and D. L. Stockton, "Boiling Rubidium as a Reactor Coolant: Preparation of Rubidium Metal, Physical, and Thermodynamic Properties, and Compatibility With Inconel," CF-55-6-49, Part 1 (April 1954)

12. "Reactor Summary Report," PWAC 271 (May 1959) (Classified)

13. S. M. Kapelner and W. D. Bratton, "The Electrical Resistivity of Sodium Potassium, Rubidium, and Cesium in the Liquid State," PWAC 376 (June 1962)

14. N. T. Crane, "Physical and Thermodynamic Properties of Lithium," FXM 4986 (1961)

15. J. Holland, "Graphs of Physical Properties of Mercury Liquid and Vapor From O°F to 1400°F," NAA-TDR-4249 (August 1959)

16. "Thermophysical Properties of Rubidium," ASD-TDR-63-133 (February 1963)

17. Lithium Corporation of America, Inc., 9th issue, January-April 1963

18. J. W. Taylor, "The Surface Tension of Liquid Metals and Alloys," A.E.R.E. M/TN 24 (May 1954)

19. E. L. Dunning, "The Thermodynamic and Transport Properties of Sodium and Sodium Vapor," ANL 6246 (October 1960)

20. R. D. Keen to A. N. Gallegos, "NaK Safety," IOL, Int. Comm., Atomics International, A Division of North American Aviation, Inc., Canoga Park, California (May 28, 1963)

21. S. Ostrach, "New Aspects of Natural-Convection Heat Transfer, Preliminary Study of Effect of Frictional Heating," trans. ASME 75, 1287-1290, Int. Comm., Atomics International, A Division of North American Aviation, Inc., Canoga Park, California (1953)

22. E. R. G. Eckert and R. M. Drake, Jr., Heat and Mass Transfer, McGraw-Hill Book Company, Inc., New York (1959)

23. S. Ostrach, NACA Technical Report 1111 (1953)

24. R. Seigle, "Analysis of Laminar and Turbulent Free Convection From a Smooth Vertical Plate With Uniform Heat Dissipation per Unit Surface Area," General Electric Data Folder

25. E. R. G. Eckert and T. N. Jackson, NACA Technical Report 1015 (1951)

26. A. de Stordeur, J. M. Morelle, and J. P. Van Dievoet, "Cooling of Irradiated Nuclear Fuel by Natural Convection," Volume 7 of Proceedings of the Second United Nations International Conference on the Peaceful Uses of Atomic Energy (1958)

27. S. C. Hyman, C. F. Bonilla, and S. W. Ehrlich, NYO 564 (1951)

28. S. J. Levy, Journal of Applied Mechanics, 22, 5-5-522 (1955)

29. S. Ostrach, NACA TN 2863, "Laminar Natural Convection Flow and Heat Transfer of Fluids With and Without Heat Sources in Channels With Constant Wall Temperatures" (1952)

30. S. Ostrach, "Combined Natural and Forced Convection Laminar Flow and Heat Transfer of Fluids With and Without Heat Sources in Channels With Linearly Varying Wall Temperature," NACA TN 3141 (1954)

31. A. F. Lietzke, "Theoretical and Experimental Investigation of Heat Transfer by Laminar Natural Convection Between Parallel Plates," NACA TN 3328 (1954)

32. M. J. Lighthill, "Theoretical Considerations on Free Convections in Tubes," Fluid Motion Sub-Committee Aeronautical Research Council, F. M. 1758 (1952)

33. D. C. Hamilton, H. F. Poppendiek, and L. D. Palmer, "Theoretical and Experimental Analyses of Natural Convection Within Fluids in Which Heat is Being Generated – Part I: Heat Transfer From a Fluid in Laminar Flow to Two Parallel Plane Bounding Walls," CF 51-12-70 (1951)

34. F. C. Steiner, "Natural Convection in a Horizontal Pipe," KAPL Memo FCS-3 (1954)

35. R. A. Tidball and T. A. Ciarlariello, "Heat Transfer in Vent and Drain Line Closure for Sodium System," MSA TR 37 (1955)

36. D. P. Timo, KAPL Memo DPT-5 (1953)

37. J. W. Mausteller and M. J. McGoff, "Natural Convection in a Sodium-Filled Annulus," MSA TR-31 (1954)

38. J. K. Powledge, "Convection Heat Transfer in a Vertical Annulus," MSA Memo Report 56 (1954)

39. R. A. Baker and Alexander Sesonske, "Heat Transfer in Sodium - Potassium Alloy," Nuclear Science and Engineering 13, 283-288 (1962)

40. R. N. Lyon, "Liquid-Metal Heat Transfer Coefficients," Chemical Engineering Progress, 47, 75-79 (1951)

41. O. E. Dwyer, "Eddy Transport in Liquid-Metal Heat Transfer," Paper submitted to A. I. Ch. E. Journal (Vol 9, No. 2, p 261-8) for Publication February 18, 1962

42. H. E. Brown, B. H. Armstead, and B. E. Short, Trans. ASME 79, No. 2, 279 (1957)

43. P. L. Kirillov et al, Soviet Journal of Atomic Energy 6, No. 4, 253 (1960)

44. E. M. Khabakhpasheva and Y. M. Il'in, Atomnaya Energiya 8, 494, p 2.14 (1960)

45. I. I. Novikov et al, Atomnaya Energiya, 1, No. 4, 92 (1956)

46. M. S. Pirogov, Atomnaya Energiya, 8, No. 4, 367 (1960)

47. B. S. Petukhov and A. Y. Yushin, Soviet Physics – Doklady 6, No. 2, 159 (1961)

48. R. A. Seban and T. Shimazaki, "Heat Transfer to a Fluid Flowing Turbulently in a Smooth Pipe With Walls at Constant Temperature," ASME Paper No. 50-A-128 (1950)

49. R. A. Seban, "Heat Transfer to a Fluid Flowing Turbulently Between Parallel Walls With Asymmetric Wall Temperatures," Trans. ASME 72, 789 (1950)

50. O. E. Dwyer and P. S. Tu, "Unilateral Heat Transfer to Liquid Metals Flowing in Concentric Annuli," submitted to Nuclear Science and Engineering for publication from Brookhaven National Laboratory.

51. V. I. Subbotin et al, Atomnaya Energiya 8, No. 4, 310 (1960)

52. V. I. Petrovichev, Atomnaya Energiya 7, No. 4, 366 (1959)

53. J. P. Hartnett and T. F. Irvine, Jr., "Nussult Values for Estimating Turbulent Liquid Metal Heat Transfer in Noncircular Ducts," A. I. Ch. E. Journal 3, No. 3, 313-317 (1957)

54. A. J. Friedland et al, "Heat Transfer to Mercury in Parallel Flow Through Bundles of Circular Rods," International Developments in Heat Transfer, Part III (also BNL 5111) (1961)

55. O. E. Dwyer and P. S. Tu, Chem. Eng. Progr. Symposium Series 56, No. 30, 183 (1960)

56. C. L. Rickard, O. E. Dwyer, and D. Dropkin, "Heat Transfer Rates to Cross-Flowing Mercury in a Staggered Tube Bank - II," Trans. ASME 80, 646 (1958)

57. M. J. McGoff and J. W. Mausteller, "Heat Transfer and Pressure Drop With NaK-56 Flowing Perpendicular to Vertical Tubes," MSA MR 87 (July 29, 1955)

58. P. D. Cohn, "Heat Transfer and Thermodynamic Properties of Mercury," NAA-SR-MEMO-4666, Int. Comm., Atomics International, A Division of North American Aviation, Inc., Canoga Park, California (1959)

59. R. E. Balzhiser et al, "Literature Survey on Liquid Metal Boiling," ASD-TR-61-594 (December 1961)

60. "Alkali Metals Boiling and Condensing Investigations," General Electric Space Power and Propulsion Section First Quarterly Report (July-September 1962)

61. "Space Power Program Semiannual Progress Report for Period Ending June 30, 1962," ORNL 3337 (CRD) (October 1962)

62. R. C. Noyes, "An Experimental Study of Sodium Pool Boiling Heat Transfer," NAA-SR-6769

63. S. L. Shulman, "Additional Data From Sodium Pool Boiling Experiments," NAA-SR-TDR-8279, Int. Comm., Atomics International, A Division of North American Aviation, Inc., Canoga Park, California (March 1963)

64. G. L. Reed, "Burnout Heat Flux of Sodium, Mercury, Sulfur, and Rubidium," NAA-TDR-3853, Int. Comm., Atomics International, A Division of North American Aviation, Inc., Canoga Park, California (January 1960)

65. K. Engelberg-Forster and R. Greif, "Heat Transfer to a Boiling Liquid - Mechanism and Correlations," J. of Heat Transfer, Trans. ASME 81, 43-53 (1959)

66. V. Nicolia and S. Tramuta, "Forced Circulation Boiling Mercury Heat Transfer in Tubes," NDA 2143-8 (Classified)(May 1961)

67. R. E. Lyon, "Boiling Heat Transfer With Liquid Metals," Thesis, University of Michigan (1953)

68. R. C. Noyes, Unpublished Data on Sodium Pool Boiling (to be published as NAA-SR-7909), Int. Comm., Atomics International, A Division of North American Aviation, Inc., Canoga Park, California (June 1963)

69. Personal Communication With C. J. Baroczy, Atomics International, A Division of North American Aviation, Inc., Canoga Park, California (July 1963)

70. J. Longo, Jr., "Alkali Metals Boiling and Condensing Investigations," General Electric Quarterly Progress Reports 2 and 3, September 31, 1962 through March 31, 1963

71. P. J. Berenson and J. J. Killackey, "An Experimental Investigation of Forced Convection Vaporization of Potassium," presented at the High Temperature Liquid Metal Heat Transfer Conference, Oak Ridge National Laboratory (September 4-6, 1963)

72. H. M. Dieckamp, R. Balent, and J. R. Wetch, "Compact Reactors for Space Power," Nucleonics 19, 4, p 73-76 (April 1961)

73. D. A. Oberacker and R. J. Ziobro, "The SNAP 2 Power Conversion System Topical Report No. 23, Compact Boiler Development," TWR-ER-5411 (Classified) (June 1963)

74. R. G. Gido and A. Koestel, "SNAP 2 Power Conversion System Topical Report No. 17, Mercury Boiling Research," TWR-ER-4833 (October 1962)

75. N. Zuber and M. Tribus, "Further Remarks on the Stability of Boiling Heat Transfer," AECU-3631 (January 1958)

76. W. Rohsenow and P. Griffith, "Correlation of Maximum Heat Flux Data for Boiling of Saturated Liquids," NP-5738, MIT (1955)

77. S. S. Kutateladze, "Heat Transfer in Condensation and Boiling," AEC-TR-3770 (1952)

78. R. E. Balzhiser et al, "Investigation of Liquid Metal Boiling Heat Transfer," Fifth Quarterly Progress Report, University of Michigan (May 1963)

79. J. N. Addoms, Sc. D. Thesis, MIT, Ch.E. Dept., also W. H. McAdams, Heat Transmission, 3rd Ed., p 385 (1948)

80. W. R. Gambill, "Generalized Prediction of Burnout Heat Flux for Flowing, Subcooled, Wetting Liquids," Ch. E. Prog. Symposium Series No. 41, Vol 59 (1963)

81. W. H. Lowdermilk et al, "Investigation of Boiling Burnout and Flow Stability for Water Flowing in Tubes," NACA-TN-4382 (September 1958)

82. G. F. Burdi to P. D. Cohn, "Plant Trip to Oak Ridge National Laboratory, IOL, Int. Comm., Atomics International, A Division of North American Aviation, Inc., Canoga Park, California (February 12-13, 1963)

83. C. F. Bonilla and B. Misra, "Boiling and Condensing of Liquid Metals," NYO-3152 (April 1953)

84. B. Misra and C. F. Bonilla, "Heat Transfer in the Condensation of Metal Vapors: Mercury and Sodium up to Atmospheric Pressure," Chemical Engineering Progress Symposium Series No. 18, Vol 52, 7-21 (1956)

85. P. D. Cohn, "Heat Transfer Coefficients for Condensation of Liquid Metal Vapors Inside a Vertical Tube," M. S. Thesis, Oregon State College (1959)

86. G. L. Reed and R. C. Noyes, "Sodium Condensing Heat Transfer: An Experimental Study of One Aspect of Sodium Cooled Reactor Safety," NAA-SR-7325 (August 1962)

87. P. F. Young and R. V. Arabian, "Determination of Temperature Coefficient of Solubility of Various Metals in Rubidium and the Corrosive Effects of Rubidium on Various Alloys at Temperatures From 1000 to 2000°F," AGN-8063 (October 1962)

88. A. Haire and L. Hays, "Energy Conversion Systems Reference Handbook - Heat Exchangers," WADD TR 60-699, Vol VII (AD 256881) (September 1960)

89. J. P. Page, "A Review of Liquid Metal Corrosion in the SNAP 8 Temperature Regime (1200 to 1500°F)," NAA-SR-6575 (August 1961)

90. J. R. DiStefano and E. E. Hoffman, "Corrosion Mechanisms in Refractory Metal - Alkali Metal Systems," presented at AGARD Conference on Refractory Metals, Oslo, Norway (to be published as ORNL 3424) (June 1963)

91. J. R. Weeks and D. H. Gurinsky, "Solid Metal Liquid Metal Reactions in Bismuth and Sodium," Liquid Metals and Solidification, ASM (1958)

92. V. W. Eldred, "Interactions Between Solid and Liquid Metals and Alloys," AERE X/R 1806 (November 1955)

93. J. W. Taylor, "Inhibition of Liquid Metal Corrosion, AERE M/TN 35 (February 1956)

94. M. Davis and A. Draycott, "Compatibility of Reactor Materials in Flowing Sodium," IGR TN/C 857 (1958)

95. R. C. Reid, Trans. ASME, Paper 51-5-13 (1951)

96. NASA-TN-D-769, NASA-AEC Liquid-Metals Corrosion Meeting, December 7-8, 1960, Washington, D. C.

97. TID-7626 (pt. 1), NASA-AEC Liquid Metals Corrosion Meeting, December 14-15, 1961, Brookhaven National Laboratory

98. J. J. Owens, J. F. Nejedlik, and J. Wm. Vogt, "The SNAP 2 Power Conversion System Topical Report No. 7," TRW-ER-4103 (June 1960)

99. D. E. Ellis, "Evaluation of Nickel Base Braze Alloys for Mercury Service," NAA-SR-TDR-6885, Int. Comm., Atomics International, A Division of North American Aviation, Inc., Canoga Park, California (December 1961)

100. J. F. Nejedlik, "The SNAP 2 Power Conversion System - Mercury Materials Evaluation and Selection," ER 5024 (CRD) (August 1962)

101. E. E. Hoffman and W. D. Manly, "Corrosion Resistance of Metals and Alloys to Sodium and Lithium," presented at the Symposium on Handling and Uses of the Alkali Metals, Dallas, Texas (April 1956)

102. R. J. Denington et al, "Space Radiator Study," ASD-TR-61-697 (April 1962)

103. R. K. Wagner and H. E. Kline, "High Strength Zirconium Alloys," NAA-SR-3481 (July 1959)

104. M. A. Perlow, "SNAP 2 Primary Coolant Development," NAA-SR-6439 (July 1961)

105. "Space Power Program Semiannual Progress Report for Period Ending December 31, 1962," ORNL 3420 (CRD) (May 1963)

106. D. V. Hammond and T. M. Littman, "Compatibility of Materials With High Temperature Potassium," NAA-R-2617-4, Final Progress Report, April 18, 1960 through December 31, 1961

107. P. F. Young and R. V. Arabian, "Determination of Temperature Coefficient of Solubility of Various Metals in Rubidium and the Corrosive Effects of Rubidium on Various Alloys at Temperatures from 1000 to 2000°F," AGN-8063 (October 1962)

108. E. E. Hoffman, "The Effects of Oxygen and Nitrogen on the Corrosion Resistance of Columbium to Lithium at Elevated Temperatures," ORNL 2675 (January 1959)

109. J. M. McKee, "Effect of Nitrogen on Corrosion by Lithium," NDA-40 (CRD) (June 1957)

110. "Lithium Corrosion Investigation of a High Power Columbium Alloy System," PWAC 381 (CRD) (February 1963)

111. D. O. Hobson, "Effect of Alloying Elements on the Strength, Stability, and Corrosion and Oxidation Resistance of Columbium - A Literature Survey," ORNL 3212 (Classified)(March 1962)

112. "Summary Report of Corrosion Tests of Several Refractory Metals in Lithium at Elevated Temperatures," AD 315553 (Classified)(November 1959)

113. E. E. Hoffman, "Corrosion of Materials by Lithium at Elevated Temperatures," ORNL 2924 (October 1960)

114. Engineering Development Handbook No. 14, Atomics International, A Division of North American Aviation, Inc., Canoga Park, California (August 1957)

115. P. L. Hill, "Alkali Metals Area Safety Guide (Supplemental Issue)," Y-811 (May 1961)

116. H. E. McCoy, Jr. and E. E. Hoffman, "Handling Techniques for Rubidium," ORNL-1991 (December 1955)

117. "Preventing, Containing, and Extinguishing Sodium and Sodium-Organic Fires," NAA-SR-1739 (October 1956)

118. H. J. Dunster, "A Review of Procedures for Disposal of Radioactive Waste, 1961," AHSB (RP)-R-29 (December 1962)

119. C. J. Baroczy and V. D. Sanders, "Pressure Drop for Flowing Vapors Condensing in a Straight Horizontal Tube," ASME Paper 61-WA-257

120. R. C. Martinelli and D. B. Nelson, "Prediction of Pressure Drop During Forced-Circulation Boiling of Water," Trans. ASME, 70, p 695 (1948)

121. R. W. Lockhart and R. C. Martinelli, "Proposed Correlation of Date for Isothermal Two-Phase, Two-Component Flow in Pipes," Chemical Engineering Progress, 45, p 39 (1949)

122. R. C. Martinelli, L. M. K. Boelter, T. H. M. Taylor, E. G. Thomsen, and E. H. Morrin, "Isothermal Pressure Drop for Two-Phase, Two-Component Flow in a Horizontal Pipe," Trans. ASME, 66, p 139 (1944)

123. C. J. Baroczy, "Correlation of Liquid Fraction in Two-Phase Flow With Application to Liquid Metals," NAA-SR-8171 (April 1963)

124. R. Kiraby and A. Koestel, "Condenser Development and Design Study," SNAP 2 Power Conversion System Topical Report No. 8, TRW-ER-4104 (June 1960)

125. G. F. Hewitt, I. King, and P. C. Lovegrove, "Holdup and Pressure Drop Measurements in the Two-Phase Annular Flow of Air-Water Mixtures," AERE-R-3764 (June 1961)

126. G. F. Hewitt, I. King, and P. C. Lovegrove, "Techniques for Liquid Film and Pressure Drop Studies in Annular Two-Phase Flow," AERE-R-3921 (March 1962)

 UNCLASSIFIED

INDEX CARD PAGE

(This page is not part of the report)

NAA-SR-8617 Vol I

Atomics International
SNAP TECHNOLOGY HANDBOOK — LIQUID METALS
G. F. Burdi (Author) 153 pages
Issued: May 30, 1964

Extensive use of liquid metals as working fluids in various reactor programs, i.e., SNAP 10A/2/8, necessitates a handbook to correlate and present the current information which is available to the engineer. The present work is not intended to be all inclusive but contains important excerpts from commonly used references along with recent developments, arranged for the convenience of the design engineer. Data selected for presentation has passed the test of being in reasonable agreement with the majority of published work; some older data not well substantiated by recent experiments has not been included. The liquid metals considered to be the most useful for present and future applications are mercury, sodium, sodium-potassium, potassium, rubidium, and lithium. As additional information becomes available, periodic revisions will be incorporated in this SNAP TECHNOLOGY HANDBOOK.

UNCLASSIFIED

NAA-SR-8617 Vol I

Atomics International
SNAP TECHNOLOGY HANDBOOK — LIQUID METALS
G. F. Burdi (Author) 153 pages
Issued: May 30, 1964

Extensive use of liquid metals as working fluids in various reactor programs, i.e., SNAP 10A/2/8, necessitates a handbook to correlate and present the current information which is available to the engineer. The present work is not intended to be all inclusive but contains important excerpts from commonly used references along with recent developments, arranged for the convenience of the design engineer. Data selected for presentation has passed the test of being in reasonable agreement with the majority of published work; some older data not well substantiated by recent experiments has not been included. The liquid metals considered to be the most useful for present and future applications are mercury, sodium, sodium-potassium, potassium, rubidium, and lithium. As additional information becomes available, periodic revisions will be incorporated in this SNAP TECHNOLOGY HANDBOOK.

UNCLASSIFIED

NAA-SR-8617 Vol I

Atomics International
SNAP TECHNOLOGY HANDBOOK — LIQUID METALS
G. F. Burdi (Author) 153 pages
Issued: May 30, 1964

Extensive use of liquid metals as working fluids in various reactor programs, i.e., SNAP 10A/2/8, necessitates a handbook to correlate and present the current information which is available to the engineer. The present work is not intended to be all inclusive but contains important excerpts from commonly used references along with recent developments, arranged for the convenience of the design engineer. Data selected for presentation has passed the test of being in reasonable agreement with the majority of published work; some older data not well substantiated by recent experiments has not been included. The liquid metals considered to be the most useful for present and future applications are mercury, sodium, sodium-potassium, potassium, rubidium, and lithium. As additional information becomes available, periodic revisions will be incorporated in this SNAP TECHNOLOGY HANDBOOK.

UNCLASSIFIED

NAA-SR-8617 Vol I

Atomics International
SNAP TECHNOLOGY HANDBOOK — LIQUID METALS
G. F. Burdi (Author) 153 pages
Issued: May 30, 1964

Extensive use of liquid metals as working fluids in various reactor programs, i.e., SNAP 10A/2/8, necessitates a handbook to correlate and present the current information which is available to the engineer. The present work is not intended to be all inclusive but contains important excerpts from commonly used references along with recent developments, arranged for the convenience of the design engineer. Data selected for presentation has passed the test of being in reasonable agreement with the majority of published work; some older data not well substantiated by recent experiments has not been included. The liquid metals considered to be the most useful for present and future applications are mercury, sodium, sodium-potassium, potassium, rubidium, and lithium. As additional information becomes available, periodic revisions will be incorporated in this SNAP TECHNOLOGY HANDBOOK.

UNCLASSIFIED